UNIVERSITÀ DEGLI STUDI DI PALERMO

Dottorato di ricerca in Oncologia e Chirurgia Sperimentali

Dipartimento di Medicina di Precisione in Area Medica, Chirurgica e Critica (Me.Pre.C.C.)

Under joint supervision with the Ri.MED Foundation, Palermo

D014 – Oncologia e Chirurgia Sperimentali

Tumour microenvironment in Non-Small-Cell Lung Cancer (NSCLC): a proteomic approach to gain insights on novel disease biomarkers and therapeutic approaches.

Doctoral Dissertation of:
Anna Paola Carreca

Tutor:
Prof. Antonio Galvano

Co-tutor:
Dr.ssa Cinzia Maria Chinnici

The Chair of the Doctoral Program:
Prof. Antonio Russo

2022–2025 Cycle XXXVIII

Per aspera ad astra.

INDEX

Abstract

Lung cancer is the most frequently diagnosed malignancy and remains the leading cause of cancer-related mortality worldwide, accounting for approximately 1.8 million deaths annually. The majority of cases (approximately 85%) are classified as non-small cell lung cancer (NSCLC), which includes adenocarcinoma, squamous cell carcinoma, and large cell carcinoma. Despite therapeutic advances, including immunotherapy, five-year survival rates remain low, with only a subset of patients—identified through biomarkers such as PD-L1—achieving meaningful clinical benefit.

A major challenge lies in the intrinsic heterogeneity of lung tumors, which is often underestimated by conventional biopsies. These provide only a limited snapshot of the disease and fail to capture its dynamic evolution or the emergence of therapy resistance. In this context, liquid biopsies have emerged as a minimally invasive and promising approach, enabling the detection of circulating tumor cells, nucleic acids, and extracellular vesicles (EVs). EVs, enriched with proteins, DNA, RNA, and lipids, represent a valuable source of biomarkers for early diagnosis, monitoring treatment response, and identifying novel driver mutations.

Unlike genomics and transcriptomics, which are already widely applied in liquid biopsy, the proteomic profiling of blood remains relatively underexplored, despite the central role of proteins in intercellular communication and biological regulation. Proteomic analysis of the tumor microenvironment (TME), combined with three-dimensional (3D) in vitro models based on cancer stem cells and tumor spheroids, offers the opportunity to better recapitulate tumor heterogeneity and to study the secretome under physiologically relevant conditions.

This project aims to identify novel biomarkers and potential therapeutic targets through mass spectrometry (MS)-based proteomic analysis of the TME focusing on EVs isolated from liquid biopsies of cancer patients and from 3D cell culture models that mimic the TME in vitro.”

1.0 Background

1.1 No Small Cell Lung Carcinoma (NSCLC)

Lung carcinoma is one of the most widespread epithelial malignancies worldwide. Although it is the second most common neoplasm in both sexes, it remains the leading cause of cancer-related mortality, with incidence trends showing significant differences between men and women. Beyond its high prevalence, lung cancer is considered one of the major oncological “big killers” because its mortality closely parallels its incidence, resulting in a diagnosis that is frequently associated with a poor prognosis and a high likelihood of fatal progression.

The natural history of non-small cell lung carcinoma (NSCLC) is strongly influenced by the clinical stage at the time of diagnosis. Prognosis varies significantly depending on whether the neoplasm is identified at an early, so-called “limited” stage, or at an advanced stage. When detected early, patients may undergo surgical treatment with curative intent, resulting in substantially better survival outcomes. Conversely, in patients diagnosed at an advanced stage, the prognosis is extremely unfavorable: five-year survival rates remain around 5%, despite therapeutic advances in recent years such as targeted therapies and immunotherapies.

Unfortunately, most cases are still diagnosed at advanced stages. This pattern reflects the insidious nature of NSCLC, often asymptomatic in its early phases, and reinforce the need for effective screening and early diagnostic strategies to enable intervention at potentially curable stages, improve clinical outcomes, and reduce associated mortality.

According to World Health Organization, in 2020 alone approximately 2.2 million new cases and as many as 1.8 million deaths were recorded. These figures highlight the devastating impact of the disease and underscore the urgency of developing increasingly effective strategies for prevention, early diagnosis, and treatment [1]. The most recent projections indicate that, despite a slight decline in incidence in high-income countries, global mortality from lung cancer remains high, particularly in low- and middle-income settings where access to early diagnosis and innovative therapies is still limited [2].

1.1.1 Epidemiology

The situation in Italy is similar concerning. According to the latest ISTAT survey published in 2023, lung cancer remains among the top three causes of cancer-related death, with a higher incidence in males, although a progressive increase is also observed among females, consistent with the rise in tobacco consumption in younger female cohorts [3]. The ISTAT "Health for All-Italia" information system, updated to 2025, shows a trend toward stabilization in overall incidence, although marked regional and socioeconomic differences persist. These findings emphasize the urgency of implementing primary prevention strategies, particularly anti-smoking initiatives, along with targeted screening programs and equitable access to personalized therapies. Moreover, the growing availability of real-world data and national cancer registries represents an opportunity to monitor the effectiveness of health policies and improve clinical outcomes in the population affected by NSCLC.

NSCLC accounts for approximately 85% of all lung cancers, making it the most prevalent form of pulmonary neoplasm. It encompasses several histological subtypes, adenocarcinoma, squamous cell carcinoma, and large cell carcinoma, each with distinct biological and clinical characteristics. Globally, lung cancer remains the leading cause of cancer-related death, with five-year survival rates varying significantly depending on the stage at diagnosis: from 45% in stage IB up to 76% in stage III, while about 70% of patients are diagnosed at an advanced stage, with survival rates below 35% (Fig. 1).

In recent years, the therapeutic landscape of NSCLC has undergone a profound transformation. The introduction of targeted therapies based on molecular alterations (such as EGFR, ALK, ROS1, and BRAF mutations) and the use of

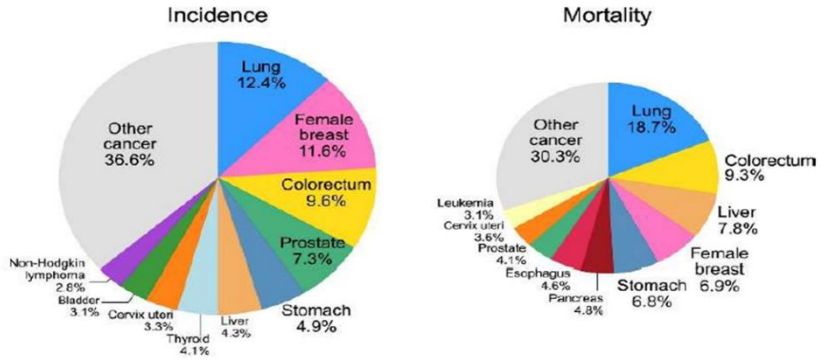

Figure 1: Percentage distribution of the incidence of new cancer cases and associated mortality worldwide. Lung cancers are the most frequent and lethal, followed by breast, colorectal, liver, and stomach cancers. [Bray et al. Cancer J Clinicians. 2024]

immunotherapy have significantly improved the prognosis of selected patient subgroups. In particular, neoadjuvant immunotherapy and combinations of checkpoint inhibitors with chemotherapy have shown promising results, contributing to the redefinition of standard treatment strategies.

From a clinical perspective, the management of NSCLC requires a multidisciplinary approach that integrates advanced imaging diagnostics, liquid biopsy, genomic profiling, and an accurate assessment of the patient's overall health status. The incresing complexity of therapeutic options necessitates a personalized clinical decision-making process, guided by biological, clinical, and individual patient factors.

1.1.2 Risk Factors

Tobacco smoke is the leading cause of lung cancer, accounting for about 85–90% of cases. Cigarettes contain dozens of carcinogenic substances that directly damage DNA and drive malignant transformations [3,4,5]. Passive smoking, as well as pipe and cigar use [6-7], also significantly increase the risk. In addition to tobacco, several environmental and genetic factors contribute to NSCLC development, including exposure to radon and asbestos, air pollution, especially fine particulate matter [8,9,10], and individual susceptibility. A family history of lung cancer further increases risk, with first-degree relatives showing nearly double the likelihood of developing the disease compared with the general population [11]. Gender-specific differences may amplify these risks: women appear to exhibit a greater susceptibility to tobacco carcinogens, and hormone replacement therapy may additionally increase the likelihood of lung adenocarcinoma [12].

1.1.3 Clinical aspects

The primary symptons of NSCLC typically include chest pain, cough, dyspnea, and hemoptysis. Cough occurs in 75% of patients, often due to endobronchial mass or post-obstructive pneumonia; dyspnea affects approximately 60% of patients and is usually related to airway obstruction caused by tumor mass; chest pain is reported in 50% of cases, while hemoptysis occurs in 35% of cases. Although acute bronchitis is the main cause of hemoptysis, lung cancer must be considered in any patient over 40 years of age presenting this sympton [13]. Clinical evaluation is essential for the initial assessment of the patient and for guiding both disease diagnosis and prognostic evaluation. It has been shown that patients with a worse prognosis at diagnosis present constitutional symptoms such as weight loss, asthenia, and/or symptoms related to

metastatic spread. Importantly, studies have demonstrated a direct correlation between the number of clinical abnormalities, encompassing symptoms, physical findings, and laboratory alterations, and the probability of identifying metastatic disease on imaging. Conversely, in asymptomatic patients or in those with symptoms limited to the primary tumor, the likelihood of detecting metastases on CT is extremely low [14,15].

1.1.4 Diagnosis and Staging

Following the formulation of a diagnostic suspicion of lung cancer, it is essential to accurately reconstruct the patient's clinical history (smoking habits, comorbidities, weight loss, performance status, and family history of neoplasms). Subsequently, diagnosis and clinical staging rely on a combination of imaging techniques and biopsy sampling methods.
The histopathological classification of lung carcinoma is primarily based on the distinction between NSCLC and small cell lung cancer (SCLC), two entities with profoundly different biological and clinical characteristics. NSCLC, which accounts for about 85% of cases, includes histological subtypes such as adenocarcinoma, squamous cell carcinoma, and large cell carcinoma, each defined by specific morphological patterns and molecular profiles. Classification today integrates traditional morphology with immunohistochemistry and genomic profiling, which are essential for identifying driver mutations that guide the use of targeted therapies. Conversely, SCLC represents about 15% of lung tumors and is characterized by rapid growth and high aggressiveness; histologically, it shows small cells with hyperchromatic nuclei and scant cytoplasm, along with a neuroendocrine phenotype. The fundamental difference between NSCLC and SCLC therefore lies not only in morphology but also in clinical and therapeutic behavior: while NSCLC requires a personalized approach based on molecular biomarkers, SCLC is generally treated with chemotherapy and radiotherapy, given its high initial sensitivity to drugs but rapid tendency to relapse [16,17,18].

Each NSCLC subtype can, in turn, be divided into many other variants and combinations of clinical subtypes, characterized by a high rate of genetic instability. For example, among patients diagnosed with NSCLC, approximately 15% present mutations in EGFR (Epidermal Growth Factor Receptor), another 15% in K-RAS (homolog of the Kirsten Rat Sarcoma viral oncogene), and around 5% in ALK (Anaplastic Lymphoma Kinase), indicating significant molecular heterogeneity within the NSCLC population. Furthermore, according to the

American Cancer Society, heterogeneity also exists within each specific mutation; it has been shown that identifying a single driver mutation in the tumor is not sufficient to understand the clinical complexity of NSCLC, highlighting the need to analyze genomic alterations in multiple genes simultaneously [19].

Adenocarcinoma is the most common NSCLC subtype; it originates from alveolar cells in the epithelium of the small airways. The WHO classification also recognizes early stages of lung cancer, such as adenocarcinoma in situ (a pre-invasive lesion), minimally invasive adenocarcinoma, and invasive adenocarcinoma, distinguished based on the degree of invasiveness and size [20].

Unfortunately, in most cases, NSCLC is not diagnosed until the disease reaches an advanced stage. Diagnosis requires a biopsy for histological confirmation and determination of tumor extent to define the stage of the lesion, which ultimately guides cancer treatment options. For this purpose, the TNM classification system is used, an international system that classifies the disease using an alphanumeric code, simplifying patient staging and prognosis. In the TNM system:

• T (Tumor): describes the size and local extent of the solid tumor, using values from 1 to 4 and “IS” for in situ lesions;

• N (Nodes): indicates the involvement of regional lymph nodes, using values from 0 to 4;

• M (Metastasis): assesses the presence or absence of distant metastatic spread from the primary tumor, categorized as M0 or M1

1.1.5 Liquid Biopsy

Given the need to obtain information on the molecular characterization of the neoplasm, which is often only partially achievable through tissue biopsy, NSCLC is one of the main cases where liquid biopsy has found significant clinical application and continues to expand rapidly.
Liquid biopsy is an innovative and promising technique that, through the analysis of body fluids (primarily blood, but also urine, ascitic fluid, pleural effusions, and cerebrospinal fluid), provides non-invasive molecular insights about the neoplasm. Liquid biopsy was first clinically adopted to detect EGFR mutations in plasma, particularly the T790M resistance mutation, which represents the main mechanism of acquired resistance to first- and second-

generation Tyrosine Kinase Inhibitors (TKIs) [21,22].
The components that can be analyzed through liquid biopsy include: circulating cell-free DNA (cfDNA), which may originate from both tumor and normal cells; circulating tumor DNA (ctDNA), a subtype of cfDNA that derives directly from tumor cells, correlates with tumor burden, and whose abundance varies depending on stage, site, and tumor size; ctDNA can also be expressed as the percentage of tumor DNA relative to cfDNA, referred to as Tumor Fraction (TF) [23,24]. Additionally, circulating tumor cells (CTCs) can be identified, which may contribute to the formation of distant metastatic foci; exosomes and extracellular vesicles (EVs), nanometer-sized structures that transport proteins, DNA, RNA, and other molecules; as well as microRNAs (miRNAs), long non-coding RNAs (lncRNAs), circular RNAs (circRNAs), and tumor-educated platelets (TEPs) [25,26] (Fig. 2). Several techniques can be used to analize liquid biopsy composition, such as real-time polymerase chain reaction (rt-PCR), which offers good sensitivity but is limited to analyzing a restricted set of predefined mutations. In contrast, next-generation sequencing (NGS) techniques allow the analysis of a broader panel of genes enabling the identifications of point mutations, insertions, deletions, rearrangements, and copy number variations (CNVs). The International Association for the Study of Lung Cancer (IASLC) recommends performing liquid biopsy using NGS both in patients who have not yet undergone any treatment and in oncogene-addicted patients with acquired resistance to targeted therapy [27]. However, liquid biopsy does not replace tissue biopsy and remains a complementary investigative technique that supports, but cannot substitute, histological and molecular evaluation of tumor tissue. The clinical applications of liquid biopsy are varied and continuously evolving, including the monitoring of disease burden, investigation of primary and acquired resistance mechanisms to targeted therapies in oncogene-addicted disease, and the assessment of

blood-based tumor mutational burden (bTMB) as a potential predictive marker of response to immunotherapy [28,29,30].

1.1.6 The Tumor Microenvironment

The tumor microenvironment (TME) is a complex ecosystem surrounding neoplastic cells, which profoundly shapes tumor initiation, progression, and therapeutic response. It consists of tumor cells and non-neoplastic components such as fibroblasts, immune cells (macrophages, myeloid cells, T and B lymphocytes), endothelial cells, extracellular matrix (ECM), and soluble molecules (cytokines, growth factors) that collectively promote survival, proliferation, and therapy resistance [31] (Fig. 3). Although immune cells are recruited to the tumor site, their antitumor functions are progressively downregulated and often co-opted to support tumorigenesis. Tumors evade immune surveillance through mechanisms that inhibit effector functions or induce apoptosis, thereby exploiting immune cell infiltration to create a growth-promoting microenvironment. This process underlies the concept of cancer immunoediting, whereby the immune system, while capable of eliminating transformed cells, also exerts selective pressure that promotes the emergence of immune-resistant tumor variants [32,33,34]. A key indicator of immune response is the presence of tumor-infiltrating lymphocytes (TILs), which correlates with favorable prognosis in several cancers. TILs are mainly T lymphocytes, divided into two major subsets: CD8+ cytotoxic T cells, which play a central role in cancer immunobiology and whose infiltration within the tumor is strongly associated with improved survival, and CD4+ helper T cells, which

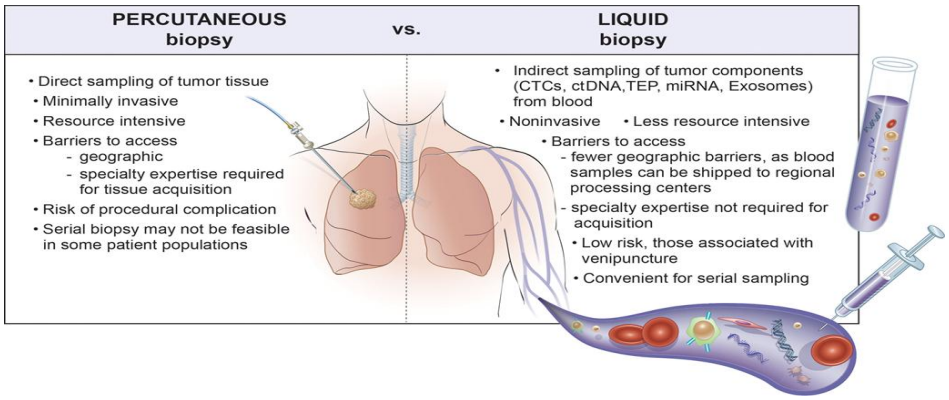

Figure 2: Illustration shows comparison of percutaneous biopsy versus liquid biopsy characteristics. CTC = circulating tumor cell, ctDNA = circulating tumor DNA, miRNA = microRNA, TEP = tumor-educated platelet [Underwood et al. 2020].

promote CD8+ recruitment and sustain an inflammatory microenvironment

through cytokines such as IL-2 and IFN-γ [35,36]. Notably, a high presence of Th1 CD4+ cells is linked to better outcomes in multiple malignancies. Conversely, regulatory T cells (Tregs), characterized by CD4+ and CD25+ expression, suppress antitumor responses both directly and indirectly, thereby supporting disease progression. High levels of Treg infiltration is associated with poor prognosis [37,38]. Tumor progression is also linked to increased expression of T-cell exhaustion markers, resulting in functional impairment: reduced IL-2 production, diminished proliferative capacity and cytotoxicity, and lower secretion of pro-inflammatory cytokines. The primary exhaustion marker is PD-1 (Programmed Cell Death-1), an immune checkpoint expressed on CD4+ and CD8+ T cells that normally regulates tolerance and limits immune response duration [39,40]. Within the TME, PD-1 interaction with its ligands (PD-L1/PD-L2) inhibits effector T-cell activity, promoting anergy. Chronic

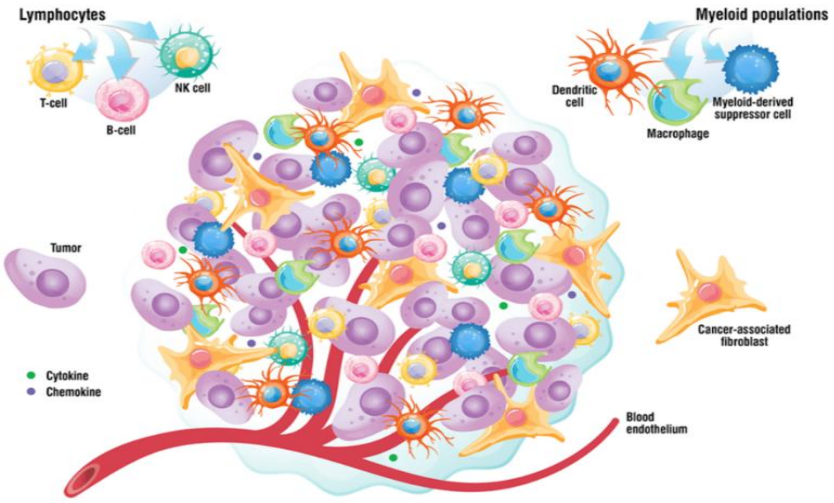

Figure 3: Schematic representation of the tumor microenvironmentTME, a complex system composed of diverse cell types and components, including tumor cells, cancer-associated fibroblasts, immune infiltrates, pericytes, and vascular and lymphatic networks. The tumor microenvironmentTME plays a critical role in tumor initiation, growth, differentiation, invasion, metastasis, angiogenesis, and treatment response, representing a potential diagnostic, prognostic, predictive, and therapeutic biomarker. (Adapted from Zhang et al.2022)

antigen exposure drives persistent PD-1 expression, a key mechanism of immune escape. Studies indicate that blocking the PD-1/PD-L1 pathway can significantly improve clinical outcomes [41].

Beyond immune cells, the TME includes Cancer-Associated Fibroblasts (CAFs), one of the most abundant stromal populations. CAFs, similar to fibroblasts activated during wound healing, fail to undergo apoptosis and remain persistently activated. Initially, they may limit tumor progression, but under the influence of tumor-derived signals, they shift toword a pro-tumorigenic phenotype, promoting growth, invasion, and angiogenesis. CAFs secrete ECM components (collagen, fibronectin, laminins) and pro-inflammatory molecules such as osteopontin (OPN), CXCL1, CXCL2, and IL-6 [42,43]. They also drive angiogenesis directly (via VEGF, MMP-9) and indirectly through the recruitement of pro-angiogenic macrophages. Recent studies show that tumor cells actively reprogram fibroblasts into CAFs through miRNAs (MiR-31, miR-214, miR-155), thereby inducing CAF-specific gene expression such as α-SMA and MMPs [44].

Given the complexity of the TME and its role in cancer progression, deeper understanding of these mechanisms is essential to identify novel therapeutic targets, enhance treatment efficacy, and develop diagnostic and prognostic biomarkers.

1.1.7 Therapies

Therapeutic approaches for NSCLC can be used individually or in combination and include surgery, radiotherapy, chemotherapy, targeted therapy, and the more recent immunotherapy. The choice of treatment depends on both the physical characteristics of the tumor and the patient's overall health status, comorbidities, age, and sex. Consequently, NSCLC treatment is highly stage-specific and divided into three clinical categories: early (stage I and II), locally advanced (stage III), and metastatic (stage IV).

For stage I or II NSCLC, treatment is primarily surgical, involving tumor resection and, if necessary, adjuvant therapy. However, most patients experience recurrence within two years [45]. Management of stage III or IV NSCLC is far more complex, as surgery is often not feasible at these stages. Treatment typically shifts toward chemotherapy and/or radiotherapy to address both locoregional disease and distant micrometastases. Unfortunately, prognosis for stage III NSCLC remains poor, with only 15% of patients alive at five years [46,47].

Targeted therapies and novel immunotherapies based on immune checkpoint inhibitors (ICIs) have significantly improved outcomes for NSCLC over the past

two decades [48]. Targeted therapies have become a major research focus due to their specificity for tumor cells and their generally lower toxicity compared to conventional treatments. These therapies aim to block or inhibit various receptor tyrosine kinases (RTKs) involved in cell growth and survival, which are frequently mutated in NSCLC. Currently available inhibitors target proto-oncogenes such as EGFR, ALK, RET (Rearranged during Transfection), BRAF (serine/threonine kinase B-Raf), ROS1 (ROS tyrosine kinase), NTRK (Neurotrophic Tyrosine Receptor Kinase), MET, and KRAS. Many of these drugs are now standard of care, while others remain under development. However, fewer than 25% of NSCLC patients benefit from targeted therapy, and most eventually develop acquired therapeutic resistance [49].

To date, among biomarkers approved by the European Medicines Agency (EMA) and the U.S. Food and Drug Administration (FDA), only PD-L1 is available for NSCLC. For patients whose tumors lack actionable molecular alterations, first-line therapy is selected based on clinical conditions and PD-L1 expression on tumor cells. Monoclonal antibodies such as pembrolizumab, cemiplimab, or atezolizumab are the preferred treatment for patients with high PD-L1 expression (≥50%) [50].

1.1.8 Immunotherapies

Over the past decade, therapies based on immune checkpoint inhibition (ICIs) have emerged as the first generation of antibody-based treatments capable of acting on immune cells within the TME by targeting inhibitory pathways such as CTLA-4 and PD-1. These therapies work by blocking the receptor-ligand interactions, which drive the tumor immune evasion [51,52,53]. Among the most studied immune checkpoints is programmed cell death receptor 1 (PD-1) and its ligands, programmed death-ligand 1 (PD-L1) and programmed death-ligand 2 (PD-L2). PD-1 plays a key role in regulating and maintaining the balance between T-cell activation and immune tolerance and is widely expressed not only on T cells but also on B cells and NK cells. Its primary function is to limit T-cell activity in peripheral tissues during cell-mediated immune or inflammatory responses. PD-L1, the major PD-1 ligand, is commonly upregulated in several human solid tumors, including lung cancer, melanoma, and ovarian cancer [54,55].

Currently, among biomarkers approved by the European Medicines Agency (EMA) and the U.S. Food and Drug Administration (FDA), only PD-L1 is routinely used for NSCLC. For patients whose tumors lack actionable molecular alterations, first-line therapy is based on clinical conditions and PD-L1

expression on tumor cells. Monoclonal antibodies such as pembrolizumab, cemiplimab, or atezolizumab are the preferred treatment for patients with high PD-L1 expression (≥50%) [50].

Compared to chemotherapy, immunotherapy is associated with fewer side effects and has been shown to prolong survival and improve quality of life. However, only a minority of cancer patients (approximately 20%) achieve durable survival with these treatments [56]. These findings highlight the need to identify robust and clinically meaningful predictive factors to select patients most likely to benefit from immune-based therapies.

1.2.0 The Evolution of EV Research

The first observations of EVs date back to 1946 thanks to the work of Chargaff and West [57], who identified them in plasma as procoagulant particles of platelet origin, later referred to as “platelet dust” by Wolf in 1967 [58]. Between the 1970s and 1980s, other studies identified EVs released into plasma from microvilli cells of rectal adenoma [59], virus-like particles secreted into the culture media of human cells or detected in bovine serum used as a culture supplement [60,61] as well as vesicles, later called prostasomes [62], in seminal fluid [63]. During this period, erly descriptions of tumor membrane fragments were reported, revealing their procoagulant properties [64]. In 1983, structural studies demonstrated that vesicles were released from multivesicular bodies (MVBs) after their fusion with the cell membrane during red blood cell differentiation [65]. More than a decade later, Raposo et al. showed that these vesicles, later named exosomes, isolated from Epstein-Barr virus–transformed B lymphocytes, were antigen-presenting particles capable of inducing a response in T cells [66]. Subsequently, it was discovered that EVs contain nucleic acids, DNA, RNA, and proteins. From that point onward, knowledge and characterization of these vesicles grew exponentially, to the extent that since 2014 the International Society for Extracellular Vesicles (ISEV) has worked to define criteria for EV classification, acknowledging the complexity of EV subpopulations defined by size, function, cargo, cell/organ type, and even species of origin [67]. The term Extracellular vescicles (EVs) refers to nanometer-sized particles released by cells, bounded by a lipid bilayer and incapable of autonomous replication, as they lack a functional nucleus [68].

1.2.1 Biogenesis

EVs display significant variability in terms of their cellular origin, molecular content, size, and biological activity [69,70]. Their first classification was based on size categorizes EVs into apoptotic bodies (1–5 μm), microvesicles (0.1–1 μm), and exosomes (30–150 nm) [71]. However, alternative classifications have been proposed, introducing considerations such as tissue of origin (e.g., prostasomes and oncosomes) and functional parameters [72]. EV proteins constitute a key aspect of their classification, reflecting both the cellular origin and the contents of the originating compartments. Exosomes (Exo) are generated by the endocytic pathway through the interaction between the endocytic vesicles and the endosomal sorting complex required for transport (ESCRT) system, and afterwards, they are released by the fusion of multivesicular bodies (MVBs) with the plasma membrane [73]. ESCRTs are involved in Exo production regulation also through the autophagy system. Autophagy-related genes (*Atg*) represent key factors for Exo release and their expression has been found to be deregulated in cancer cells, promoting proliferation and metastasis [74]. The complex network between autophagy and Exo trafficking includes many regulatory proteins and was recently revised by Zubkova and coworkers [75]. Conversely, microvesicles (MV) and apoptotic bodies arise directly from the plasma membrane. In particular, MVs derive from membrane budding, whereas apoptotic bodies form from the blebbing of cells that undergo apoptosis. Cancer cells markedly enhance EV release to promote cancer development, proliferation, and metastasis. Among the EVs released from cancer cells are oncosomes, a subtype that differ in size and composition from other EVs, and associated with the transfer of oncogenic material.

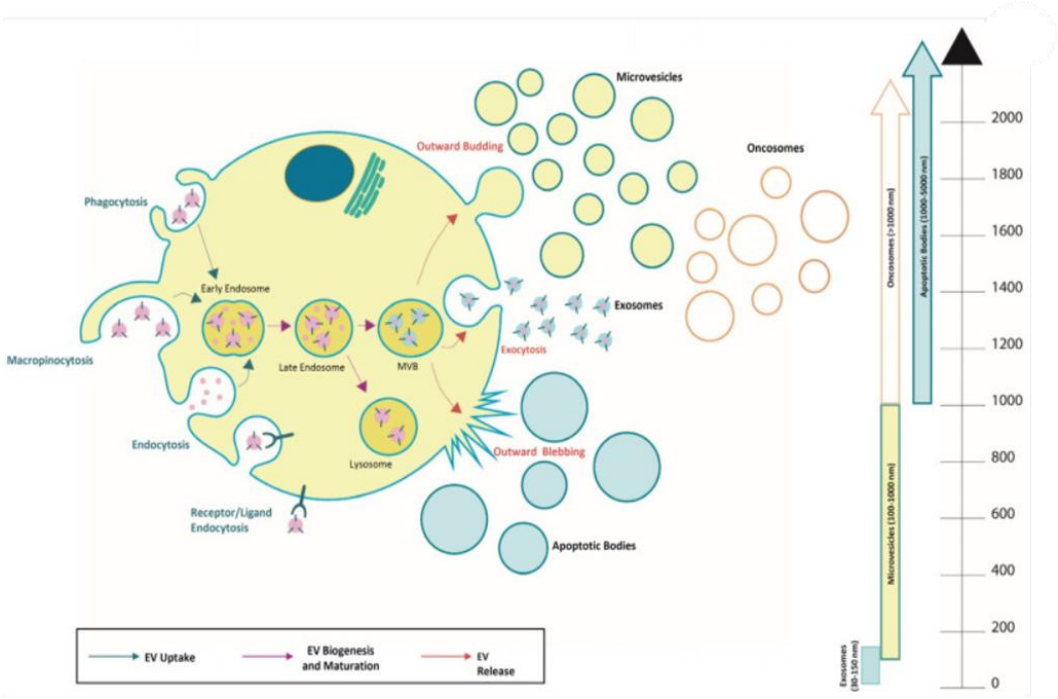

Figure 4: Overview of extracellular vesicleEV subtypes and their uptake, biogenesis, and release. They are classified into different sub-classes and are generated through the endosomal pathway, released as exosomes (30–150 nm), microvesicles (0.1–1 µm), apoptotic bodies (1–5 µm), and oncosomes (>1 µm) (Carreca et al. Cancers 2024).

1.2.2 EVs in Lung Cancer Diagnosys and Therapy

EVs represent a mechanism of intercellular communication adopted by cells and are involved in both physiological and pathological processes. They are implicated in tumor formation and development by participating in mechanisms such as migration, invasion, angiogenesis, hypoxia, and immune system evasion [76]. By exploiting their ability to mediate cell-to-cell communication and thereby enable the transfer of the cancerous phenotype, EVs constitute an important biological mechanism underlying the conditioning of the TME, leading to the formation of pre-metastatic niches [77]. The information they carry can influence the behavior of target cells in multiple ways. In particular, they can act as carriers, transferring membrane proteins and receptors to target cells, or modifying their phenotype through the

horizontal transfer of genetic information. It has been demonstrated that EVs can deliver not only proteins or lipids, but also miRNAs, other ncRNAs, and mRNAs [78]. The analysis of EV miRNA levels in lung cancer patients has shown a significant difference compared to control samples, suggesting that circulating EV miRNAs might represent a useful screening tool [79]. Compared to other circulating biomarkers such as cell-free DNA (cfDNA) and CTC, EVs have the advantage of being more abundant and more stable, given their lipid layer, which also protects the transported cargo. These characteristics are crucial for establishing sensitive and easily repeatable protocols for the early diagnosis of disease. Their role is central in certain pathological phenomena; for instance, it is now widely demonstrated that a tumor cell can release more than 20,000 of these vesicles in 48 h [80], highlighting their contribution to shaping the TME. The analysis of EVs can represent a low-impact source for lung cancer characterization; notably, it has been demonstrated that EVs derived from bronchoalveolar lavage fluid (BALF) liquid biopsy can be used proficiently for epidermal growth factor receptor (EGFR) genotyping and the evaluation of EGFR mutations [81]. This method, together with digital droplet PCR (ddPCR) and next-generation sequencing (NGS) techniques, can allow for the stratification of patients for TKI treatment without invasive methods such as tissue biopsy [82].

Over the last ten years, EV research has focused on their potential application as therapeutic agents. As already underlined, EVs can carry molecules, particularly non-coding RNAs, influencing cancer growth, progression, metastasis, or drug resistance. EVs can be considered a promising vector for anti-cancer delivery systems due to their natural and advantageous properties, such as their high biocompatibility and limited systemic toxicity. Specific nanocarrier-targeted action can be improved by engineering and functionalizing their surface, for example, by inducing the expression of specific proteins on the EV membrane or through the loading of miRNA, which can be inserted exogenously on isolated EVs (electroporation, sonication, and RNA cholesterol conjugation), or indirectly by genetic modification of the donor cells before EV isolation (RNA transfection, RNA encoding plasmid transfection, and virus transfection) [83].

1.3 In vitro models: from 2D to 3D approaches

In biomedical field, experiments are conducted on models consisting of cell cultures derived from human or animal sources. These cultures, defined in vitro, allow researchers to study and investigate various aspects of cellular functions, aiming to reproduce as faithfully as possible the physiological characteristics of a tissue or organ. A classic model is represented by two-dimensional (2D) cultures, in which cells grow as a monolayer within flasks or Petri dishes. Although these systems are highly useful for evaluating parameters such as cytotoxicity, cell proliferation, inflammatory response, gene and protein expression, and the pharmacokinetics and pharmacodynamics of new compounds, they present certain limitations. Specifically, the reproduction of biological phenomena observed in vivo is limited, as these cultures fail to fully mimic the cellular and extracellular interactions typical of living tissues, resulting in reduced biomimetic capacity. Due to these discrepancies between in vitro and in vivo environments, the development of 3D models has become essential. These systems recreate a more complex and realistic microenvironment, promoting cell-cell and cell-ECM interactions through the formation of three-dimensional structures (Fig. 5).

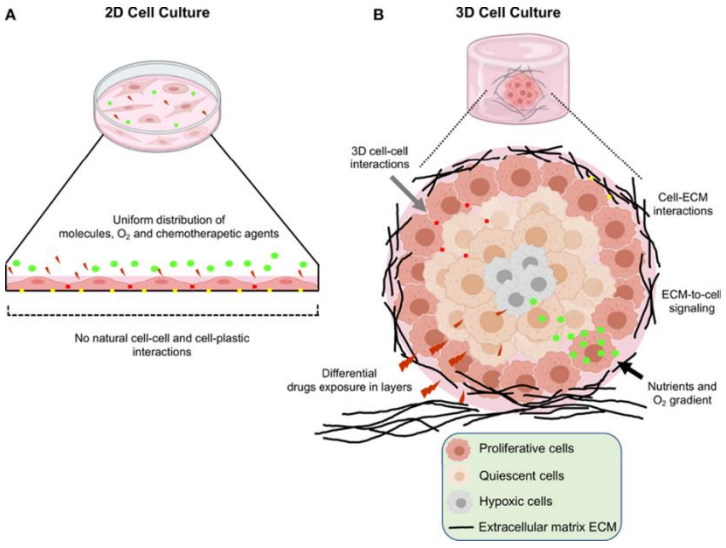

Figure 5: Schematic representation of conventional 2D (A) and advanced 3D cell culture systems (B), highlighting their structural organization and key biological characteristics. (Salinas-Vera et al. ront Oncol. 2022)

Cells can be cultured within artificial 3D matrices or using scaffold-free approaches, such as ultra-low attachment plates (ULA) [84]. Among the most representative 3D models, arranged in increasing order of biomimetic complexity, are spheroids, organoids, bioreactors, and organ-on-chip systems.

These models allow for a more accurate simulation of *in vivo* complexity and represent highly relevant tools for advanced biomedical research [85].

1.3.1 Spheroids

Spheroids are the simplest 3D models, consisting of aggregates of cells, and are often used as in vitro models for studying neoplastic conditions. Spheroids are able to develop gradients of oxygen, nutrients, metabolites, and soluble signals eventually producing a heterogeneous cell population. They also display a defined geometry, with cell-to-cell and cell-to-ECM interaction. Spheroid formation occurs through the action of integrins, a class of membrane proteins. This process can occur through several mechanisms: (i) dispersion of cell aggregates due to a long chain of ECM fiber consists of RGD motifs that can allow the binding of the integrin leading to the upregulation of cadherins; (ii) cadherin aggregates on the surface of the cell; and (iii) hemophilic cadherin-to-cadherin binding between adjacent cells, which strengthens the connection between cells and spheroids [86]. Spheroids exhibit a spherical geometry and are structurally organized into three main regions: (i) Proliferative Zone: the outermost region, where conditions are optimal for oxygen and nutrient diffusion, and waste products can be rapidly removed; (ii) Quiescent Zone: an intermediate area where most cells remain viable but exhibit very low metabolic activity; under certain conditions, these cells can regain full functionality; (iii) Necrotic Core: the innermost region, where limited oxygen and nutrients diffusion lead to cell death [87].

Cells adhere to each other, forming small aggregates with a diameter of 50-100 microns, which can be collected using standard micromanipulation techniques and individually seeded into culture medium. As cell proliferation continues, these aggregates increase in size, reaching volumes on the order of a cubic millimetre, corresponding to approximately one million cells. Thanks to their 3D architecture, spheroids acquire unique biological properties that are not observed in traditional monolayer cultures.

Spheroid cultures can be established using either immortalized cell lines or primary human cells. Immortalized lines allow long-term testing but offer limited biomimicry compared to human tissue, whereas primary cells provide higher physiological relevance but cannot be cultured for extended periods due to the risk of senescence [88].

Moreover, 3D spheroids can be generated using homotypic or heterotypic cell combinations, allowing a more faithful representation of in vivo cellular

heterogeneity and enabling the study of environmental interactions that influence tumor progression and treatment responses.
Tumor-derived spheroids are unique because they are often used for the enrichment of cancer stem cells (CSCs) or cells with stem cell-related characteristics. These spheroids are grown as floating spheres and have been used as surrogate systems of solid tumors in vitro [89].

1.3.2 Cancer Stem Cells (CSCs)

CSCs, first identified in 1990 [90] are a small group of cancer cells that possess properties of normal stem cells, such as self-renewal and pluripotency [91]. The CSC model, also known as the hierarchical model, provides a paradigm for people to understand intratumoral heterogeneity, as they can differentiate into various cancer cell phenotypes while maintaining their own population [92]. CSCs are also characterized by an enhanced ability to initiate tumor growth, proliferate, invade, migrate, and resist therapeutic effects. This implies a central role of CSCs in cancer development and makes their targeting an invaluable strategy for anti-cancer treatments. The CSC population exhibits both typical tumor cell activities and features similar to normal stem cells (NSCs), namely the cell population responsible for physiological tissue homeostasis, such as self-renewal capacity, undifferentiated state, and multipotency (i.e., the ability to generate mature cells belonging to different cell types) [93]. CSCs have been shown to give rise to tumors again when transplanted in vivo into immunodeficient mice [94,95].

The main distinctive characteristics of CSCs, which differentiate them from NSCs, are multiple. First of all, they have marked plasticity, as they can recreate intra-tumoral and inter-tumoral heterogeneity, giving rise to different cell populations [96,97,98]. They also possess a high and uncontrolled proliferative capacity, which allows them to escape the normal control of tissue homeostasis. CSCs, due to specific genetic alterations, tend to undergo a greater number of symmetric divisions (i.e., from one stem cell two stem daughter cells originate) rather than asymmetric divisions (i.e., from one stem cell a stem daughter cell and a more differentiated cell originate), which are instead typical of normal stem cells [99]. CSCs are capable of accumulating various mutations in their DNA and transmitting them to subsequent generations, due to alterations in DNA repair mechanisms.

Another fundamental peculiarity is their ability to resist the main therapeutic treatments, such as chemotherapy [101] and radiotherapy [102]. In this way, they constitute a small reservoir of cells responsible for tumor relapse and metastasis formation. Among the multiple characteristics of CSCs are their ability to initiate and sustain tumor growth, their plasticity [103,104], and their genetic instability, which make them capable of establishing specialized niches that support metastatic development [105,106]. Given all these peculiarities, CSCs are able to replicate by forming clones in in vitro cell cultures, which grow in suspension and have the characteristic spherical shape [107,108]. Many of the tumors with the highest incidence worldwide are heterogeneous tumors, containing cell populations with various stem-like properties [109]. The onset of a tumor can be driven either by transformed differentiated cells or by transformed stem cells residing in tissues. Transformation may occur during tissue regeneration and can also be initiated and/or accelerated in response to infections, toxins, radiation, or metabolic influences that cause mutations [110, 111]. During the transformation process (Fig. 6), oncogenes are overexpressed and tumor suppressors are inactivated, promoting uncontrolled proliferation. As a result, cells dedifferentiate and acquire stem cell-like characteristics [112]. CSCs have the peculiarity of expressing specific surface markers that allow their isolation in culture. These markers are shared with normal stem cells and progenitor cells, highlighting their probable derivation and origin. The spheroids originating from them are defined as oncospheres, or more

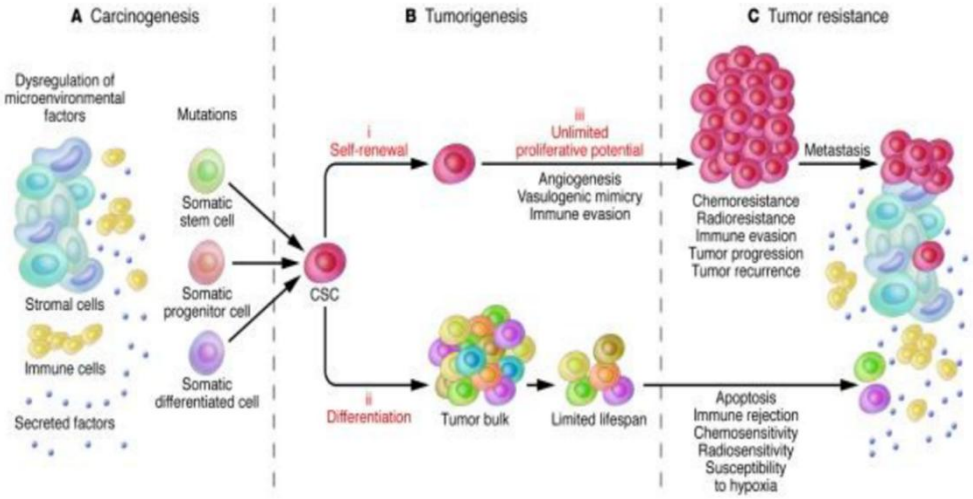

Figure 6: CSTs exhibit multiple characteristics that make them particularly invasive and capable of generating tumors, both in primary and secondary sites, thus leading to metastasis formation. Among their distinctive features, a key aspect is their ability to evade major treatments, including chemotherapy and radiotherapy. (Frank NY, et. al., J. of Clinical Investigation 2010).

specifically according to the tissue of origin, for example, colon-spheres or lung-spheres. The first studies on oncospheres were carried out on cells isolated from colon tumors [113], showing that CD133+ cells exhibited high aggressiveness and replicative capacity. Isolated CD133+ cells were able to form spheres in suspension culture and, when transplanted into immunodeficient mice, were capable of regenerating the tumor [95]. Subsequently, it was demonstrated that CD44, a transmembrane protein involved in cell adhesion, could be proposed as an alternative marker [114]. CD44+ cells isolated from carcinomas display CSC-like characteristics, as they can form spheres in culture starting from a single cell and regenerate the tumor when transplanted in vivo [115,116]. The microenvironment in which stem cells reside (the stem cell niche) plays a crucial role in maintaining their characteristics and regulating differentiation and proliferation processes. Stem cells are located within a dense network of blood vessels, immune system cells, adipocytes, fibroblasts, and components of the ECM, which collectively maintain a proper environment for preserving stemness. Stem cells communicate with the microenvironment through adhesion molecules, which bind to the ECM, and soluble molecular signals, such as cytokines and growth factors, which they exchange with the different components of the niche [117]. Ultimately, a reciprocal exchange of signals occurs between CSCs and the TME, establishing conditions suitable for tumor growth and development. This environment is sustained by CSCs, which have been recognized as an essential component of the TME and actively contribute to tumor progression [118,119].

2.0 Aim

The study aims to identify new predictive and/or prognostic biomarkers or therapeutics targets of NSCLC through a proteomic approach called “bottom-up,” to shed new light on the proteins that play a central role in the complex TME of NSCLC patients. These new potential biomarkers may be present in the cargo of EVs and carried into the bloodstream, or they may be “secreted” directly by tumor cells. Both components could be important for early detection and diagnosis of the disease, for determining prognosis, and for predicting therapeutic efficacy through a molecular model that differs from that found in healthy patients.

The main objective of this project is to evaluate the potential value of secretome and exosome analysis as predictive and prognostic markers using a simple and non-invasive method in patients with NSCLC at the early stage of the disease. Once specific molecular signatures are defined for each patient, better patient stratification and application of more appropriate therapies will be possible.

Secondary Objective: in parallel, the development of a 3D model based on CSCs will be pursued to recreate in vitro the pathophysiological conditions of the TME. The use of heterotypic 3D cell culture model in vitro will allow the evaluation of individualized therapies and treatment responses, as well as the identification of new potential biomarkers.

3.0 Materials and Methods

3.1.0 Proteomic analysis of plasma samples: defining procedures

3.1.1 Plasma sample collection

Two and a half milliliters of plasma were collected from four different healthy donors from 10 mL of blood in Vacutainer K2-EDTA collection tubes, blood cells were removed from plasma by centrifugation for 15 min at 1100 × g at 4 °C. The samples were maintained at 2–8°C while handling and were aliquoted into 0.5 ml fractions and stored at –80°C.

3.1.2 EV isolation from plasma

The isolation of EVs from body fluids is challenging because they are prone to contamination with non-EV proteins, lipoproteins, and high-density lipoproteins (HDL). Such contaminants interfere with obtaining pure EVs for therapeutic, diagnostic, or prognostic purposes. The various EV isolation methods can be categorized based on the physicochemical properties exploited for isolation: centrifugation-based methods, size-based isolation, affinity-based isolation, precipitation, and recently developed microfluidic techniques. Each method has advantages and disadvantages, and the choice largely depends on the intended application of EVs.

In this study, two methods were initially tested to determine the most suitable for our purpose:

- differential ultracentrifugation (DU) as described in literature [120];
- affinity-based enrichment using VN96, a synthetic peptide incorporated in the ExoSel Kit (Exosomics) [121]. This synthetic peptide binds selectively EVs from plasma due to its affinity for specific membrane proteins, particularly heat shock proteins (HSPs), which are abundant on EV surfaces. The method exploits a molecular affinity mechanism, forming stable complexes with EV surface proteins that can be easily separated from the plasma matrix, allowing rapid and reproducible isolation to enrich the EV sample. This approach was developed to be compatible with diagnostic workflows, offering reduced processing times and high yield, supporting its application in liquid biopsy for the detection of DNA, RNA, and protein biomarkers.

Plasma from three healthy donors was processed using both isolation methods, after which the resulting EV pellet was resuspended in Laemmli

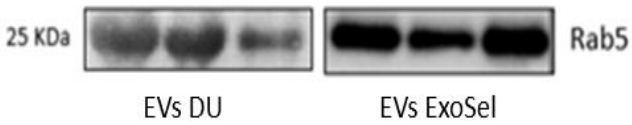

Fig.7: Western Blot analysis of EVs extracts from plasma samples with two different isolation methods: differential ultracentrifugation (DUC) or ExosSel kit from Exosomics. Probed forRab5.

buffer and analyzed by Western blot using an antibody against the EV surface marker RAB5. The results show that affinity-based EV isolation was more effective compared with DU (Fig. 7).

3.1.3 Analysis of EVs by Nanoparticle Tracking Analysis

Nanoparticle Tracking Analysis (NTA) (NanoSight NS300) is the gold standard method for assessing both concentrations and size of EVs. This method relies on measuring the characteristic movement of EVs as a function of Brownian motion [122]. Following laser illumination, the instrument records the scattered light produced by individual particles, allowing the software to calculate their hydrodynamic diameter through the Stokes-Einstein equation,

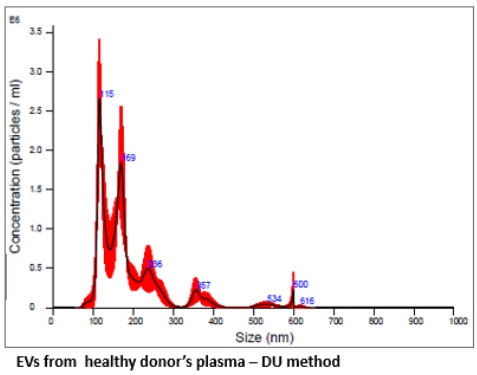

EVs from healthy donor's plasma – DU method
Mode: 115.0 nm
Concentration: 1.55e+08 particles/ml

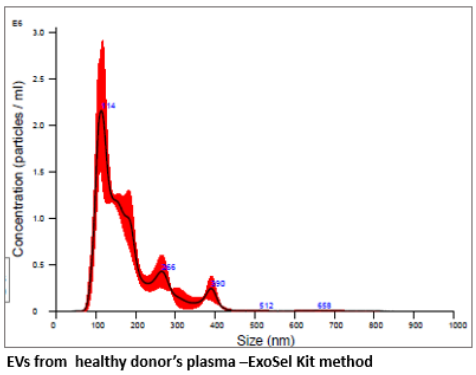

EVs from healthy donor's plasma –ExoSel Kit method
Mode: 113,6 nm
Concentration: 1,97e+08 particles/m

Figure 8: NTA analysis shows size distribution and concentration of EVs isolated from healthy donor plasma using two different approaches: DU method and ExoSel Kit method.

together with particle tracking information. Figure 8 shows the NTA profiles of EVs isolated using the DU method and the ExoSel Kit method, respectively.

Both methods show a predominant population of particles around 115 nm, which is consistent with the expected size range of EVs. However, the EV sample obtained through the DU method displayed a more heterogeneous profile, with multiple peaks extending beyond 400 nm, suggesting the presence of larger aggregates or contaminants. In contrast, the EV sample isolated with the ExoSel Kit method yielded a more defined distribution, with fewer secondary peaks and a slightly higher concentration. These observations indicate that the ExoSel Kit provides superior enrichment and purity compared to the DU, which is particularly advantageous for downstream proteomic analyses requiring highly consistent EV populations.

3.1.4 Reduction of plasma volume: new perspectives in EV isolation

Optimizing a protocol for isolating EVs from small plasma volumes is essential when working with NSCLC patients. These patients, already in fragile clinical conditions, should not undergo invasive or excessive blood draws, as each procedure may adversely affect their health and well-being. Liquid biopsy offers a less invasive alternative to tissue biopsy, but its true clinical value depends on requiring minimal amounts of blood. Further reducing the plasma volume needed for analysis helps preserve patient comfort, minimize sampling-related risks, and increase the sustainability and feasibility of the protocol in real clinical settings, without compromising data quality. A promising approach to enhance EV purity is to combine different isolation methods to reduce contamination rate [123]. For this purpose, plasma samples collected from healthy donors were processed using different isolation methods and their combinations, to identify the most effective procedure for EV isolation and high abundant protein (HAP) depletion starting from 1 mL of plasma. These procedures are summarized in Figure 9.

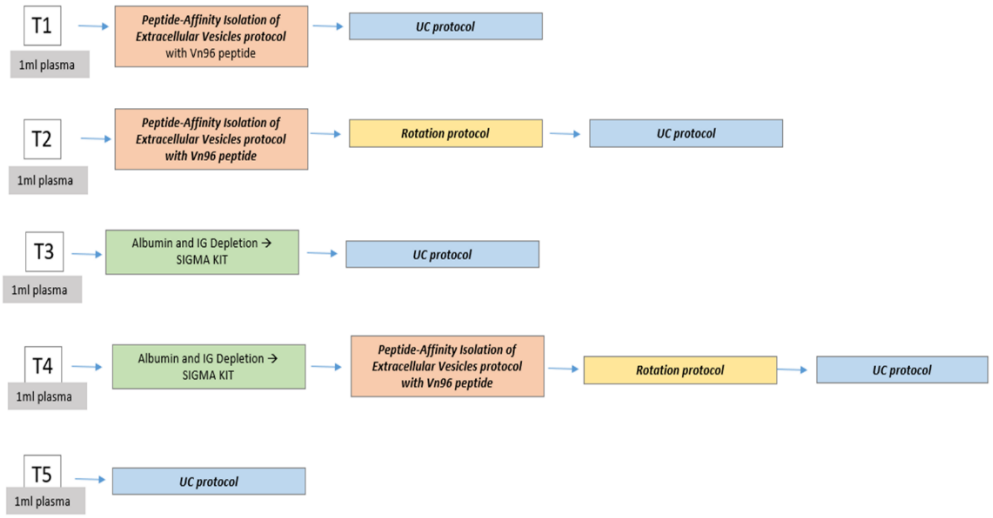

Figure 9: Schematic overview of the processing workflows tested for EV isolation from 1 ml plasma. Five protocols (T1–T5) were compared, incorporating different combinations of peptide-affinity isolation (Vn96 peptide), albumin and IgG depletion (Sigma kit), rotation protocol, and ultracentrifugation (UC protocol.)

As illustrated in Figure 10, western blot was performed to assess the suitability of the various combined isolation workflows. Lanes 4 and 5 clearly indicate that workflows T4 and T5 introduce interfering substances that fail to migrate properly through the polyacrylamide matrix.

This impaired migration renders the identification of these components unfeasible, leading to the exclusion of these workflows from further analyses. Consequently, only EVs isolated using workflows T1-T3 were characterized.

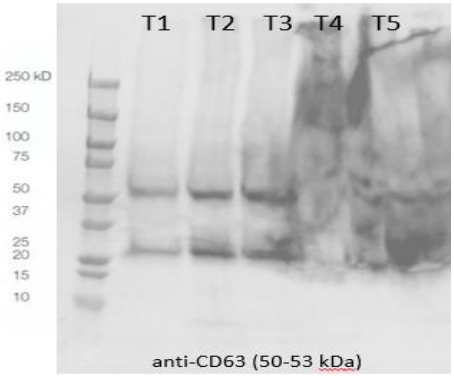

Figure 10: Western blot analysis of EVs isolated from plasma using five different protocols (T1–T5) and the anti-CD63 antibody (50–53 kDa) . Band intensities reflect variable isolation efficiency across workflows. T4 and T5 ehibited an altered signal, likely due to incomplete albumin removal from the sample and impaired electrophoretic migration. In contrast, T1-T3 workflows produced cleaner profiles, with distincts CD63 band, despite a nonpecific 25 kDa band present in all samples. Overall, T1-T3 yielded the strongest CD63 signal, suggesting superior EV recovery compared to other methods.

As shown in the Western blot in Figure 11, these three methods yielded EV preparations with clearly detectable and well-expressed markers.

.

Based on these results, workflows T1, T2, and T3 were identified as the most effective. Importantly, they allow reliable processing from a minimum starting volume of 1 mL of plasma, allocating 500 µL for proteomic analysis of plasma after HAP depletion and 500 µL for EV isolation. Efficient EV recovery from such limited limited volumes was achieved using the Vn96 peptide, which binds to heat shock proteins (HSPs) on the EV surface, enabling effective enrichment. These standardized procedures establish a robust framework for plasma processing and EV isolation for subsequent MS-based proteomic analyses.

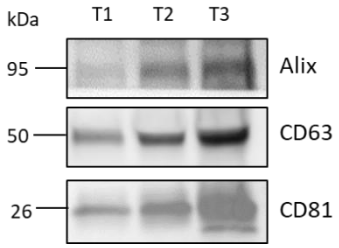

Figure 11: Western blot characterization of EVs isolated using three different protocols (T1-T3). EV markers Alix (95 kDa), CD63 (50 kDa), and CD81 (26 kDa) were detected in all samples, confirming successful isolation and enrichment of EVs across all workflows.

3.1.5 Plasma high abundant proteins (HAP) depletion

To define SOPs for MS analysis and remove HAPs, two commercial depletion kits (BioRad and Sigma Aldrich), both designed for the selective binding and simultaneous removal of albumin and IgG from plasma were used. To validate albumin and IgG depletion, protein concentration was measured by using the colorimetric 562nm bicinchoninic acid assay (BCA). Depleted plasma samples were resuspended in Laemmli sample buffer (Bio-Rad) and analyzed by SDS-PAGE followed by Coomassie Blue staining (Fig. 12).

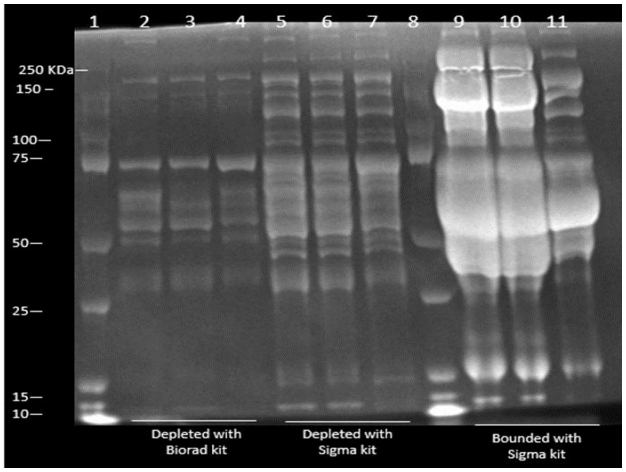

Figure 12: SDS-PAGE of human plasma protein fractions after depletion using the Aurum Serum Protein Mini Kit and PROTEOPREP columns. Lane1: Unstained Marker (10-250kDa); Lanes 2-4: Depleted plasma obtained with the Aurum Serum Protein Mini Kit; Lanes 5-7: Depleted plasma obtained with the Proteoprep; Lane 8: Unstained Marker (10-250kDa); Lanes 9-11: HAPs bound to the Proteoprep columns.

3.1.6 Sample preparation for liquid chromatography tandem mass spectrometry (LC-MS/MS)

EV protein concentration was determined by BCA, and 30 μg per sample was processed using filter aided sample preparation (FASP) [124] with 10 kDa Vivacon 500 spin filters. Briefly, proteins were reduced and free cysteine residues were alkylated to allow enzymatic digestion of the proteins by LysC and trypsin (Promega). The resulting peptides were eluted into collection tubes and acidified with formic acid (Sigma Aldrich) at a final concentration of 0.1%. Afterward, proteolytic peptides were desalted by stop-and-go extraction (STAGE) with self-packed C18 tips (Empore) [125]. Peptides were eluted with 60% acetonitrile (Sigma Aldrich) and 0.1% formic acid, dried by vacuum centrifugation, and concentrated and dissolved in 20μl of 0.1% formic acid. Final peptide concentrations were measured using NanoDrop 2000 spectrophotometer (Thermo Fisher Scientific).

3.1.7 Proteomic analysis using LC-MS/MS

A total of 1.2 µg peptide per sample was injected into a Vanquish UHPLC system (Thermo Scientific) coupled to an Exploris 480 Hybrid Quadrupole-Orbitrap mass spectrometer (Thermo Fisher Scientific). Data-independent acquisition (DIA) was used for label-free quantification (LFQ). Plasma samples was analyzed with MaxQuant (maxquant.org, Max-Planck Institute Munich). MS data were searched against the reviewed canonical *Homo sapiens* UniProt FASTA database. Protein LFQ values generated by MaxQuant were further analyzed in Perseus. Peptide and protein LFQ intensities were log_2-transformed, and proteins were retained only if detected in at least one biological replicate per group. A comprehensive list of identified proteins was also generated. When comparing the performance of the two depletion kits, Sigma Kit achieved a more efficient removal of serum albumin than the BioRad kit (Fig. 7). However, these results show minor discrepancies compared with the SDS-PAGE analysis (Fig. 13), likely reflecting methodological differences between gel-based visualization and MS-based quantification (Fig. 13).

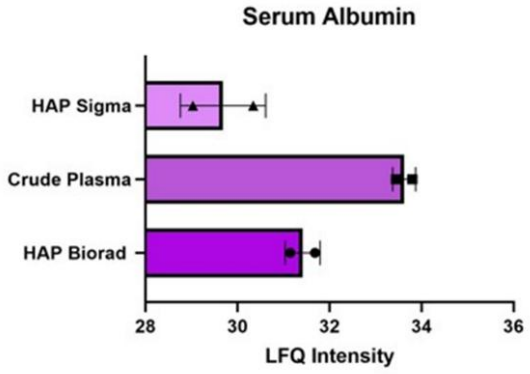

Fig 13: Serum albumin LFQ intensity detected by LC-MS/MS after depletion with BioRad or Sigma kits compared to undepleted, crude plasma.

The Venn diagram in figure 14, which represents the distribution of proteins identified across the two depletion conditions, including both shared and unique proteins, indicates that the Sigma HAP depletion kit enables the recovery of 10.4% unique proteins, compared to only 1.8% with the BioRad kit.

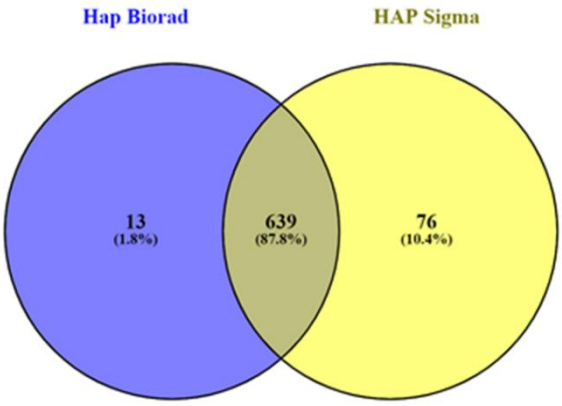

Figure 14: Venn diagram showing the distribution of plasma proteins indentified by LC-MS/MS, after depletion of high abundant proteins (HAPs) using BioRad or Sigma commercial kits, as part of SOP development for NSCLC patient plasma processing.

These findings highlight how interference from HAPs cansignificanly affect the LC-MS/MS performance and the overall protein identification. Based on these results, the Sigma kit appears to be the most appropriate option for continuing our investigations. LC-MS/MS analysis also provided insights into the subcellular localization of the proteins identified following HAP depletion (Fig. 15).

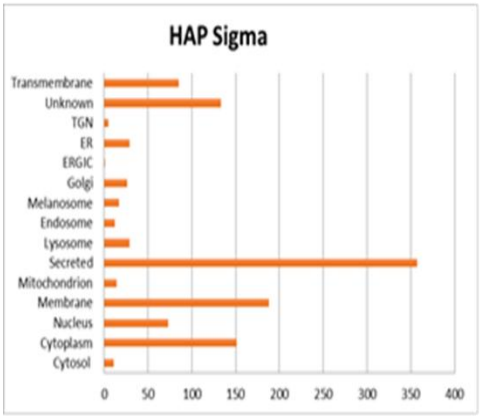

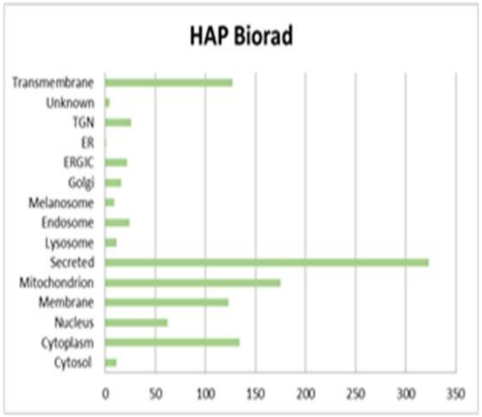

	Proteins tot	Cytosol	Cytoplasm	Nucleus	Membrane	Mitochondrion	Secreted	Lysosome	Endosome	Melanosome	Golgi	ERGIC	ER	TGN	Unknown	Transmembrane
Sigma	717	11	151	73	188	14	357	29	12	17	26	1	29	5	133	85
Biorad	654	11	134	62	123	175	11	24	323	9	16	22	1	26	4	127

Figure 15: Subcellular localization of proteins identified in plasma following depletion of HAPs using two commercial kits, Sigma and BioRad.

Additional MS analyses were subsequently performed on EVs isolated from plasma either by Differential ultracentrifugation (DU) or using the ExoSel Kit, comparing the protein profiles obtained after plasma HAP depletion with those derived from combined HAP and EV depletion by DU. As shown in figure 16, EVs isolated with the ExoSel kit yielded a substantially higher number of identified proteins compared with EVs isolated by DU.

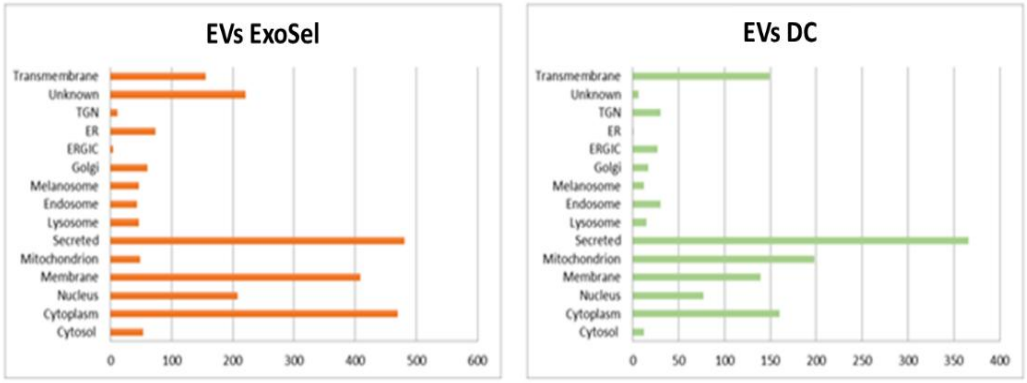

	Proteins	Cytosol	Cytoplasm	Nucleus	Membrane	Mitochondrion	Secreted	Lysosome	Endosome	Melanosome	Golgi	ERGIC	ER	TGN	Unknown	Transmembrane
Evs DU	757	12	160	77	139	198	366	15	30	12	17	27	1	30	6	149
EVs ExoSel	1352	53	470	208	408	48	481	46	43	46	60	4	73	11	221	156

Figure 16: Subcellular localization of proteins identified in EVs isolated from plasma using two different isolation methods, the ExoSel kit and differential ultracentrifugation (DU).

3.2 Exploring Plasma and EV Proteomes in Patient Samples

Plasma samples were obtained through liquid biopsies from patients diagnosed with advanced-stage NSCLC undergoing treatment at the Oncology Unit of the Policlinico of Palermo. Samples were stratified according to the time of collection, with baseline samples (P0) collected prior to treatment initiation and follow-up samples (P1) obtained at the time of radiological assessment. Furthermore, patients were grouped based on the therapeutic regimen received, including chemotherapy, immunotherapy, or combined chemo-immunotherapy. For each treatment category and time point, three plasma samples were collected, ensuring a representative distribution for comparative analyses. This sampling strategy enabled the evaluation of both plasma and EV proteome profiles across different treatment modalities and time points, providing insights into dynamic molecular changes associated with therapy

response. Starting from 5-15 ml peripheral blood was collected in tubes containing EDTA. To obtain plasma samples, the blood was centrifuged for 15 min at 1500g and stored at -80°C in aliquots until use.

Once again, in accordance with the 2023 guidelines of the ISEV, characterization of the isolated vesicles was performed using two complementary approaches: Nanoparticle Tracking Analysis (NTA) and Western blot assay. Both methods confirmed successful EV isolation, as evidenced by the clear detection of EV surface markers, CD63 and CD81, shown in Figure 17. For Western blot, 20 µg of EV protein were mixed with 4x Laemmli sample buffer, loaded on 4-15% mini-PROTEAN TGX stain-free gels, transferred using a trans-blot turbo system and visualized with the ChemiDoc Touch System (all from BioRad).

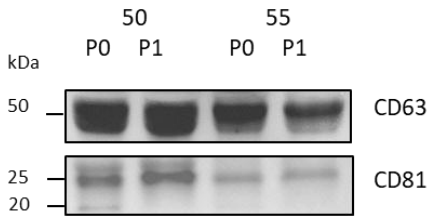

Figure 17: Rappresentative Western blot analysis of EV markers CD63 and CD81 in plasma-derived extracellular vesicles EVs isolated from two plasma patients at different times of treatment.

Primary antibodies included mouse anti-CD63 (Clone MX49; Santa Cruz) and mouse anti-CD81 (Clone: B11; Santa Cruz). After overnight incubation at 4°C, membranes were washed and incubated with an HRP-conjugated secondary antibody (Promega). Immune complexes were visualized using the Clarity Max chemiluminescence substrate (BioRad).

Plasma from the same patients was processed to remove high-abundance proteins (HAPs) using the Bio-Rad Aurum Serum Protein Kit, following the manufacturer's instructions and starting from 500 µL of plasma. Both the isolated EVs and the HAP-depleted plasma were then subjected to protein characterization using a bottom-up approach, data processing with a DIA (Data-Independent Analysis) strategy, and interpolation with protein databases for the identification of proteins present in the sample. Figure 18 summarizes the complete experimental workflow, from blood collection to LC-MS/MS analysis, using plasma from patients with advanced-stage NSCLC, collected at baseline (P0) and at the time of radiological assessment (P1). FASP protocol was performed as already mentioned.

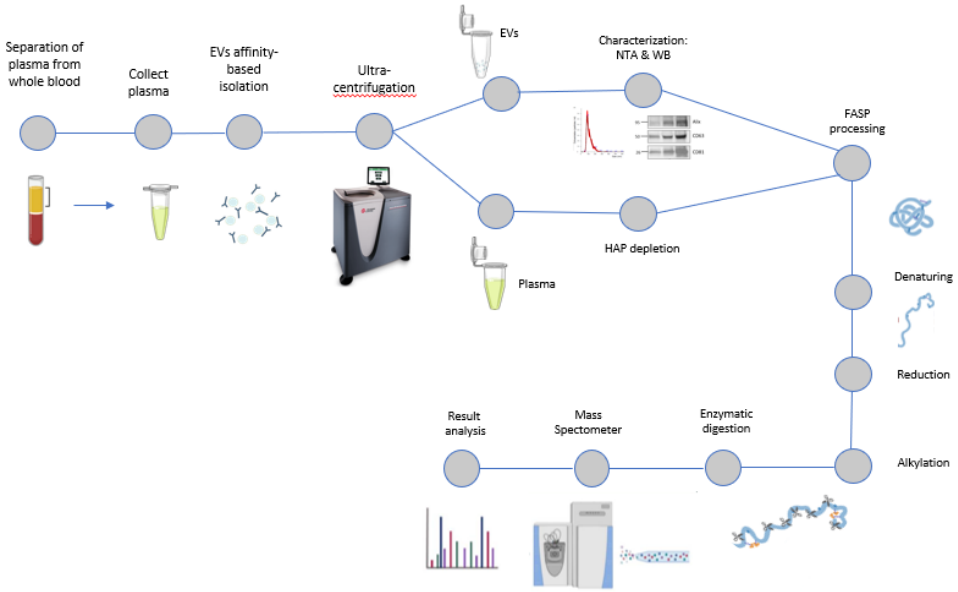

Figure 18: Workflow outlining sample processing, from patient plasma collection through EV isolation, followed by LC-MS/MS and subsequent bioinformatic data processing.

3.2.1 Mass Spectrometry

The FDR for peptide and protein identification was set at 0.01%. LFQ was used for protein quantification and analyzed with Perseus (version 1.6.15.0) [126]. LFQ values were log2 transformed, and a two-sided Student's *t* test was used to evaluate statistical changes in relative protein abundance between groups, with a significance threshold set at a *p*-value of less than 0.05. Protein groups were retained for statistical analysis only if they were quantified in at least 70% of the samples in one or more of the study groups.

Subsequently, the resulting protein lists were subjected to functional analysis using enrichment tools such as Gene Ontology (GO)[127] and KEGG [128], which enable data interpretation in terms of biological processes and molecular pathways [129]. Finally, platforms like STRING [130] allowed the construction of protein–protein interaction networks based on experimental evidence and computational predictions, providing an integrated view of the functional relationships among the identified proteins. This workflow enables the transition from spectrometric data to a biological and systemic understanding of the mechanisms involved. In the bioinformatic analyses for

this study, GO and KEGG were essential tools for interpreting the biological significance of the identified proteins. The integration of GO and KEGG in enrichment analyses thus allowed the transformation of protein lists into structured biological information, facilitating the interpretation of tumor progression mechanisms and treatment responses in NSCLC.

Principal Component Analysis (PCA), which is particularly useful in proteomics because it helps visualize sample clustering, detect outliers, and identify sources of variance across experimental groups, was performed on the proteomic data obtained and revealed substantial differences between whole plasma and EVs from NSCLC patients. PCA of plasma, figure 19, showed a marked overlap among groups, with an Adjusted Rand Index (ARI) of 0.144, indicating poor discriminative power. The dispersion of samples along the principal components suggests that the overall protein content of plasma does not provide sufficiently robust information to distinguish patient subgroups. This reduces the relevance of further investigations based exclusively on plasma, as the lack of clustering limits the possibility of identifying specific biomarkers. Conversely, EV-derived proteomes exhibited a clearer tendency to separate according to clinical groups, with an ARI of 0.305, indicative of a moderate consistency between data distribution and clinical classification. This behavior suggests that EVs preserve distinctive biological signals, likely reflecting tumor- and treatment-related molecular changes, and therefore represent a more promising matrix for patient stratification and biomarker identification. For this reason, the study proceeded by focusing on EV analysis, as EVs more effectively reflect biological differences among groups, as illustrated in the results section. They represent selective molecular microenvironments that are less influenced by systemic factors, making them ideal candidates for biomarker identification and for elucidating pathogenic mechanisms in NSCLC.

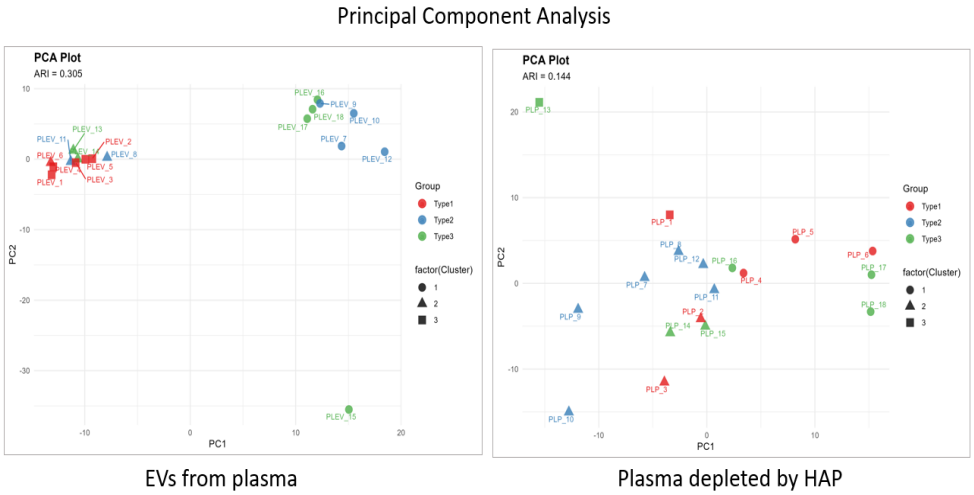

Figure 19: Principal Component Analysis (PCA) of proteomic profiles across three treatment-based experimental groups. Left panel: PCA of EVs isolated from plasma. Right panel: PCA of plasma samples depleted of high-abundance proteins (HAPs). Colors represent experimental groups, while point shapes indicate sample clustering sectors.

.

3.3.0 3D heterotypic NSCLC cell cultures for TME studies

3.3.1 Cell Lines

NSCLC-derived cell lines A549 and H460 were kndly donated by Prof. Ugo Cavallaro, Director of Unit of Gynecological Oncology Research at IEO in Milan.

A549 and H460 are two widely used cell lines serving as experimental models for the study of NSCLC, the most common form of lung cancer. The A549 cell line originates from a human lung adenocarcinoma and exhibits well-defined epithelial characteristics. It is particularly employed to investigate biological processes such as cell proliferation, drug response, and interactions with the tumor microenvironment, thanks to its ability to produce surfactant and maintain a phenotype similar to type II alveolar cells.

Conversely, the H460 cell line derives from a large-cell carcinoma and exhibits a more aggressive phenotype, with high proliferative and invasive capacity. This makes it a valuable model for studying mechanisms of tumor progression and treatment resistance. From a molecular perspective, both cell lines harbor

common mutations found in NSCLC, such as alterations in TP53 and KRAS, making them representative of clinically relevant disease subtypes.

3.3.2 Generation of Homotypic 3D cell culture and Flow Cytometry

A549 and H460 tumor cell lines were tested for the absence of mycoplasma and cultured initially in 2D cultured, using high glucose Dulbecco's Modified Eagle Medium (DMEM) and Roswell Park Memorial Institute 1640 (RPMI1640) respectively, both supplemented with 10% fetal bovine serum (HyClone) and 1% penicillin-streptomycin (Gibco). Cells were maintained at 37 °C in a humidified atmosphere with 5% CO_2 until reaching confluence and underwent one passage to recover from thawing. To allow sphere formation, cells were cultured in a serum-free DMEM-F12 medium supplemented with specific growth factors, including EGF (1 ng/µL), FGF (10 ng/µL), and B27 supplement (50X), under low-adhesion conditions. This approach enables the selection of CSCs from the bulk cancer cell population. To obtain the first generation of oncospheres (F1), tumor cells previously grown in 2D were enzymatically detached, collected, and centrifuged at 125 × g at 4 °C for 5 minutes. The resulting cell pellet was washed with sterile PBS and resuspended in complete medium. Cells (2×10^5 per well in 1.5 mL of medium) were plated in low-attachment 6-well plates, exploiting their ability to grow in suspension and form spheres (Fig. 20). The cells were incubated for four days, after which 500 µL of fresh complete medium was added, and the cultures were examined under a light microscope to verify oncosphere formation in suspension.

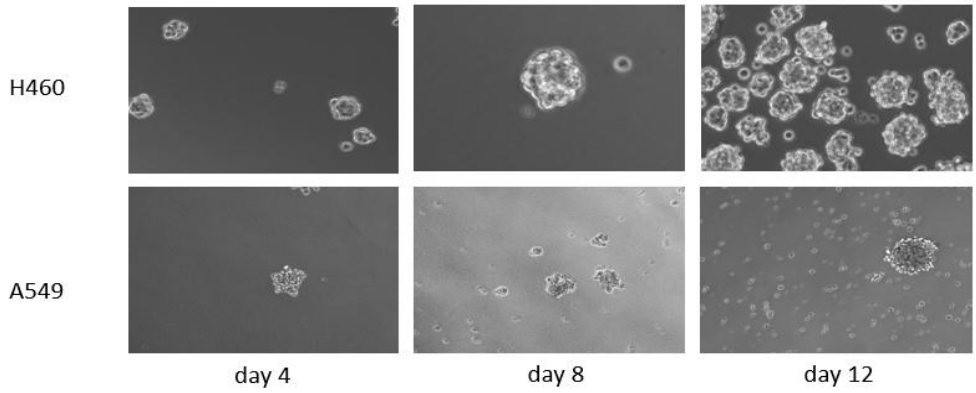

Figure 20: Morphological evolution of 3D spheroids from H460 and A549 cell lines under low-attachment conditions.

Oncospheres were collected on the eighth day of culture in ultra low-attachment (ULA) plates and dissociated both enzymatically and mechanically. The resulting single-cell suspension was then analyzed by flow cytometry to verify whether the oncospheres have been successfully selected and enriched in stem-like cells.

Under these conditions, CSCs are able to replicate and form clones that grow in suspension as spherical aggregates, whereas non-stem cancer cells fail to adhere to the flask and consequently undergo apoptosis. Upon the appearance of the first CSC clones, the supernatant containing the spheres was collected, centrifuged for 10 minutes at 800 rpm, and the pellet was subsequently dissociated using TrypLE. The oncospheres were then washed with sterile PBS and labeled with antibodies such as anti-CD44 and anti-CD133, well-known cancer stem cell markers in lung cancer [131]. Cells were incubated in the dark for 30 minutes, washed with PBS, and analyzed by flow cytometry (BD FACSDiva 9.0). The results, shown in Figure 21, indicate positivity for stemness markers such as CD44 and CD133, which are also associated with increased tumorigenic potential. The expression of CD44 is significantly correlated with early-stage lung adenocarcinoma and with mutations in the epidermal growth factor receptor (EGFR)[132 133].

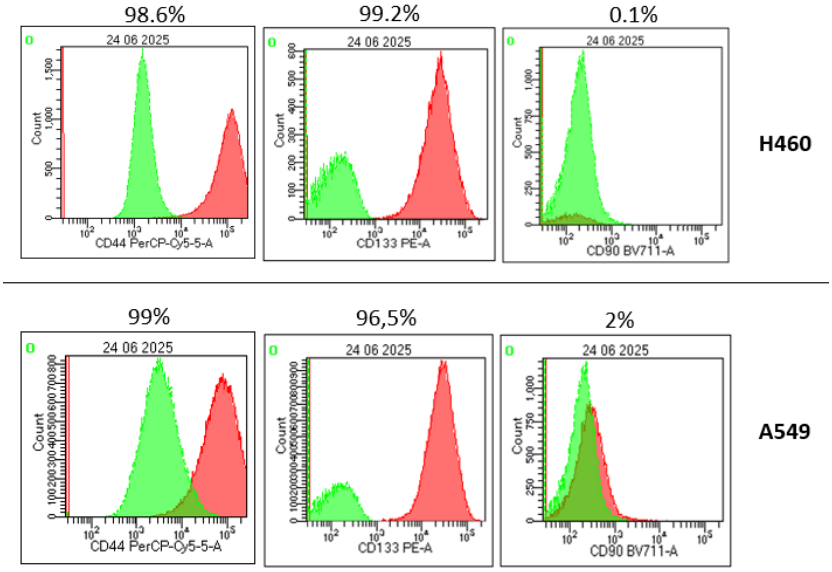

Figure 21 : Characterization of CSCs by flow cytometry analysis using a panel of stemness markers. Red peaks represent markers positive cells, green peaks indicate unstained controls

.

These markers have different structures and functions but are closely associated with stemness potential and the uncontrolled proliferation of

cancer cells [133]. CD44 is a biomarker expressed not only in solid tumors but also in hematological malignancies. Its expression is associated with increased proliferation, self-renewal, and metastasis. In other studies, CD44^high/CD133^high cells have shown enhanced tumorigenic capacity [134]. Compared to CD44^low/CD133^low cells, those with high CD44 and CD133 expression exhibited more stem cell-related genes and demonstrated greater tumorigenic potential.

Furthermore, the absence of CD90, a marker characteristic of fibroblasts from various species and tissues and proposed as a CAF marker [135], confirms the non-fibroblast nature of H460 cells. To better simulate the TME, MRC5 cell line was also used. MRC5 are a diploid cell derived from fetal lung fibroblasts, which are commonly used as feeder cells and to maintain stem cells in an undifferentiated state. Therefore, these cells were also characterized by flow cytometry, confirming their fibroblastic identity through high CD90 expression (fig. 22).

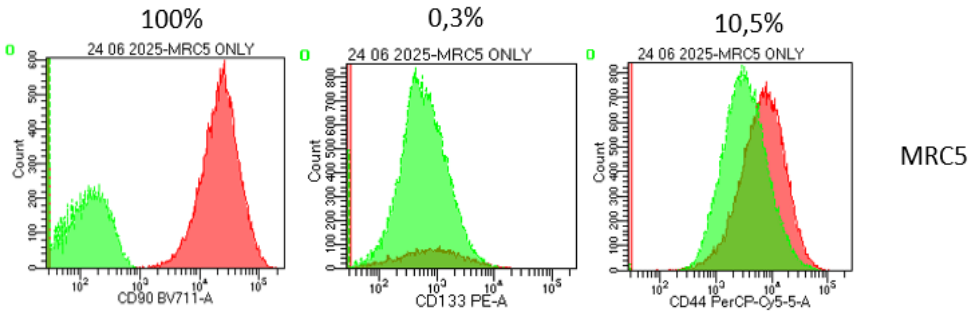

Figure 22: Marker expression in MRC5 cells. Flow cytometry histograms show high CD90 positivity in fibroblasts. Red peaks represent markers positive cells, green peaks indicate unstained controls.

3.3.3 Tumor cells expressing GFP or RFP through lentiviral transfection

To identify the relationships between cell types within the 3D co-cultures by fluorescence, third-generation lentiviral vectors (LV-GFP and LV-RFP) were used to transduce either Green Fluorescent Protein (GFP) or Red Fluorescent Protein (RFP). Both cell lines, H460 and A549, previously cultured in 2D, were infected with the indicated lentiviral vectors.

Lentiviral particles were produced in human embryonic kidney HEK 293T cells. Approximately six million cells were seeded in 100 mm plates to reach about 70% confluence. The following day, each plate was co-transfected with the plasmid of interest and the lentiviral packaging plasmids in appropriate

proportions. In this system, one plasmid (LV-GFP, ~7500 bp) encodes the EGFP gene under a strong promoter, enabling green fluorescent protein expression for cell tracking.

The second plasmid (LV-RFP, ~7539 bp) carries the mCherry gene, which encodes a red fluorescent protein enabling stable expression of red fluorescent protein (Fig. 23). Two hours before transfection, the culture medium was replaced with fresh medium containing serum but without antibiotics, and a transduction-enhancing compound was added to enhance viral production.

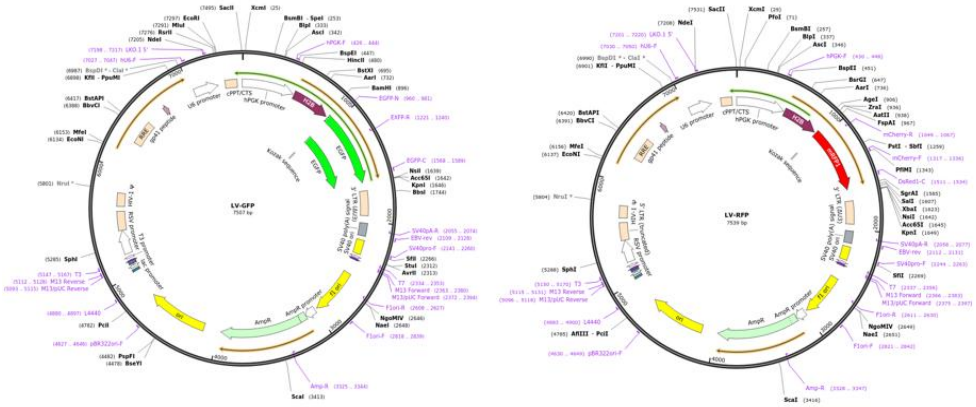

Figure 23: Lentiviral vector maps showing the organization of key genetic elements, including promoters, selection markers, and regulatory sequences.

DNA mixes were prepared using a transfection reagent at a 1:3 ratio (DNA: reagent), incubated at room temperature for 20 minutes, and then added to the cells. The day after transfection, the medium was replaced with fresh complete medium. After 48 and 72 hours, the supernatant containing lentiviral particles was collected, centrifuged, and filtered. Aliquots were then stored at -80 °C until use.

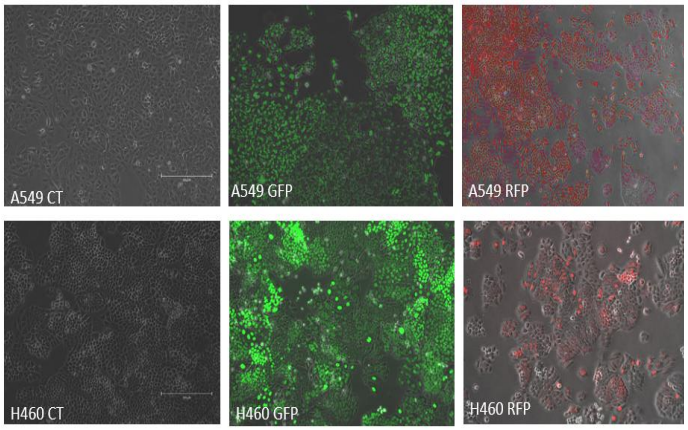

Figure 24: Lentiviral transfection of A549 and H460 cells in 2D culture. Representative images show control cells (CT), GFP-expressing cells (green), and RFP-expressing cells (red) after lentiviral transduction. A549 (top row) and H460 (bottom row) exhibit robust fluorescence signal, confirming efficient lentiviral transduction and stable transgene expression.

To perform the infection with the produced lentiviral particles, each cell line of interest was seeded in 6-well plates at a concentration of 2.5 x 10^5 cells per well. The next day, cells were infected with the lentiviral particles using different virus concentrations at a final volume of 1.5 mL per well (Fig. 24).

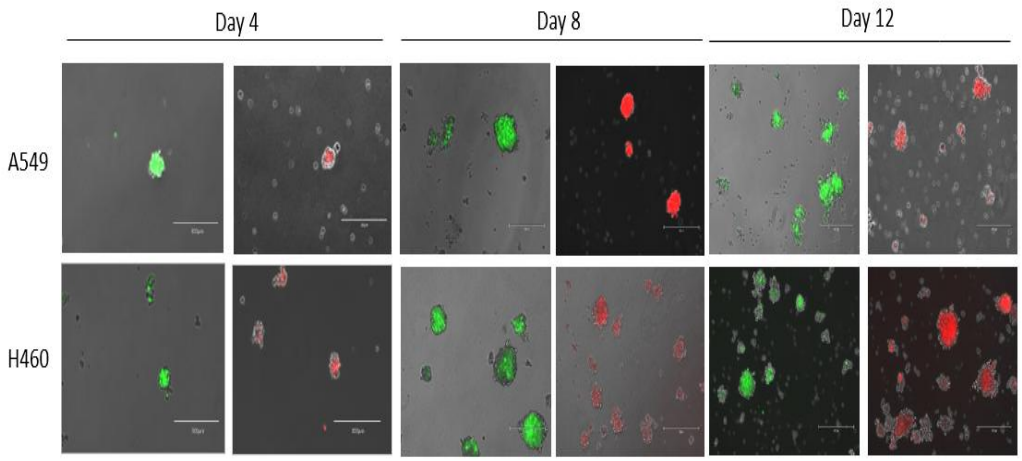

Figure 25: Lentiviral transduction of A549 and H460 cells forming oncospheres in 3D culture. Representative images at Day 4, Day 8, and Day 12 show GFP-expressing (green) and RFP-expressing (red) oncospheres. Both cell lines maintain stable fluorescence signals over time, confirming efficient lentiviral integration and transgene expression during spheroid growth.

Subsequently, the selection process was repeated to allow the cells to grow as oncospheres, following the previously described protocol. The images in figure 25 clearly show that both lentiviral vectors successfully integrated into both cell lines, A549 and H460, without affecting their capacity to form spheroids.

3.3.4 Volumetric analysis of oncospheres

For further characterization of the spheroids, the area of each oncosphere was measured on days 4, 8, and 12 after seeding in low-attachment plates, and their volume was calculated in mm^3. We observed an increase in size and diameter of the spheroids over time for all cell lines, both those treated with lentivirus and those untreated. By day 12, there appeared to be a slowdown in volumetric growth, although the trend continued even after lentiviral transduction (Fig. 26)

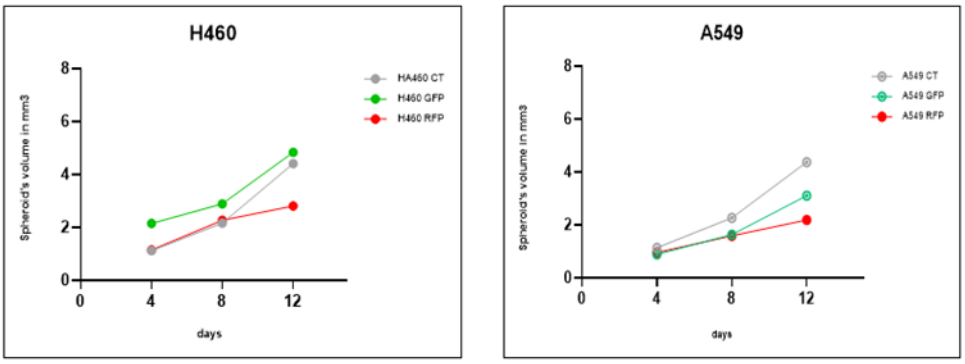

Figure 26: Measurement of spheroid volume at days 4, 7, and 12 for H460 (left) and A549 (right) cell lines. Growth curves compare control (CT, gray), GFP-expressing (green), and RFP-expressing (red) spheroids.

Moreover, assessing PD-L1 expression in tumor spheroids is essential because this immunomodulatory ligand enables neoplastic cells to evade immune surveillance through interaction with PD-1 on T cells. Analyzing it first in 2D and then in 3D allows us to highlight how microenvironment complexity influences its regulation: 2D models provide a controlled and simplified condition, whereas 3D spheroids reproduce oxygen, nutrient, and paracrine signaling gradients typical of in vivo tumors, which can increase or modulate PD-L1 expression. This characterization is crucial for designing heterotypic co-cultures so a flow cytometry was performed and results are showed in fig. 27.

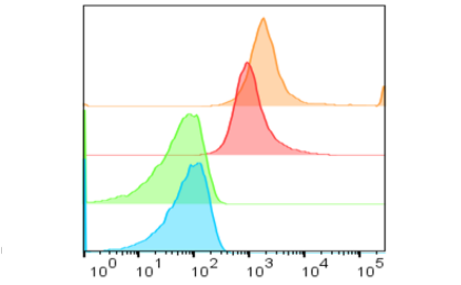

	Sample Name	PD-L1 (CD274)
	A549 2D	97%
	A549 3D	99%
	A549 2D Unstain	0.3%
	A549 3D Unstain	0.1%

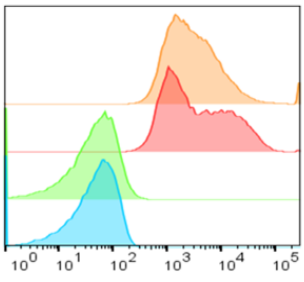

	Sample Name	PD-L1 (CD274)
	H460 2D	99.2%
	H460 3D	99.4%
	H460 2D Unstain	0.1%
	H460 3D Unstain	0.1%

Figure 27: Flow cytometry analysis of PD-L1 (CD274) expression in A549 and H460 tumor cell lines cultured under 2D and 3D conditions.

Flow cytometry analysis shows PD-L1 (CD274) expression in the tumor cell lines A549 and H460, cultured under 2D (red) and 3D (orange) conditions, with unstained controls correctly included to define the background.

The comparison reveals that both cell lines express PD-L1 at very high levels, regardless of the culture type. However, the transition from 2D to 3D results in a marginal but consistent increase (approximately 1–2%), suggesting that three-dimensional culture may further enhance PD-L1 expression, likely due to microenvironmental factors such as hypoxia and nutrient gradients. This finding is biologically relevant because it confirms that 3D models better reproduce in vivo conditions and could influence immune response and the effectiveness of immune checkpoint therapies.

3.3.5 Generation of Heterotypic Spheroids

The TME generally consists of irregularly formed tumor vessels, ECM, cancer-associated fibroblasts (CAF), and immune cells [135]. It interacts with cancer cells via paracrine signalling and cell-to-cell contact mechanisms, allowing growth factors, cytokines and chemokines, ECM proteins and EVs to promote tumor formation [136]. The proportion of cancer cells and non-cancer cells varies interindividually and intraindividually during disease progression [137,138]. Previous studies have demonstrated a crucial impact of fibroblasts and CAFs in proliferation and the initial steps of ovarian cancer metastasis by secreting cytokines and chemokines. Despite this importance of CAFs in tumour behaviour, little is currently known about how cancer cells convert normal fibroblasts into CAFs. Through the release of soluble factors, CAFs actively promote tumour progression by stimulating survival, proliferation, and invasion. Paracrine signalling between cancer cells and fibroblasts showed mutual proliferative stimulation and the induction of drug resistance. Therefore, in the development and analysis of new tumour models, consideration of the microenvironment is essential to better represent the in vivo situation and to better assess the long-term effects of anti-cancer drugs. In recent years, there have been numerous ideas to improve the development of in vitro tumour models. One approach is to create 3D multicellular tumour spheroids with physiological properties that are similar to in vivo tumour tissue and TME for efficient drug screening and successful drug development [139, 140].

Traditional spheroid culturing using exclusively tumour cells is now extended to co-culturing cancer cells with fibroblasts. More in vivo-like properties were observed for co-culture models, strongly supporting their usefulness as preclinical tumour models for drug screening and TME interactions [141,142]. Therefore, the MRC-5 fibroblasts cell line was chosen. MRC5 were first cultured in 2D in complete DMEM medium and subsequently, like the other cell lines, grown as spheroids using the same culture medium enriched with growth factors and without FBS serum. To enable traceability of MRC5 fibroblasts within the 3D heterotypic model, MRC5 cells were transduced with a lentiviral vector encoding the GFP (Fig. 1B), as previously done for tumor cells using lentiviral plasmids. Just like the cancer cells, fibroblasts also formed stable spheroids in monoculture and were subsequently seeded in co-culture with the oncospheres from both cell lines.

To better mimic the immune component of the tumor microenvironment, peripheral blood mononuclear cells (PBMCs) isolated from healthy donor blood were incorporated into this in vitro model. PBMCs are a heterogeneous population of different cell types found in peripheral blood. They include monocytes, lymphocytes (B cells, T cells), and Natural Killer (NK) cells, and may also comprise dendritic cells and differentiated macrophages. In humans, the frequency of these populations varies among individuals, but generally lymphocytes account for 70–90%, monocytes for 10–20%, while dendritic cells are rare, representing only 1–2% [143].

PBMCs are widely used in biomedical research, translational studies, and clinical applications, where they serve to evaluate the efficacy of immunomodulatory treatments, support vaccine development, and assist in pharmacological screening. For this study, PBMCs were isolated from the blood of three healthy donors for subsequent in vitro experiments using Lympholyte-H, a density gradient medium specifically designed to isolate viable lymphocytes and monocytes from human peripheral blood. After centrifugation at 700 × g for 30 minutes without brake, distinct layers were observed: plasma at the top, an opalescent white ring containing PBMCs, the Lympholyte-H layer, and at the bottom, the erythrocyte and polymorphonuclear cell fraction. PBMCs were labeled with CellTrace™ Violet (Thermo Fisher Scientific) (Fig. 28C), a fluorescent dye primarily designed for tracking cell proliferation, but also used in fluorescence microscopy with a readout at 450 nm. The three cell lines were initially cultured separately under spheroid conditions, then dissociated, counted, and combined in co-culture at

a ratio of cancer cells: fibroblasts: PBMCs of 5:3:2. Fluorescence imaging using the EVOS microscope enabled detection of the signal from each cell line. The corresponding images, including those from individual cultures and the heterotypic co-culture, are presented in the Results section (Fig. 28).

3.3.6 Protocol for TME 3D-model

The in vitro TME model was established as follows:

Spheroid formation:

- Tumor cells (A549 or H460) were seeded at 100,000 cells per well together with 60,000 MRC5 fibroblasts in 6-well Ultra-Low Attachment (ULA) plates using serum-free oncosphere medium.
- Cultures were maintained at 37 °C with 5% CO_2 for 4 days, monitoring spheroid formation by phase-contrast or fluorescence microscopy.

PBMC preparation:

- Peripheral blood mononuclear cells (PBMCs), after gradient isolation and washing, were stimulated with IL-2 (10 U/mL) for 24 h in RPMI-1640 medium. Subsequently, $CD8^+$ T cells were activated by incubation for 48 h with anti-CD3 (1 µg/mL) and anti-CD28 (1 µg/mL) in RPMI-1640 supplemented with IL-2.

Co-culture assembly:

- On day 5, PBMCs were added to the cancer cell–fibroblast spheroids and incubated for 24 h.

Drug treatments:

- The following conditions were applied:

  Chemotherapy: Carboplatin (50 µM)

  Immunotherapy: Pembrolizumab (anti–PD-1 monoclonal antibody) (10 µg/mL)

  Chemo-immunotherapy: Pembrolizumab + carboplatin + pemetrexed (10 µg/mL + 100 µg/mL + 10 µM)

Before treatment, 50% of the culture medium was replaced with fresh medium containing the drugs. Each experimental condition included a heterotypic co-culture control.

Culture maintenance:

- Spheroids were maintained for 8 days, with IL-2 supplementation every 48 h.

At the end of the 8-day period, spheroids were dissociated and analyzed by flow cytometry using lineage-specific markers: CD45 for PBMCs, CD90 for MRC5 fibroblasts, and CD44 for cancer cells (A549 or H460). After dissociation and washing, cells were analyzed using a FACSCelesta™ flow cytometer (Becton Dickinson). The gating strategy included FSC/SSC selection, doublet exclusion (FSC-A vs. FSC-H), and viability assessment using 7-AAD (Becton Dickinson). To evaluate CD4+ T and CD8+ T maturation status, the lymphocyte component was analyzed in all 3D culture conditions. Specifically, the maturation status (naïve, central memory (CM); effector memory (EM); terminal effector memory (TEM) of CD4+ and CD8+ cells was analyzed and compared to the control lymphocytes. We phenotyped T cells using a panel of markers that distinguish lymphocyte cell subsets in T helper CD4+ or cytotossic T CD8+. In detail, we analyzed the CD4+ T cells' differentiation states using different marker combinations, CD4+ naïve (CD45+CD62L+), CD4+ CM (CD45RA- CD62L+), CD4+ EM (CD45RA- CD62L-), and CD4+ TEM (CD45RA+ CD62L-). Same panel of markers was used to evaluate CD8+ naïve (CD45+CD62L+), CD8+ CM (CD45RA- CD62L+), CD8+ EM (CD45RA- CD62L-), and CD8+ TEM (CD45RA+ CD62L-). Data were analyzed with FlowJo software (FlowJo LLC, Ashland, OR, United States), with fluorescence intensity and marker expression evaluated relative to isotype controls. Flow cytometry analysis and evaluations are shown in results session.

4.0 Results

4.1.0 Impact of standard therapies on a 3D Heterotypic Model Mimicking the NSCLC TME

The EVOS inverted microscope, equipped with fluorescent filters, enabled visualization of the 3D cultures of individual spheroids for each cell line, as well as the heterotypic co-culture, in which the interaction among the three cell lines and the formation of 3D structures are clearly evident. The panel in Figure 28 provides a representative overview of these results.

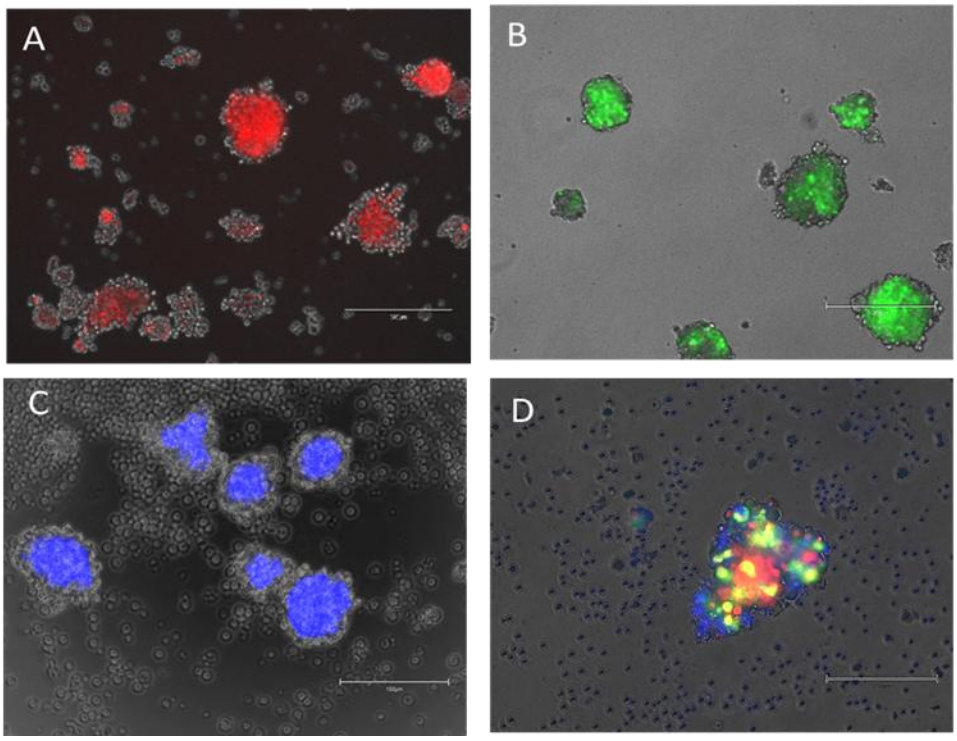

Figure 28: 3D heterotypic co-culture. A) Cancer cell oncospheres (H460) expressing RFP; B) MRC5 fibroblast spheroids expressing GFP; C) PBMC spheroids labeled with Cell Trace Violet (CTV); D) Heterotypic spheroid formed from the co-culture, after 24h, of the three previously labeled cell lines.

The heterotypic co-cultures, set up accordingly, were further exposed to the most commonly used therapeutic agents in accordance with international NSCLC treatment guidelines, namely chemotherapy, immunotherapy, and combined chemo-immunotherapy, as previously described in the Materials and Methods section.

Flow cytometry analysis of heterotypic 3D spheroid models derived from NSCLC cell lines (H460 and A549) highlights distinct responses to chemo, immuno, and combined chemo-immunotherapy, are shown in figures 29 and

30. Cell mortality remained low (<13%) across all treatments, consistent with the inherent drug resistance conferred by 3D culture systems. Notably, A549 spheroids exhibited the lowest mortality under immunotherapy (2.9%), confirmed that anti–PD-1 treatment primarily induces immunomodulatory rather than direct cytotoxic effects [144]. Immunotherapy significantly increased CD45+ immune cell proliferation in both models (≈35-40%), whereas the chemo-immuno combination diminished these levels (8-13%), reflecting chemotherapy-induced PBMC toxicity. Remarkably, immunotherapy led to near-complete fibroblast depletion (CD90+, 0.3-0.4%), conferming potent immune-mediated stromal remodeling, while chemotherapy alone or in combination left fibroblast levels largely stable [145].

Crucially, both cell lines showed a reduction in tumor stem-like cells (CD44+) following immunotherapy, with effects more pronounced in A549 (15.1%) than H460 cells (23.3%), whereas the chemo-immunotherapy regimen failed to further decrease this population (≈31–36%). This suggests that anti–PD-1 therapy preferentially targets aggressive subpopulations, while chemotherapy alone or in combination lacks such selectivity [146].

Our findings are consistent with emerging evidence that immune-checkpoint blockade primarily remodels the TME, enhancing T cell infiltration, depleting stromal support, and reducing stem-like phenotypes, rather than inducing widespread cytotoxicity. This is in line with preclinical spheroid studies reporting similar immune-stromal reprogramming and with clinical data demonstrating improved outcomes when checkpoint inhibitors modulate both the TME and tumor cells [147].

The low overall mortality underscores the physiological relevance of 3D models, suggesting that additional functional endpoints, such as immune-cell activation, cytokine production, ECM remodeling, and invasion metrics, are required to fully evaluate therapeutic efficacy [148].

Finally, the differential responses between H460 and A549 spheroids, particularly in immune infiltration and retention of $CD44^+$ cells under combination therapy, in support of literature examining genetic drivers of immunotherapy resistance, such as KEAP1 and SMARCA4 mutations, point to the need for model-specific strategies. These data underscore the complexity

of TME interactions and reinforce that model selection is critical for translational relevance.

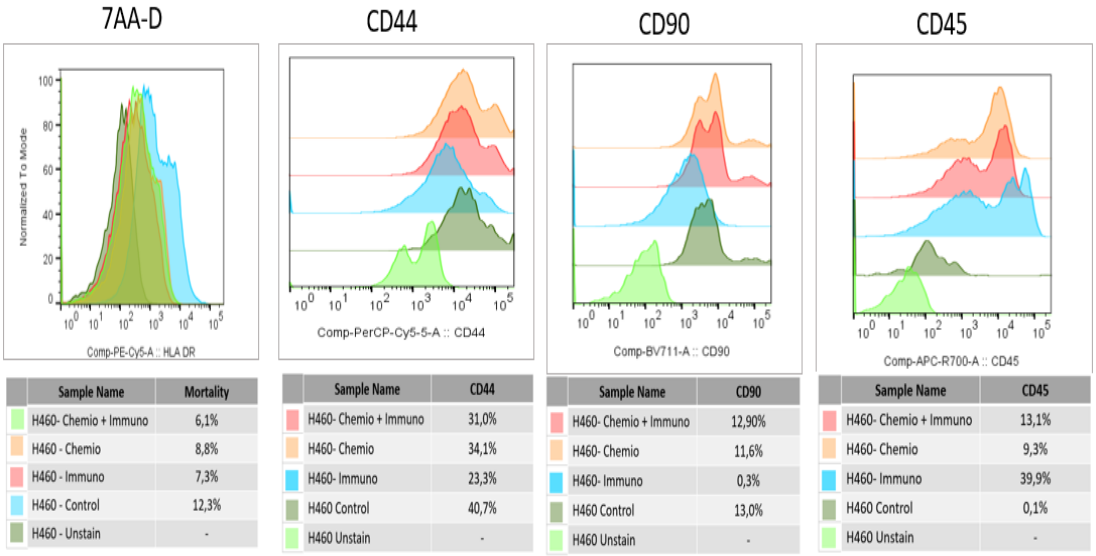

Sample Name	Mortality
H460- Chemio + Immuno	6,1%
H460 - Chemio	8,8%
H460 - Immuno	7,3%
H460 - Control	12,3%
H460 - Unstain	-

Sample Name	CD44
H460- Chemio + Immuno	31,0%
H460- Chemio	34,1%
H460- Immuno	23,3%
H460 Control	40,7%
H460 Unstain	-

Sample Name	CD90
H460- Chemio + Immuno	12,90%
H460- Chemio	11,6%
H460- Immuno	0,3%
H460 Control	13,0%
H460 Unstain	-

Sample Name	CD45
H460- Chemio + Immuno	13,1%
H460- Chemio	9,3%
H460- Immuno	39,9%
H460 Control	0,1%
H460 Unstain	-

Figure 29: Flow cytometry profiles of H460 heterotypic 3D spheroids under different treatment conditions.

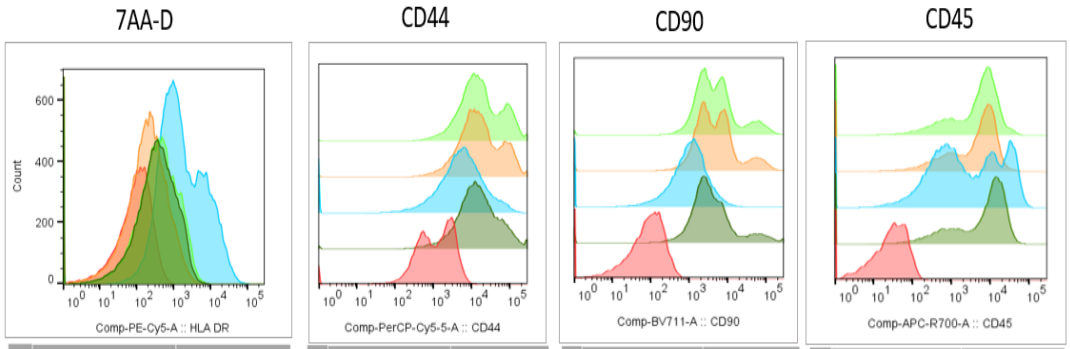

Sample Name	Mortality
A549- Chemio + Immuno	5,2%
A549 - Chemio	7,6%
A549 - Immuno	2,9%
A549 - Control	10,4%
A549 - Unstain	-

Sample Name	CD44
A549- Chemio + Immuno	35,6%
A549 - Chemio	35,8%
A549 - Immuno	15,1%
A549 - Control	37,4%
A549 - Unstain	-

Sample Name	CD90
A549- Chemio + Immuno	16,3%
A549 - Chemio	17,9%
A549 - Immuno	0,4%
A549 - Control	15,6%
A549 - Unstain	-

Sample Name	CD45
A549- Chemio + Immuno	8,6%
A549 - Chemio	9,6%
A549 - Immuno	35,3%
A549 - Control	17,4%
A549 - Unstain	-

Figure 30: Flow cytometry profiles of A549 heterotypic 3D spheroids under different treatment conditions.

In summary, our results demonstrate that anti–PD-1 immunotherapy effectively remodels the TME within 3D NSCLC spheroids, targeting immune and stromal components as well as stem-like cancer populations. In contrast, combinating anti-PD-1 with standard chemotherapy did not improve cytotoxicity or enhance TME modulation, suggesting that simple additive regimens may not provide benefit in this context. Future works should focus on optimizing combination treatment strategies by adjusting dosing, sequencing and timing, and applying advanced profiling technologies such as spatial transcriptomics and single-cell analyses to dissect cellular heterogenicity and uncover mechanisms of therapeutic resistance [149].

In conclusion, the heterotypic 3D NSCLC model developed in this study represents a physiologically relevant and versatile platform for exploring multiple dimensions of the TME. By integrating cancer cells, fibroblasts, and immune components, this system enables comprehensive evaluation of therapeutic effects beyond cytotoxicity, including stromal remodeling, immune cell dynamics, the persistence of stem-like populations, and biomarker discovery. Its complexity and resemblance to in vivo conditions make it a powerful tool for preclinical research, offering opportunities to investigate drug resistance mechanisms, optimize combinatorial strategies, and advance translational approaches in NSCLC.

4.2.0 LC-MS/MS proteomic bioinformatic analysis of EVs

As previously mentioned, since the PCA analysis did not yield data of interest for the in-depth study of EV-depleted plasma, the investigation focused on the protein content derived from the analysis of EVs isolated from patient plasma, following the procedures described in the Materials and Methods section. The analysis of the isolated EVs revealed differential expression and the logarithmic value of the p-value (-LOG (p-value)) between patients at time point P0 and those at P1, as shown in the volcano plot in Figure 31.

The volcano plot displays proteins significantly expressed in P0 patients in blue; proteins significantly expressed in P1 patients in red; and proteins with no significant variation in gray. Overall, this analysis identified a total of 418 proteins, of which 65 were more highly expressed in EVs from P1 patients (red), and 43 were more highly expressed in P0 patients (blue).

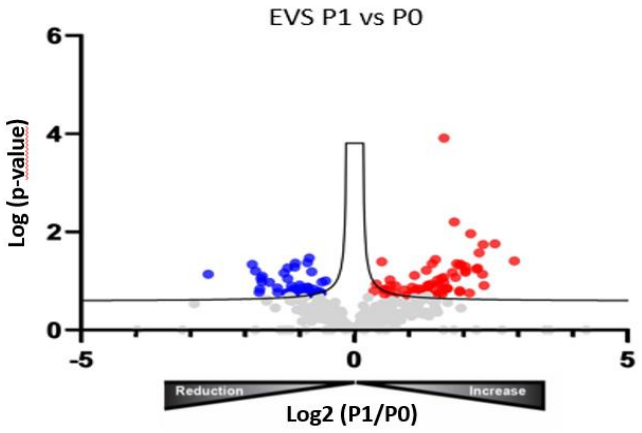

Figure 31: Volcano plot showing differential expression of EV proteins between groups P1 (in red) and P0 (in blue). Proteins that do not reach statistical significance are shown in gray.

4.2.1 Protein expression analysis in EVs from patients at P0 and P1

To explore the molecular heterogeneity associated with different therapeutic regimens in NSCLC, protein expression profiles in EVs were analyzed at two time points: P0 (baseline, pre-treatment plasma) and P1 (post-treatment plasma collected at the time of radiological assessment). Samples were stratified according to treatment type, chemotherapy (CHEMIO), immunotherapy (IMMUNO), and chemo-immunotherapy (CHEMIO-IMMUNO), based on current NSCLC treatment guidelines. To visualize the distribution and overlap of EV proteins among the groups, two Venn diagrams were generated (Fig. 32), representing protein profile at P0 and P1, respectively. These diagrams are useful in identifying both unique and shared elements among the therapeutic groups, aiding the discovery of potential biomarkers and providing insights into the mechanisms of treatment response. For clarity, P0 refers to baseline protein profile, while P1 refers to post-treatment protein profile (plasma collected at the time of radiological assessment).

The P0 Venn diagram reveals a notable heterogeneity in protein contents across the three groups. The CHEMIO-IMMUNO P0 group exhibited the highest number of unique elements (97), followed by IMMUNO P0 with 78exclusive elements, whereas CHEMIO P0 displayed only 11 exclusive elements; furthermore, the overlap among all three sets is limited (11 elements). This suggests that in EV protein expression, initially, distinct pathways are active with limited molecular convergence, which could complicate patient stratification in the early phase.

The intersection between CHEMIO-IMMUNO P0 and IMMUNO P0 included 54 shared elements, suggesting a strong similarity between these two patient groups even before treatment initiation. These findings underline the intrinsic biological heterogeneity of NSCLC prior to therapy and suggests that unique EV signatures in the IMMUNO and CHEMIO-IMMUNO groups may be harnessed to stratify patients or predict responsiveness to specific therapeutic strategies.

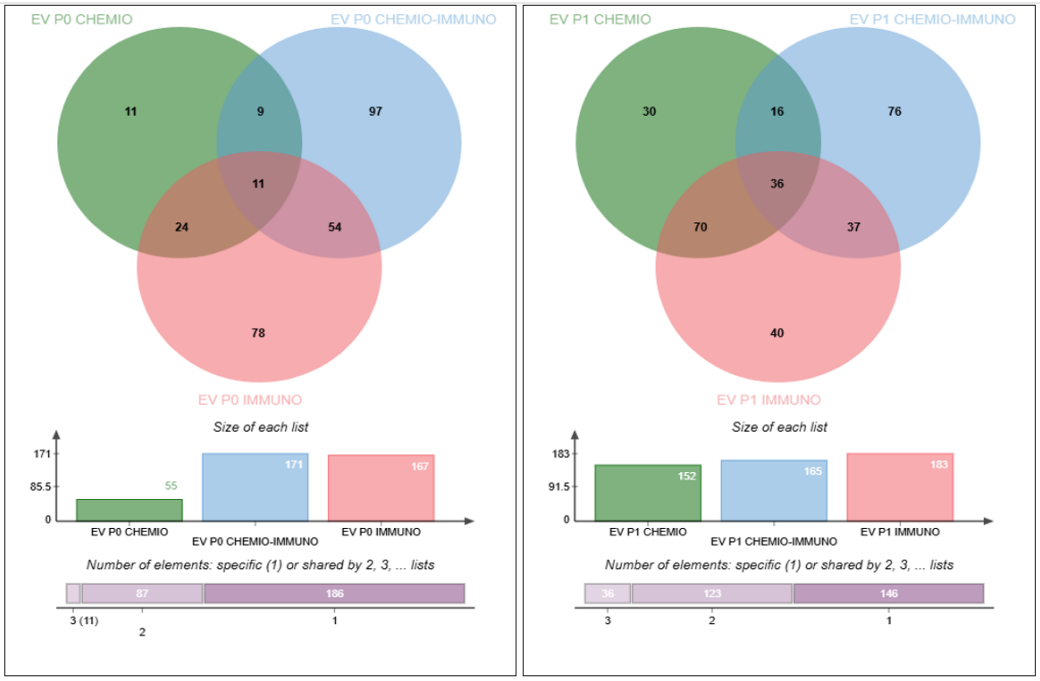

Figure 32: Venn diagrams and numerical distribution of elements identified in samples P0 (XA) and P1 (XB) for the three treatment groups: CHEMO (green), CHEMO-IMMUNO (blue), and IMMUNO (pink). The diagrams show the number of exclusive and shared elements among the groups, while the bar charts report the total size of each set. The bottom bar indicates the distribution of elements specific to one list (1) or shared by two or three lists.

The P1 Venn diagram further highlights the heterogeneity in EV expression following treatment. Here, the CHEMIO P1 group demonstrated the highest number of unique elements (30), indicating a distinctive proteomic reprogramming in response to chemotherapy. IMMUNO P1 and CHEMIO-IMMUNO P1 groups showed 40 and 76 exclusive proteins, respectively. A significant finding is the large intersection (70 proteins) between IMMUNO P1 and CHEMIO P1, suggesting a progressive integration of biological mechanisms. Notably, 36 proteins were shared across all three treatment groups at P1, representing a central post-treatment EV signature, possibly

associated with common mechanisms of response or regulation across treatment modalities.

In the P1 phase, following exposure to treatment, a significant increase in overlap among the groups is observed: the triple intersection rises from 11 to 36 elements, and pairwise overlaps also expand (e.g., CHEMIO–IMMUNO from 24 to 70). This convergence indicates a progressive integration of biological mechanisms induced by therapy, likely related to cellular adaptation phenomena, metabolic stress, or cross-talk between immune and chemotherapeutic pathways. Furthermore, the reduction in exclusive elements and the more balanced size of the sets in P1 reflect a more coordinated and less heterogeneous response compared to the pre-treatment phase.

Three main trends emerge from this analysis: (i) an increase in shared elements post-treatment, suggesting a reduction in initial specificity and greater molecular interaction; (ii) a decrease in exclusive elements, indicative of a more uniform response across groups; (iii) persistence of a substantial overlap between IMMUNO and CHEMO-IMMUNO, both before and after therapy, supporting the existence of a shared immune-related molecular program throughout the treatment course. These observations highlight the potential value of both unique and shared EV proteins as biomarkers of response and resistance, and as functional indicators of treatment-induced molecular dynamics.

To identify biologically and clinically relevant proteins within the shared subsets, a detailed analysis was performed on the proteins commons to all three treatment groups at both P1 and P0.

These proteins were cross-referenced with data from the Human Protein Atlas (HPA), an open-access, high-resolution resource that maps the expression and localization of human proteins in tissues, cells, and organelles. The HPA database integrates multiple data types, including immunohistochemistry, immunofluorescence, RNA-seq, and proteomics, providing insights into protein function, spatial distribution, and associations with normal and tumor tissues. It includes specific annotations for various cancers, including NSCLC, making it

a valuable tool for spatial proteomics and biomarker discovery [150]. Two lists (Table 1) summarize the proteins identified as common to all three therapeutic groups at P0 and P1, respectively, and indicate their known association with cancer prognosis based on HPA annotations. This integrative strategy supports the identification of candidate biomarkers for response prediction, disease monitoring, and future therapeutic targeting in NSCLC patients.

	Gene	tipo di cancro correlato
Proteins in EVs at P0	CDH5	Kidney renal clear cell carcinoma, Kidney renal papillary cell carcinoma
	SLC2A1	Kidney chromophobe, Kidney renal papillary cell carcinoma, Liver hepatocellular carcinoma, Lung adenocarcinoma, Pancreatic adenocarcinoma
	LTF	Kidney renal clear cell carcinoma, Liver hepatocellular carcinoma
	TFRC	ervical squamous cell carcinoma and endocervical adenocarcinoma, Glioblastoma multiforme, Kidney chromophobe, Liver hepatocellular carcinoma, Lung squamous cell carcinoma
	SERPINA5	Glioblastoma multiforme, Kidney renal clear cell carcinoma, Lung squamous cell carcinoma
	SELENOP	Kidney renal clear cell carcinoma, Lung adenocarcinoma
	S100A8	Glioblastoma multiforme
	SERPINA10	Liver hepatocellular carcinoma, Pancreatic adenocarcinoma, Stomach adenocarcinoma
	APOA1	Pancreatic adenocarcinoma

	Gene	tipo di cancro correlato
Proteins in EVs at P1	MASP2	Liver hepatocellular carcinoma
	APOC4	Liver hepatocellular carcinoma
	APOC2	Kidney renal clear cell carcinoma, Liver hepatocellular carcinoma
	STOM	Kidney chromophobe, Kidney renal clear cell carcinoma, Kidney renal papillary cell carcinoma
	PROS1	Cervical squamous cell carcinoma and endocervical adenocarcinoma, Kidney renal clear cell carcinoma, Stomach adenocarcinoma
	EFEMP1	Kidney renal clear cell carcinoma, Kidney renal papillary cell carcinoma
	FGL1	Kidney renal clear cell carcinoma, Stomach adenocarcinoma
	LBP	Kidney renal clear cell carcinoma, Kidney renal papillary

Table 1: Proteins shared across all three treatment groups (chemotherapy, immunotherapy and chemo-immunotherapy), identified at baseline (P0 highlighets in blue) and post-treatment (P1, highlighted in red), and previously reported as potential tumor biomarkers. The correlatio with specific cancer types was determined using data from The Human Protein Atlas database.

4.2.2 Bioinformatic Tools for Pathway and Network Interpretation

To support the functional interpretation of EV proteomics, additional bioinformatic analyses were performed using Enrichr and STRING. Enrichr is an enrichment tool that enables the identification of associations between gene lists and biological pathways, diseases, or experimental datasets, providing a statistical overview of the most significant perturbations [151,152]. In this study, Enrich was applied to analyze a list of genes derived from shared EV protein subsets, using both GO categories and KEGG pathways to identity biological processes and molecular functions, potentially involved in common

mechanisms of treatment response. STRING, on the other hand, is a platform dedicated to constructing protein-protein interaction networks based on experimental evidence, computational predictions, and co-expression data, which is useful for understanding functional relationships among proteins [153].

4.2.3 Overlap of EV Profiles Between Treatment Groups and Stages

Enrichment analysis of proteins shared across all three treatment groups at P0 revealed significant functional terms in particular, the GO Biological Process category (Fig. 33A) highlighted enriched pathways such as blood coagulation, lipid metabolism, and response to external stimuli; in parallel, the GO Molecular Function analysis (Fig. 33B) identified key functions including lipid-binding activity, endopeptidase inhibition, and coagulation emerge. These findings suggest that shared baseline EV proteins may be involved in host defence, hemostasis, and inflammatory regulation, processes frequently associated with tumor progression and systemic effects in NSCLC. The protein interaction map using STRING (Fig. 33C) revealed a well-defined functional module, centered around APOH, HPX, APCS, PLG, C9, and FCN3. These proteins are primarily involved in complement cascade and coagulation [154,155].

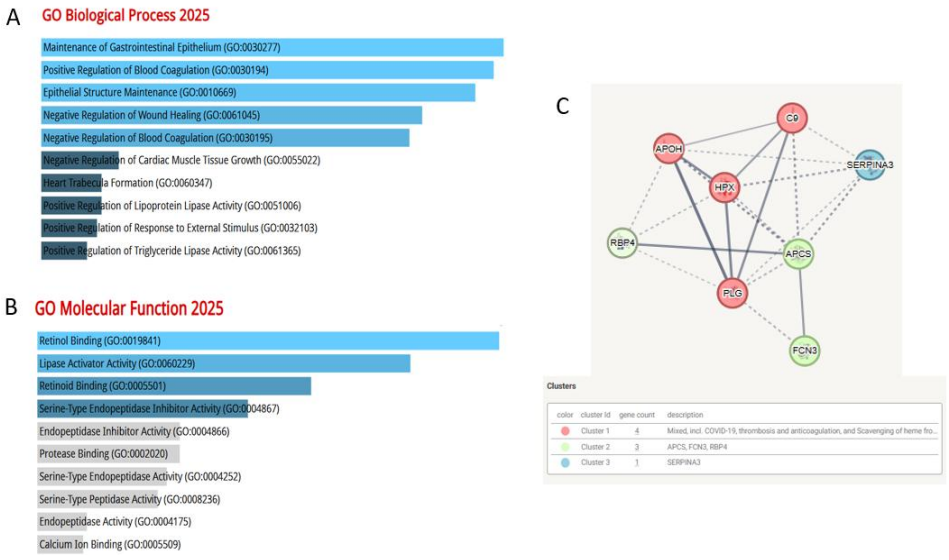

Figure 33: Functional enrichment analysis of EV proteins across all three treatment groups at basaseline (P0).(A) GO Biological Processes and (B) GO Molecular Functions associated with the identified EV proteins. (C) Protein–protein interaction network generated using STRING, showing functional clusters among shared EV proteins.

Among the ten EV proteins common to all treatment groups (RBP4, APOH, HPX, APCS, SERPINA3, PLG, IGHG1, C9, IGHG4, FCN3, IGKV1-27) [156], several show strong functional and clinical relevance in cancer biology, particularly in NSCLC:

- SERPINA3: it belongs to the serine protease inhibitor superfamily. Its downregulation in tumors has been linked to cell growth and invasiveness. In preclinical models, SERPINA 3 increases sensitivity to osimertinib,a third-generation EGFR inhibitor [157-159].
- Retinol-binding protein 4 (RBP4): although not NSCLC-specific, has been associated with poor survival in papillary renal carcinoma and mesothelioma. Furthermore, RBP4 emerged as an independent prognostic marker in hepatocellular carcinoma and pancreatic adenocarcinoma [160].
- APOH (β2-glycoprotein I): it participates in coagulation/inflammation complexes [161], often altered in cancer patients.
- PLG, HPX, and C9: members of the complement/coagulation cascade. All of which are involved in TME modulation in EV NSCLC models [162]. Moreover, GO and KEGG analyses show significant enrichment for “complement/coagulation” and “cholesterol metabolism” [163].

Consistent with early findings, the integrated dataset continues to support a central role for the complement system and related immune/coagulation pathways in NSCLC. Proteins such as SERPINA3, RBP4, and APOH/PLG/HPX were identified across all treatment groups. Because these proteins appear consistently and have supportive from both the HPA database and studies on tumor-derived EVs, they could emerge as candidate biomarkers for NSCLC detection or monitoring.

Regarding the proteins commonly expressed by patients at P1, the GO charts (Fig. 34A) highlight strong enrichment in processes related to “intermediate filament organization” and “supramolecular structure assembly”. These findings ar consistent with the presence of several keratins (KRT2, KRT4, KRT10, KRT13, KRT77, KRT78), as wells as proteins such as Filaggrin-2 (FLG2) and Hornerin (HRNR). These proteins are typically associated with skin functionality and regeneration, reflecting the epithelial origin of the tumor. Additionally, the analyses revealed activation of immune and coagulation pathways (Complement Activation, Lectin Pathway), involving proteins such as MASP1, FCN2, and COLEC11. Their presence suggests a role for EVs in modulating both the TME and systemic immune responses, potentially contributing to immune evasion or inflammation associated with NSCLC progression.

In figure 34B, molecular functions identified through Enrichr, including endopeptidase activity, calcium binding, cholesterol transfer activity, indicate the involvement of both plasma proteins (APOA2, CETP, AHSG) and metabolic enzymes (TXN, ENO1, GAPDH, CAT), associated with oxidative stress and lipid metabolism, processes known to influence tumor progression and response to immunotherapy in NSCLC.

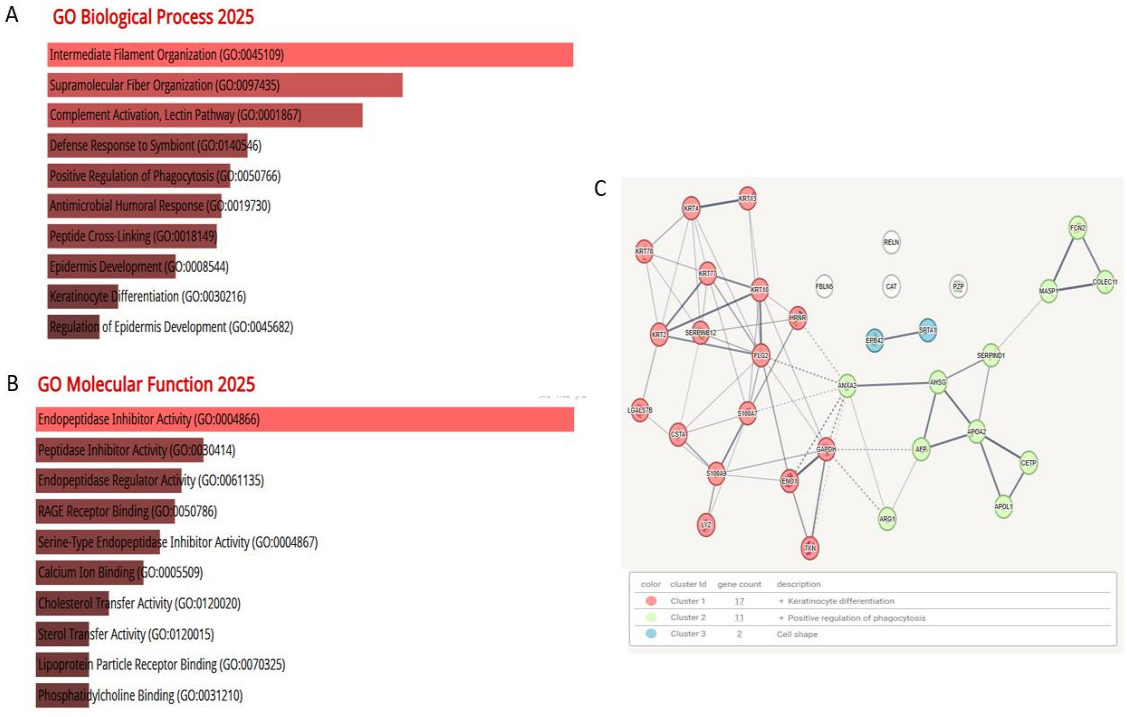

Figure 34: Functional enrichment analysis of EV proteins shared to all three treatments at P1. (A) GO Biological Processes and (B) GO Molecular Functions associated with the identified EV proteins. (C) Protein–protein interaction network generated using STRING, highlighting functional clusters among the shared EV proteins.

The STRING network (Fig. 34C) confirms this organization into functional clusters: an epithelial cluster (keratins and structural proteins), an immune cluster (ANXA2, ARG1, MASP1, FCN2), and a metabolic cluster (ENO1, TXN, GAPDH). Some central nodes, such as ANXA2, AFP, ENO1, S100A7/A9, and ARG1, are already described in the literature as biomarkers or mediators of aggressiveness and immunomodulation in NSCLC. Specifically:

- Annexin A2 (ANXA2) is a calcium-dependent phospholipid-binding protein that regulates cell growth [164,165]. ANXA2 is involved in various pathophysiological processes, including epithelial-to-mesenchymal transition (EMT), fibrinolysis, and resistance to anticancer drugs [166,167].
- α-fetoprotein (AFP) is a well-known marker for hepatocellular carcinoma but is also present in advanced lung cancer contexts [168].
- α-Enolase (ENO1) is a multifunctional oncoprotein. Its glycolytic function deregulates cellular energy, supports tumor proliferation, and inhibits apoptosis. ENO1 also evades growth suppressors and helps tumors escape immune destruction. Furthermore, ENO1 relocates to the cell surface and acts as a plasminogen receptor, promoting tumor invasion and metastasis by inducing angiogenesis [169].
- S100A7 and S100A9 proteins are involved in cancer by promoting tumor growth and metastasis through mechanisms such as cell proliferation, migration, and invasion, often by activating inflammatory pathways and recruiting immune cells [170].
- ARG1, the enzyme arginase 1, is a well-known modulator of the immune microenvironment and an emerging target for combination with checkpoint inhibitors. Neutrophils infiltrating NSCLC appear to release ARG1, which inhibits T-cell proliferation by degrading extracellular arginine [171]. This phenomenon seems to contribute to local immune suppression, and possible vaccines to combine with ICI-based immunotherapies are already under investigation [172].

In summary, these findings support the hypothesis that plasma EVs capture not only the epithelial origin of the tumor, but also the systemic immunomodulation and metabolic adaptations induced by therapy. Together, these observations position plasma EVs as dynamic biomarkers of the TME for monitoring immunotherapy response in NSCLC.

4.2.4 Exclusive EV Protein Profiles in the Immunotherapy Group at Baseline (P0) and Post-Treatment (P1)

The analysis of proteins contained in EVs isolated from plasma of NSCLC patients at baseline (P0), prior to immunotherapy, reveals a complex molecular profile reflecting both the epithelial origin of the tumor and systemic processes of immune and metabolic regulation. GO enrichment charts (Fig. 35A) show strong representation of processes such as “intermediate filament organization” and “supramolecular structure assembly”, consistent with the presence of multiple keratins (KRT) and adhesion proteins (DSP, DSC1, JUP), indicating maintenance of epithelial characteristics and structural integrity. In parallel, enrichment for coagulation and complement pathways (F7, F8, F9, F10, F12, F13A1, SERPINC1, SERPINA1, SERPINA5, SERPINA10, SERPINF1, C6, C8G, CFH, CFI) emerges, associated with modulation of inflammation and the TME, features known to influence progression and response to immunotherapy in NSCLC.

The GO molecular functions (Fig. 35B) include calcium and metal binding, endopeptidase activity, and serine protease inhibitor activity, suggesting an active role for EVs in proteolytic regulation and tissue remodelling.
The STRING network highlights well-defined functional clusters: an epithelial cluster (keratins and junction proteins), an immune-coagulative cluster (complement factors and serpins), and a metabolic-antioxidant cluster (PRDX, PKM, IGF2).
Several central nodes, such as APOA1, LTF, IGF2, S100A8/A11, SELENOP (Fig. 34C) have been already described in the literature as biomarkers or mediators of aggressiveness and immunomodulation in NSCLC. In details:

- Apolipoprotein A1 (APOA1), involved in lipid metabolism and inflammation regulation, has been associated with tumor prognosis and immune response. Reduced serum ApoA-I levels correlate with progression of lung, liver, breast, kidney, endometrial, and cervical cancers, and with metastasis development [173].
- Lactoferrin (LTF), a protein with immunomodulatory activity, is reported as a modulator of the TME [174] and has been shown to effectively block migration and/or invasion in a wide range of tumor cell models, making it a potential molecular target in NSCLC [175].

- IGF2, an insulin-like growth factor, is associated with cell proliferation, invasiveness, and therapeutic resistance in lung carcinoma. Through IGF2, lung cancer cells activate fibroblasts into CAFs, which in turn stimulate tumor cell migration and invasion via the AKT/NF-κB pathway [176].
- S100A8 and S100A11, members of the calcium-binding S100 protein family, are associated with immunosuppression and tumor progression. S100A8, involved in cancer-related inflammation, has been linked to multiple malignancies, including breast, colorectal, leukemia, cutaneous squamous cell carcinoma, laryngeal, hepatocellular, head and neck, and bladder cancers; its overexpression correlates with poor overall and progression-free survival in solid tumors [177,178]. S100A11 is primarily associated with breast, ovarian, and pancreatic cancers [179];
- SELENOP is the major selenium transport protein in plasma, and its circulating levels reflect systemic selenium availability [180,181]. Low SELENOP expression in tumors or plasma correlates with poor overall survival in several cancers, including lung adenocarcinoma (LUAD) and hepatocellular carcinoma. Conversely, abnormal SELENOP activity can promote colorectal cancer progression via WNT signaling [182]. In NSCLC, SELENOP supports tumor resilience by maintaining redox homeostasis and selenium supply; its expression inversely correlates with immune-exhausted microenvironments, and restoring SELENOP may enhance anti-tumor immunity by modulating oxidative stress and immune cell function [183].

- Peroxiredoxin-6 (PRDX6), an antioxidant enzyme, is frequently present in various tumors and can promote proliferation, migration, and invasion of A549 cells, making it a potential molecular target for further study [184].

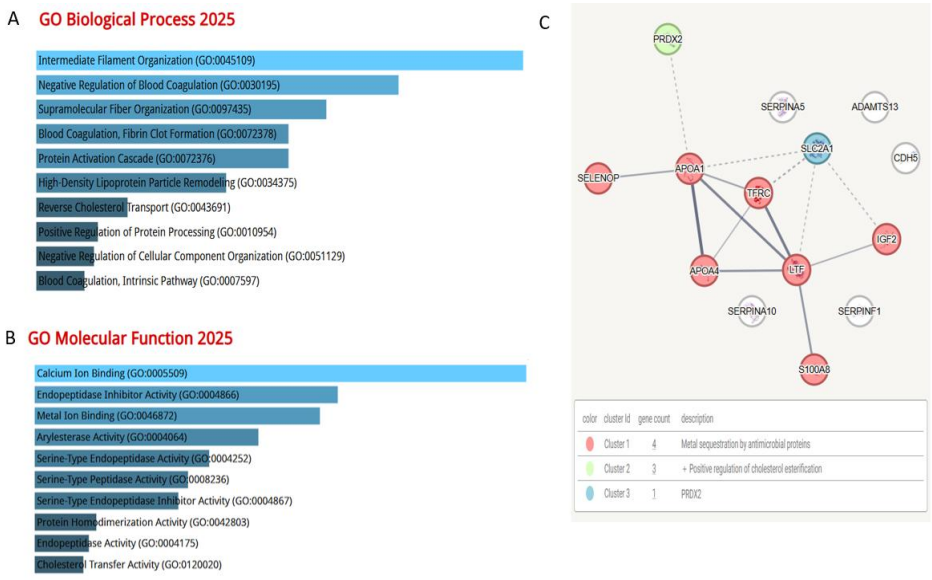

Figure 35: Functional enrichment analysis of EV proteins from the IMMUNO group at P0.

Beyond these clusters, the presence of variable immunoglobulins (IGHV, IGKV, IGLV) and proteins such as PIGR (Polymeric Immunoglobulin Receptor) and CLEC3B (Tetranectin) suggests that EVs contribute in transporting immune components and may participate in immune communication. Notably, high CLEC3B levels have been recently associated with favorable prognosis in NSCLC [184].

In summary, these data indicate that plasma EVs at baseline in NSCLC patients eligible for immunotherapy are not mere reflections of the tumor but instead carriers of complex signals integrating epithelial differentiation, immune modulation, lipid metabolism, and stress response: Together, these features position EVs as dynamic and informative biomarkers with sgrong potential for predicting therapeutic response and improving patient stratification in immunotherapy-based treatment strategies.

After the first cycle of immunotherapy (P1), the analysis of proteins contained in extracellular vesicles (EVs) isolated from plasma reveals a molecular profile of interest for studying the impact of therapy on the TME and the immune system. The GO diagramm shows enrichment (Fig. 36A) in processes such as positive regulation of protein maturation, plasminogen activation, and coagulation and complement cascades. These findings are consistent with the presence of proteins including F13A1 [185], F7 [186], F12 [187], SERPIN's family with members C1, A1 and F1 [188], all of wich known for their roles in inflammation modulation and tumor progression. The GO molecular functions in figure 36B highlight enrichments in calcium and metal ion binding, endopeptidase activity, and serine protease inhibitor activity, suggesting that EV proteome reflects proteolytic and immune remodeling induced by therapy.

The STRING network highlights distinct functional clusters (Fig. 35C):

- Coagulation–immune cluster: coagulation factors (F7, F12, F13A1) and complement regulators (C6, CFH, CFI) interact with serpins (SERPINA1, SERPINC1, SERPINF1), indicating a functional axis linking hemostasis, inflammation and innate immunity.
- Metabolic–antioxidant cluster: proteins such as PKM (glycolytic enzyme) and PRDX6 (peroxiredoxin) suggest mechanisms that support tumor survival under oxidative stress and may contribute to treatment resistance.
- Immunomodulatory cluster: Variable immunoglobulins (IGHV, IGKV, IGLV), and immune-related proteins such as CLEC3B and CLEC11A suggest a role for EVs in immune component transport and in mediating intercellular immune communication [189].

Among central nodes, IGF2 is associated with proliferation and therapeutic resistance in NSCLC, while S100A11, a pro-inflammatory protein, is linked to tumor progression and immunosuppression. Plasma proteins such as APOA1 and AZGP1 further reflect the interplay between lipid metabolism, inflammation and immune response, both of which with prognostic implications.

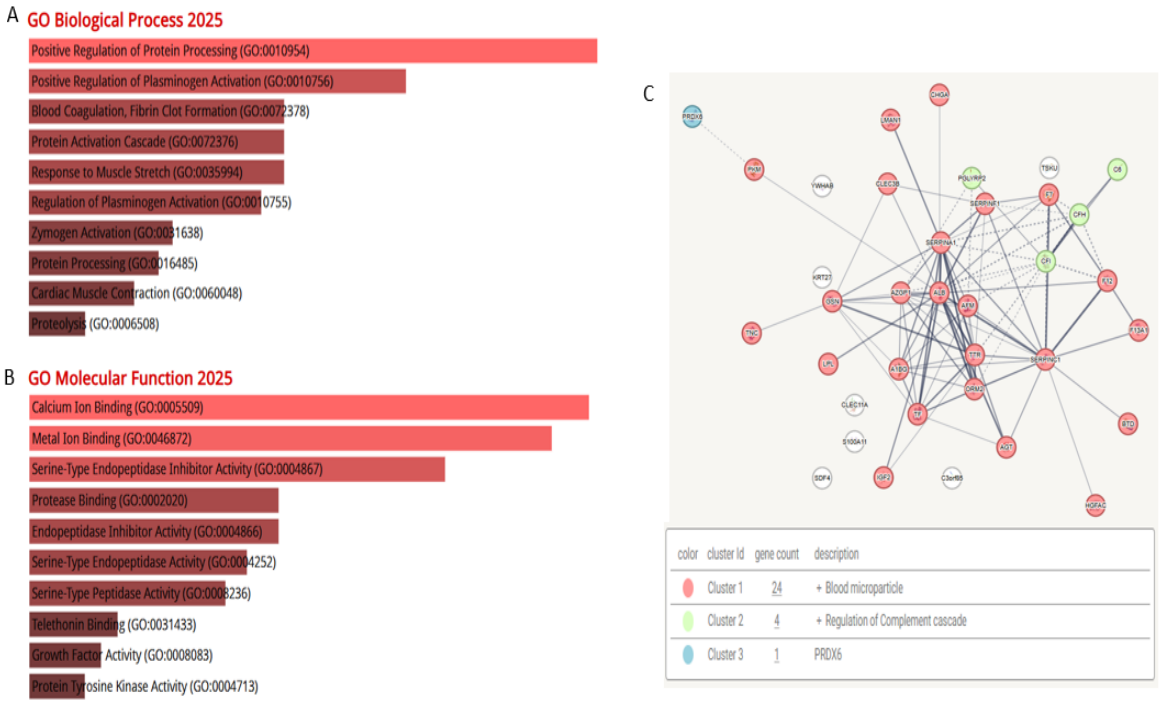

Figure 36: Functional enrichment analysis of EV proteins expressed exclusively in the IMMUNO group at P1.

A comparison between EVs at baseline (P0) and post-treatment (P1) in NSCLC patients reveals significant functional shift associated with the initiation of immunotherapy. At P0, GO enrichment in processes related to intermediate filament organization, lipid metabolism regulation, and activation of complement and coagulation cascades, suggests a procoagulant and structural remodelling EV phenotype.

Following immunotherapy (P1), GO enrichment analysis indicates an accentuation of coagulation and proteolytic processes, with molecular functions such as serine protease inhibition, calcium and metal ion binding. These changes suggest that immunotherapy not only modulates immune reprogramming but also reshapes the TME through enhanced hemostatic and protease-inhibitory processes.

4.2.5 Analysis of proteins expressed exclusively in the Chemo-Immuno group at P0 and P1

The analysis of EVs at baseline (P0) in NSCLC patients scheduled to receive chemo-immunotherapy reveals a complex molecular profile, characterized by biological processes and molecular functions that reflect both the epithelial origin of the tumor and a systemic predisposition to inflammatory and metabolic responses. The GO Biological Process enrichment (Fig. 37A) indicates involvement in heterochromatin formation, intermediate filament organization, negative regulation of gene expression, and activation of complement and coagulation cascades. These findings are consistent with the presence of structural proteins, such as numerous keratins, junctional proteins (DSP, DSC1, JUP), multiple coagulation factors (F7, F8, F9, F10, F12, F13A1), and complement regulators (C1S, C6, C8G). Collectively, this enrichment indicates a procoagulant and inflammatory baseline state, known to favor tumor progression and metastasis formation in NSCLC patients [190,191].

Complemeting these findings, the GO Molecular Function analysis highlights terms related to calcium and metal ion binding, endopeptidase activity, and serine protease inhibition. These functions are consistent with the presence of

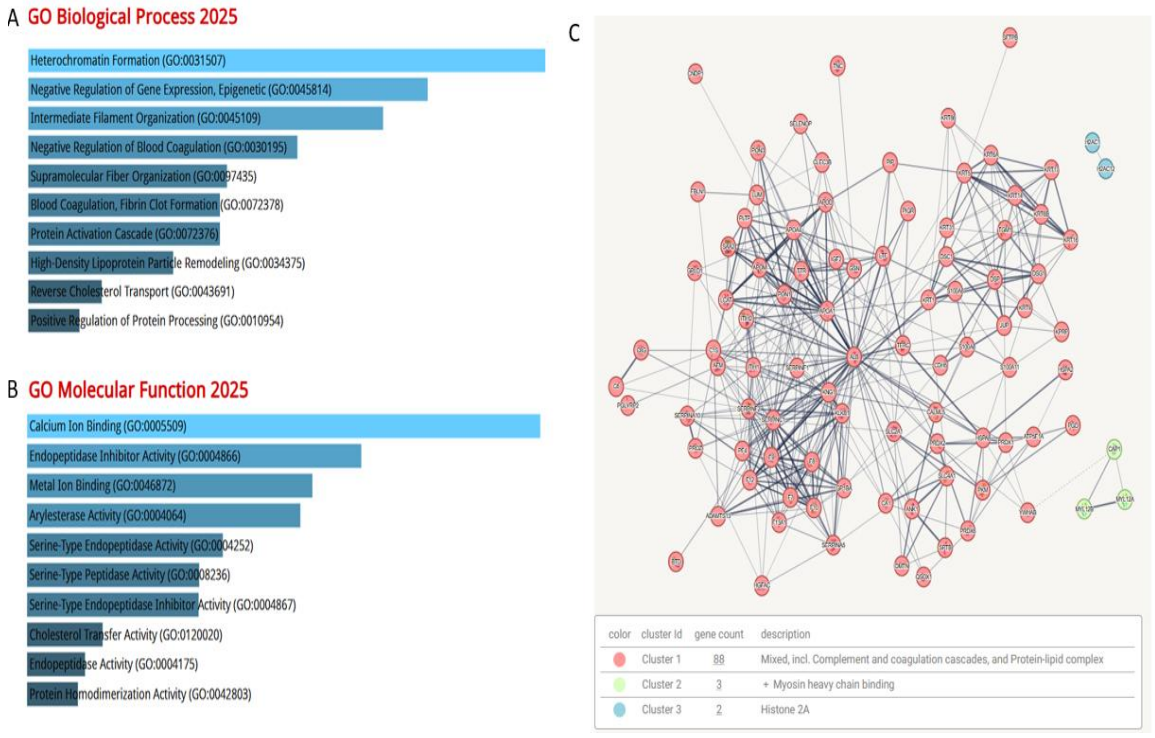

Figure 37: Gene Ontology (GO) enrichment analysis of EV proteins expressed exclusively in the Chemio-Immuno group at P0

serpins (SERPINA1, SERPINA5, SERPINC1, SERPINF1, SERPINF2), as well as proteins involved in proteolytic regulation [192,193] (Fig. 37B). Such proteins play essential roles in tissue remodeling, immune regulation, and tumor–stromal interactions, further supporting the interpretation of EVs as active participants in systemic responses relevant to chemo-immunotherapy outcomes.

Although complex, the STRING network (Fig. 37C) confirms the organization of EV proteins into well-defined functional clusters, including an epithelial cluster, an immune-coagulative cluster, and a metabolic-antioxidant cluster. Numerous immunoglobulins (IGHV, IGKV, IGLV) are present, along with proteins such as Tetranectin (CLEC3B), which is significantly downregulated in NSCLC and correlates with poor progression-free and overall survival. Its expression positively associates with immune infiltration and activation, acting as an independent prognostic risk factor [195]. Also notable is PIGR polymeric immunoglobulin receptor), which has been correlated with poorer outcomes, altered immunity, and EMT [196]. In summary, the EV profile at P0 in patients scheduled for chemo-immunotherapy reveals signals of structural remodeling, coagulation activation, and metabolic adaptation processes that may influence therapeutic response and serve as predictive biomarkers in NSCLC.

The analysis of EVs at P1 in NSCLC patients treated with chemo-immunotherapy reveals a molecular profile strongly oriented toward immune processes and tissue remodeling. GO Biological Process enrichment (Fig. 38A) include processes such as negative regulation of complement activation, adaptive immune response, regulation of defense response, and cell adhesion mediated by synaptic junctions. These features indicate a potential role for EVs in modulating cell–cell communication and suppressing pro-inflammatory pathways.

GO Molecular Function terms highlight binding to complement components, interaction with immunoglobulins, and binding to growth factor receptors. These functions align with the presence of numerous variable immunoglobulin chains (IGHV, IGKV, IGLV), immunoglobulin light chains (IGLC3, IGLL1, IGLL5), and regulatory complement proteins such as C4BPA, C4BPB, CFHR1-5, indicating fine control of the complement cascade during the early therapeutic phase (Fig. 38B).

The STRING network (Fig. 38C) further of distinct functional EV clusters:

- Immune cluster: dominated by immunoglobulins and complement components [197].
- Metabolic cluster: characterized by proteins such as A2M (Alpha-2-Macroglobulin), a broad-spectrum protease inhibitor in plasma, which binds growth factors and inflammatory mediators [198]. Furthermore, a reduced A2M expression in NSCLC correlates with tumor tissue presence, while higher levels are linked to improved prognosis in lung and colorectal cancers [199]. Also present is HP (Haptoglobin), an acute-phase protein which, when elevated in NSCLC, associates with advanced stage, metastasis, and shorter survival [200].
- Structural cluster [201]: includes cytoskeleton proteins such as VIM (vimentin), whose high expression in NSCLC correlates with poor prognosis [202], and FLNA (filamin A), a scaffold protein promoting aggressive phenotype, metastasis, chemo-resistance, and poor clinical outcomes [203].

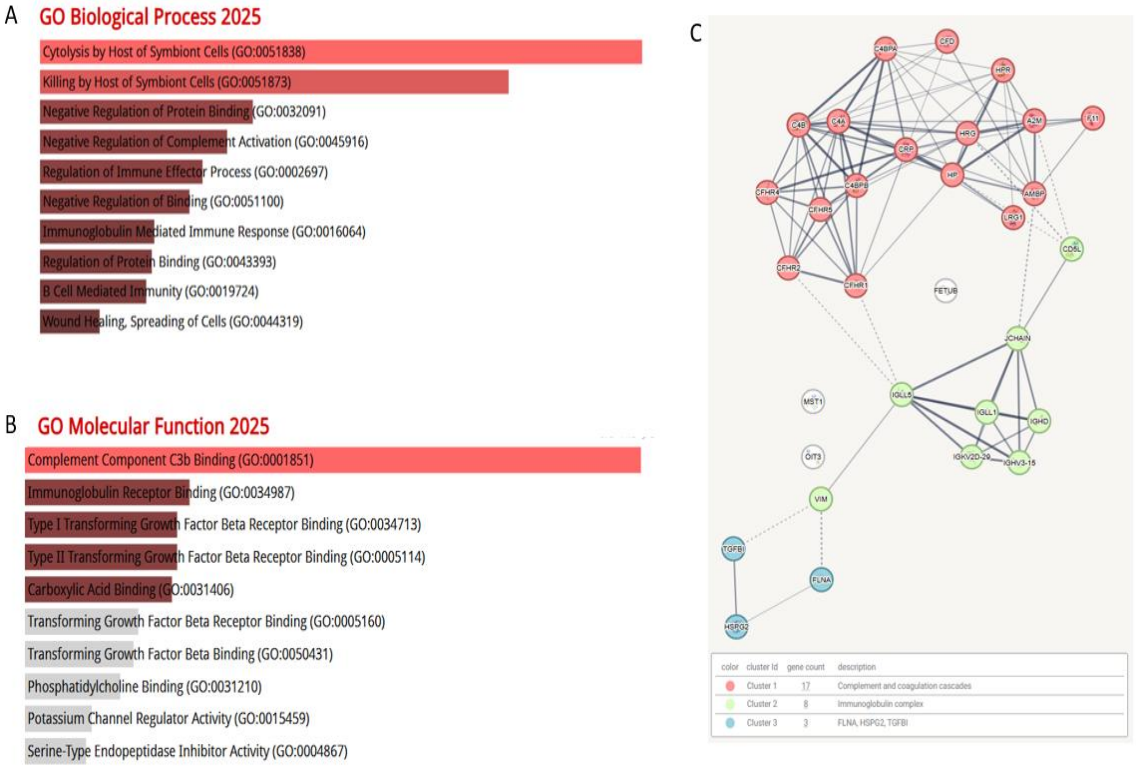

Figure 38: GO enrichment analysis of EV proteins expressed exclusively in the Chemio-Immuno group at P1.

Additionally, proteins such as C-reactive protein (CRP) and leucine-rich alpha-2-glycoprotein (LRG1) indicate a persistent systemic inflammatory response. The presence of Transforming Growth Factor Beta-Induced (TGFBI) further suggests involvement in tumor–stroma interaction, immune infiltration, prognostis sgratification, and metastatic spread in NSCLC [204].

The concurrent presence of inflammatory mediators, EMT-related proteins, and metabolic regulators suggests that EVs actively contribute to shaping the TME and may serve as dynamic biomarkers for treatment response and resistance in NSCLC.

4.2.6 Protein expression in the Chemoterapy group: comparison between P0 and P1.

Baseline EV analysis (P0) in NSCLC patients scheduled for chemotherapy reveals a distinctive molecular profile dominated by processes related to metal ion homeostasis, particularly copper and iron regulation. The GO Biological Process (Fig. 39A) indicates enrichment in pathways such as intracellular copper ion homeostasis, cellular defense response, and intracellular iron ion homeostasis, suggesting an early involvement of metal-dependent oxidative balance. Correspondingly, GO Molecular Functions terms (Fig. 38B) highlight endopeptidase and serine protease activities, suggesting involvement in proteolytic regulation and cellular defense.

These enrichments align with STRING network analysis (Fig. 39C), which reveals presence of proteins central to copper and iron metabolism, inflammation and extracellular remodelling. Among these ceruloplasmin (CP), a copper transport protein, involved in angiogenesis and tumor neovascularization [205]. High CP serum levels have been associated with recurrence in pancreatic carcinoma [206], lung carcinoma [207], leukemia and Hodgkin's lymphoma [208,209,210]. Moreover, elevated urinary CP levels are independent predictors of recurrence in bladder tumors [211]. Complement Factor B (CFB), a crucial component of

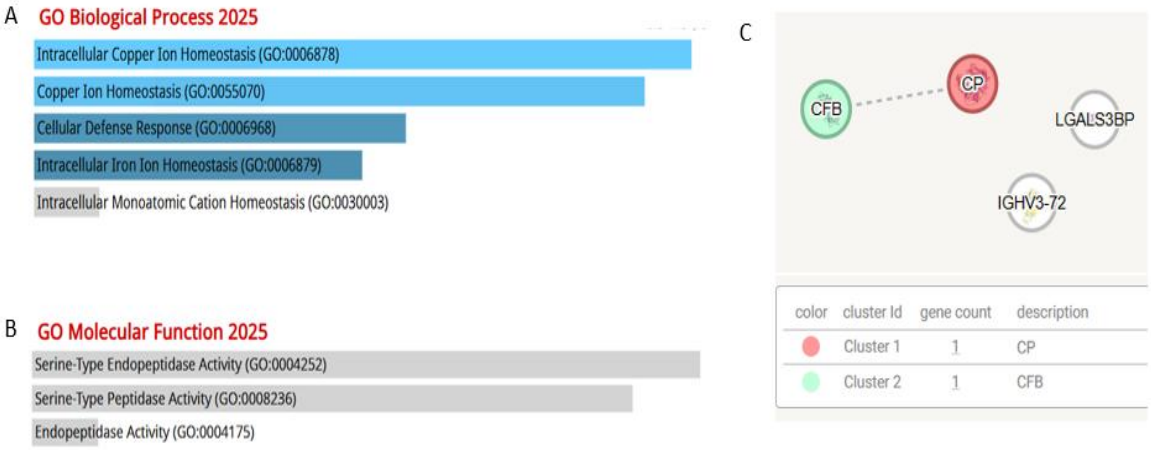

Figure 39: GO enrichment analysis of EV proteins expressed exclusively in the Chemioterapy group at P0.

the alternative complement pathway, has been involved in the progression of many tumors, including pancreatic cancer [212], cutaneous squamous cell carcinoma, and nasopharyngeal carcinoma. Notably, CFB has recently been shown to act as a tumor suppressor in lung adenocarcinoma through inhibition of the Ras/MAPK pathway. Indeed, reduced CFB expression correlates with poor prognosis [213], suggesting it as a potential biomarker and therapeutic target [214]. STRING analysis also identified variable immunoglobulin chains (IGHV, IGKV, IGLV) and Galectin-3-binding protein (LGALS3BP), a highly glycosylated oligomeric protein that is produced at low levels by healthy cells and tissues, whose overexpression is associated to poor prognosis in NSCLC [216], breast cancer[215], head and neck squamous cell carcinoma[217], and melanoma [218].

Analyzing the circulating EV profile in NSCLC before (P0) and after (P1) chemotherapy reveals a clear shift in molecular signatures. At P1, EVs exhibit a profile dominated by pro-coagulant, inflammatory, and lipoprotein remodeling mechanisms, indicating substantial systemic and TME changes induced by treatment. In particular, the post-chemotherapy condition ids characterized by enhance activation of complement and coagulation pathways, lipid transport, as well as the induction of proteins frequently associated with cellular stress and therapeutic resistance (Fig. 40A-B). Notably, these features are highly consistent with EV signatures described in cisplatin-resistant NSCLC, which typically show increased levels of APOA1/APOE apolipoproteins [219].

Protein–protein interaction analysis shows a cohesive cluster (highlighted in red) that includes coagulation factors (F2, F5, PROC), lipid-binding proteins (APOE, APOB, APOC1/3, LPA), and inflammatory molecules (SAA1, SAA4), all of which strongly interconnected (Fig. 40C). Among these, HABP2, a serine protease detected in this study group, appears particularly relevant. HABP2 is involved in extracellular matrix remodeling and regulation of proteolytic activities, ans is known to interact with the urokinase-type plasminogen activator (uPA) pathway. Through this interaction, HABP2 enhances the conversion of plasminogen into plasmin, promoting extracellular matrix degradation and thereby increasing tumor cell invasiveness [220].

Apolipoproteins alspo emerge as crucial biological mediators in NSCLC. APOE plays a central role in regulating cholesterol metabolism, promoting tumor cell invasiveness [221], and modulating inflammation and immune response [222].

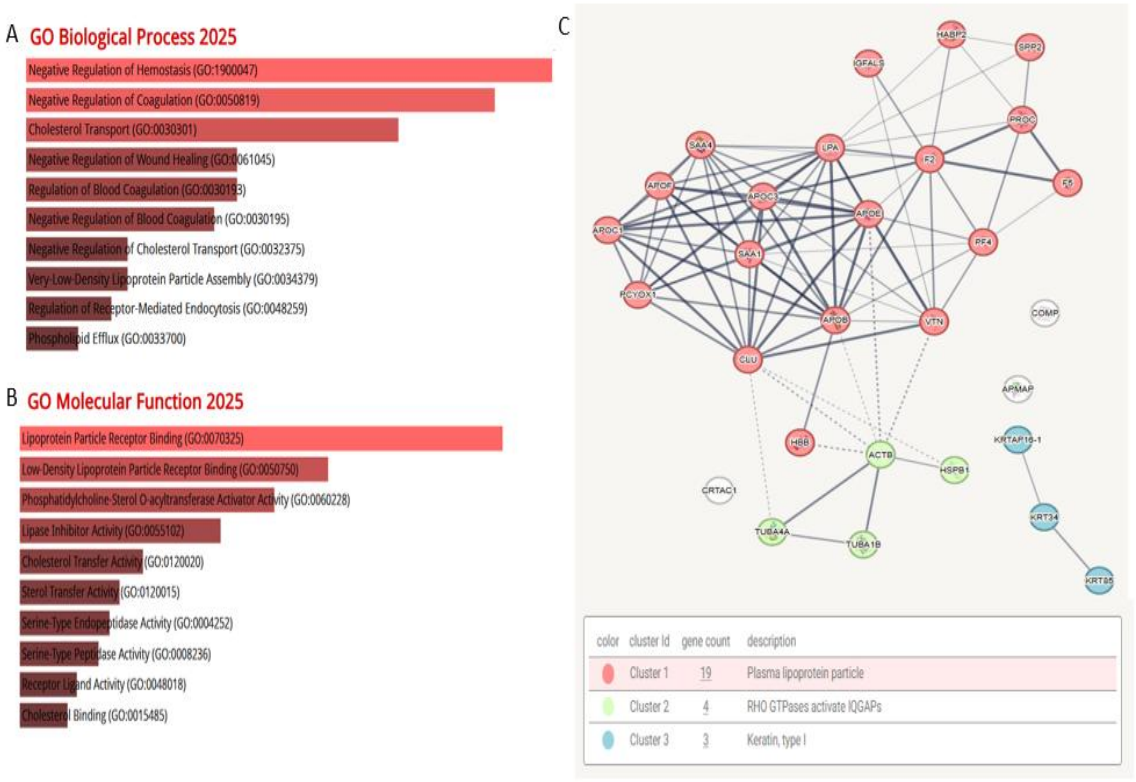

Figure 40: GO enrichment analysis of EV proteins expressed exclusively in the Chemotherapy group at P1.

Meanwhile, APOB is associated with worsening clinical prognosis, and may contribute to angiogenesis and vascular remodeling in the TME [223].

The second cluster (highlighted in green) containing ACTB, various tubulins, and HSPB1, a group of proteins linked to cell motility and structural plasticity, all key processes in NSCLC metastasis. β-actin (ACTB) is frequently overexpressed in NSCLC and correlated with poor prognosis, as it facilitates cellular plasticity and EMT [224]. 1 Heat Shock Protein Beta-1 (HSPB), a chaperonin that stabilizes actin filaments and protects cells from oxidative stress, also plays a critical role in tumor progression. In NSCLC, HSPB1 promotes cell survival, drug resistance, and motility, thereby promoting metastatic potential [225].

In contrast, the baseline sample (P0) shows a more generalized EV profile, dominated by proteins involved in cellular homeostasis rather than the pronounced pro-motility, pro-coagulant and inflammatory signatures observed in P1. This shift further supports the notion that chemotherapy induces a measurable remodeling of the EV proteome, emphasizing pathways associated with stress adaptation, cytoskeletal reorganization, and tumor aggressiveness.

5.0 Conclusions

NSCLC is one of the most frequent cancer types and remains responsible for the majority of cancer-related deaths worldwide. Although its management has considerably improved, especially over the past decade, advanced-stage disease continues to pose major therapeutic challenges. In the early 2000s, the median survival of a patient diagnosed with stage IV NSCLC rarely exceeded one year [226]. Today, in 2025, thanks to targeted therapies and immunotherapy, the 5-year survival rate has increased to 12–15%, with some molecular subgroups achieving even better outcomes according to the 2025 American Society of Clinical Oncology (ASCO) guidelines. This progress reflects a paradigm shift linked to the expanding knowledge of lung cancer biomarkers and their role in prognosis, treatment selction, and patient stratification [227].

Tumor markers are crtical tools in early diagnosis, surveillance of recurrecy and prognosis. Their reliability depends on sensitivity, specificity, and

reproducibility, parameters still far from optimal for many circulating cancer biomarkers. Human plasma represents an ideal biological matrix for biomarker discovery: it is readily accessible, minimally invasive, and reflects systemic physiological and pathological conditions. For this reason, extensive research has been devoted to exploring plasma proteomes in search of clinically meaningful tumor markers [228]. EVs have emerged as central mediators of intercellular communication in cancer. Tumor-derived EVs present in blood and other body fluids encapsulate proteins, lipids, and nucleic acids that mirror the molecular state of their cells of origin. This makes EV-derived proteomes particularly promising for liquid biopsy applications, with potential use in early detection, disease monitoring, treatment response assessment, and therapy resistance prediction [229].

Cancer deeply perturbs the proteome, altering both protein abundance and post-translational modifications. Here, the plasma proteome functions as a integrated biological entity, reporting physiological and pathological events occurring throughout the body. MS-based proteomics offers unprecedented depth for profiling these changes and is increasingly regarded as a future component of routine clinical practice [230].

In this study, proteomic analysis of EVs isolated in NSCLC patients revealed significant heterogeneity of molecular profiles across different therapeutic regimens and between pre- and post-treatment time points. The data show that EVs are not mere cellular byproducts, but dynamically reflect complex biological processes, including extracellular matrix remodeling, lipid metabolism, coagulation, and immune modulation.

In patients undergoing chemotherapy, the post-treatment profile is characterized by an increase in proteins related to the coagulation cascade and lipid transport, suggesting a role for these pathways in the response to drug-induced stress and in tumor progression.

In the immunotherapy group, EVs show enrichment of immunomodulatory proteins and metabolic factors, indicating a complex adaptation that integrates epithelial and immune signals.

Finally, chemo-immunotherapy induces a marked reorganization toward functions of complement control, cell adhesion, and structural plasticity, with proteins associated with EMT and treatment resistance.

Collectively, these results indicate that EVs have a strong potential as dynamic biomarkers to monitor therapy response and to stratify patients. Therefore accurate analysis of the vesicular cargo could substantially improve early diagnosis, guide treatment tailoring, and reveal novel oncogenic drivers [231,232]. Unlike genomics and transcriptomics, which are widely studied through liquid biopsies, the complete plasma proteomic profile remains, to date, relatively unexplored, yet holds enormous diagnostic and prognostic promise. Further studies on larger patient cohorts will be necessary to validate the observed associations, and to define a robust panel of markers with high specificity and sensitivity. Such biomarkers should undergo rigorous functional and clinical evaluation to yield diagnostic and predictive tools truly applicable in clinical oncology.

Alongside clinical samples, 3D cell cultures are becoming essential platforms for cancer research. These models provide an intermediate level of complexity between standard 2D cultures and in vivo tumors. Therefore, we developed a 3D culture method applicable to NSCLC lines, designed to simulate the TME as closely as possible. To study and analyze in a more physiological manner, heterotypic tumor spheroids were chosen, as they present a cellular organization and a 3D structure that can more efficiently mimic the TME. Thus, to optimize the parameters that could in some way influence spheroid formation and growth, it was necessary to perform cell titrations that considered not only the initial number of cells for the individual phenotypes, but also the ratio between the cell populations. The most effective ratios are those already mentioned in section 4.1.0 of this thesis.

Three-dimensional (3D) in vitro models have been used in cancer research as an intermediate model between in vitro tumor cell line cultures and the in vivo tumor. The 3D microenvironment allows the imitation of different types of cellular heterogeneity observed in vivo in various contexts. Among the different 3D models, tumor spheroids, or oncospheres, derived from cultures of cancer stem cells (CSCs), emerge. These cells display particular characteristics such as high clonal capacity, self-renewal ability, expression of embryonic stem cell markers, and a very high level of resistance to the main chemo- and radiotherapeutic drugs most commonly used. Moreover, CSCs are more aggressive than the majority of the tumor cell population, so tumor malignancy could be correlated with the degree of cellular differentiation and the abundance of the CSC fraction within the tumor mass [233,234].

Several co-culture systems based on the use of spheroids have been developed. The most frequently used cell types are tumor cells, immune cells, fibroblasts, and endothelial cells. Generally, immune cells are added in suspension to preformed spheroids, while endothelial cells and fibroblasts are added either in suspension together with tumor cells or to preformed tumor spheroids, as in this thesis study. The experimental system adopted shows that the presence of tumor cells together with stromal and immune cells appears able to mimic, albeit in a clearly simplified manner, the in vivo tumor microenvironment [235].

From flow cytometry analyses performed after 10 days on heterotypic 3D cultures and applying the most common therapies against NSCLC, it emerges that the model appears suitable for further studies focused on the TME. Specifically, these models could be used to culture primary tumor cells derived from patients under clinical care, to be subjected to the action of the main therapeutic agents used in clinical practice, leading to evidence that provides an in-depth understanding of the tumor in each patient category, predicting treatment response and improving outcomes by refining what is a personalized therapy.

Proteomics, counted among the “omics” sciences now well established at the international level, is the main tool for the study of the proteome, that is, the entire set of proteins expressed in a given cell. Knowledge of the components of the proteome can be a valuable tool for the discovery of new candidate biomarkers detectable in blood through liquid biopsy [236]. Analogous to the clinical objectives of genomics and transcriptomics-namely, to provide a deeper understanding of a given disease that goes beyond the standard clinical parameters of cancer diagnosis-proteomics offers a comprehensive view of the molecular actors in a cell at a particular moment and in a specific state [237]. Especially in cancer research, proteomic analysis of tumors is fundamental to gaining a complete understanding of dynamic molecular aberrations, including protein phosphorylation, protein–protein interactions, protein structure, and protein function [238, 239].

6.0 Bibliography

1. https://www.who.int/news-room/fact-sheets/detail/lung-cancer
2. Ward, Zachary J- Estimating trends in non-communicable disease mortality: implications for global health data and policy research- The Lancet, Volume 406, Issue 10509, 1195 – 1197 P1195-1197September 20, 2025
3. https://www.istat.it/informazioni-sulla-rilevazione/rilevazione-sulle-cause-di-morte/
4. R. N. Proctor, "The history of the discovery of the cigaretteelung cancer link: Evidentiary traditions, corporate denial, global toll," Tobacco Control, vol. 21, no. 2, pp. 87–91, 2012, doi: 10.1136/tobaccocontrol-2011-050338.
5. W. EL, G. EA, "Tobacco smoking as a possible etiologic factor in bronchiogenic carcinoma: A study of six hundred and eighty-four proved cases," J Am Med Assoc, vol. 143, no. 4, pp. 329–336, 1950.
6. Doll R., A. B. Hill, "The mortality of doctors in relation to their smoking habits: A preliminary report," British Medical Journal, vol. 328, no. 7455, 2004, doi: 10.1016/s0084-3954(07)70287-7.
7. Christensen C.H. et al., "Association of cigarette, cigar, and pipe use with mortality risk in the US population," JAMA Internal Medicine, vol. 178, no. 4, pp. 469–476, 2018, doi: 10.1001/jamainternmed.2017.8625.
8. "IARC Working Group on the Evaluation of Carcinogenic Risks to Humans: Silica, Some Silicates, Coal Dust and Para-Aramid Fibrils. Lyon, 15-22 October 1996.," in IARC monographs on the evaluation of carcinogenic risks to humans / World Health Organization, International Agency for Research on Cancer, 1997, vol. 68, pp. 1–475.
9. S. Klebe, J. Leigh, D. W. Henderson, M. Nurminen, "Asbestos, smoking and lung cancer: An update," International Journal of Environmental Research and Public Health, vol. 17, no. 1. p. 258, 2020. doi: 10.3390/ijerph17010258.
10. P. Brennan et al., "Secondhand smoke exposure in adulthood and risk of lung cancer among never smokers: A pooled analysis of two large studies," International Journal of Cancer, vol. 109, no. 1, pp. 125–131, 2004, doi: 10.1002/ijc.11682.
11. J. Yokota, K. Shiraishi, T. Kohno, "Genetic Basis for Susceptibility to Lung Cancer. Recent Progress and Future Directions," in Advances in Cancer Research, vol. 109, no. C, 2010, pp. 51–72. doi: 10.1016/B978-0-12- 380890-5.00002-8.
12. A. Zang, E. L. Wynder, "Differences in lung cancer risk between men and women: Examination of the evidence," J Natl Cancer Inst, vol. 88, no. 3–4, pp. 183–192, 1996, doi: 10.1093/jnci/88.3-4.183.
13. S. G. Spiro, M. K. Gould, G. L. Colice, "Initial evaluation of the patient with lung cancer: Symptoms, signs, laboratory tests, and paraneoplastic syndromes. ACCP evidenced-based clinical practice guidelines (2nd edition)," Chest, vol. 132, no. 3 SUPPL., 2007, doi: 10.1378/chest.07-1358.
14. A. R. Feinstein, "Symptomatic Patterns, Biologic Behavior, and Prognosis in Cancer of the Lung," Annals of Internal Medicine, vol. 61, no. 1, pp. 27– 43, 1964, doi: 10.7326/0003-4819-61-1-27
15. A. R. Feinstein, C. K. Wells, "A clinical-severity staging system for patients with lung cancer," Medicine (United States), vol. 69, no. 1, pp. 1–33, 1990, doi: 10.1097/00005792-199001000-00001
16. Linee guida NEOPLASIE DEL POLMONE- AIOM 2024 9e22916b-799c-3966-7dc9-01762112ce94
17. Raffaele Bianco, S. de Placido, G. Tortora, P. Conte, Core curriculumoncologia clinica, 2nd ed. 2016.

18. W . D. Travis et al., “International Association for the Study of Lung Cancer/ American Thoracic Society/European Respiratory Society: International multidisciplinary classification of lung adenocarcinoma - An executive summary,” Proc Am Thorac Soc, vol. 8, no. 5, 2011, doi: 10.1513/pats.201107-042ST.
19. Rosell R, Karachaliou N. Large-scale screening for somatic mutations in lung cancer. The Lancet. 2016 Apr;387(10026):1354–6
20. Osmani L, Askin F, Gabrielson E, Li QK. Current WHO guidelines and the critical role of immunohistochemical markers in the subclassification of nonsmall cell lung carcinoma (NSCLC): Moving from targeted therapy to immunotherapy. Seminars in Cancer Biology. 2018 Oct;52:103–9
21. Acquired EGFR C797S mutation mediates resistance to AZD9291 in non-small cell lung cancer harboring EGFR T790M; Kenneth S Thress, Cloud P Paweletz, Enriqueta Felip, Byoung Chul, et al; DOI: 10.1038/nm.3854
22. Liquid Biopsy in Non-Small Cell Lung Cancer: Highlights and Challenges; Erika Rijavec, Simona Coco, Carlo Genova, Giovanni Rossi, et al; DOI: 10.3390/cancers12010017
23. Liquid biopsies come of age: towards implementation of circulating tumour DNA; Jonathan C M Wan, Charles Massie, Javier Garcia-Corbacho, Florent Mouliere, et al; DOI: 10.1038/nrc.2017.7.
24. Circulating tumor DNA and liquid biopsy in oncology; David W. Cescon , Scott V. Bratman , Steven M. Chan and Lillian L. Siu ; DOI: https://doi.org/10.1038/s43018-020- 0043-5
25. Nikanjam M, Kato S, Kurzrock R. Liquid biopsy: current technology and clinical applications. J Hematol OncolJ Hematol Oncol. 12 settembre 2022;15(1):131.
26. Gijtenbeek RG, Jong K, Venmans BJ, Vollenhoven FH, Ten Brinke A, Van der Wekken AJ, et al. Best first-line therapy for people with advanced non-small cell lung cancer, performance status 2 without a targetable mutation or with an unknown mutation status. Cochrane Database Syst Rev. 7 luglio 2023;2023(7):CD013382.
27. Rolfo C, Mack P, Scagliotti GV, Aggarwal C, Arcila ME, Barlesi F, et al. Liquid Biopsy for Advanced NSCLC: A Consensus Statement From the International Association for the Study of Lung Cancer. J Thorac Oncol. 1 ottobre 2021;16(10):1647–62.
28. Li W, Liu JB, Hou LK, Yu F, Zhang J, Wu W, et al. Liquid biopsy in lung cancer: significance in diagnostics, prediction, and treatment monitoring. Mol Cancer. 20 gennaio 2022;21(1):25
29. Zulato E, Attili I, Pavan A, Nardo G, Del Bianco P, Boscolo Bragadin A, et al. Early assessment of KRAS mutation in cfDNA correlates with risk of progression and death in advanced non-small-cell lung cancer. Br J Cancer. luglio 2020;123(1):81–91
30. Bonanno L, Dal Maso A, Pavan A, Zulato E, Calvetti L, Pasello G, et al. Liquid biopsy and non-small cell lung cancer: are we looking at the tip of the iceberg? Br J Cancer. agosto 2022;127(3):383–93.
31. Anderson, N. M. & Simon, M. C. The tumor microenvironment. Current Biology vol. 30 (2020).
32. Dunn, G.P., Old, L.J. & Schreiber, R.D. The Immunobiology of Cancer Immunosurveillance and Immunoediting. Immunity vol. 21 (2004).
33. Swann, J.B. & Smyth, M.J. Immune surveillance of tumors. Journal of Clinical Investigation vol. 117, 1137–1146 (2007).
34. Dunn, G.P., Old, L.J. & Schreiber, R.D. The three Es of cancer immunoediting. Annual Review of Immunology vol. 22, 329–360 (2004).
35. Chraa, D. et al. T lymphocyte subsets in cancer immunity: Friends or foes. Journal of Leukocyte Biology vol. 105, 243–255(2019).
36. Balkwill, F.R., Capasso, M. & Hagemann, T. The tumor microenvironment at a glance. Journal of Cell Science vol. 125, 5591–5596 (2012).
37. Curiel, T.J. et al. Specific recruitment of regulatory T cells in ovarian carcinoma fosters immune privilege and predicts reduced survival. Nature Medicine 10, 942–949 (2004).
38. Worzfeld, T. et al. The unique molecular and cellular microenvironment of Ovarian cancer. Frontiers in Oncology vol. 7, (2017).

39. Fridman, W.H. et al. The immune contexture in cancer prognosis and treatment. Nature Reviews Clinical Oncology vol. 14, 717–734 (2017).
40. Dyck, L. & Mills, K.H. G. Immune checkpoints and their inhibition in cancer and infectious diseases. European Journal of Immunology vol. 47, 765–779 (2017).
41. Iwai, Y., Hamanishi, J., Chamoto, K. & Honjo, T. Cancer immunotherapies targeting the PD-1 signaling pathway. Journal of Biomedical Science vol. 24 (2017).
42. Chang HY, Sneddon JB, Alizadeh AA, Sood R, West RB, Montgomery K, Chi JT, van de Rijn M, Botstein D, Brown PO. Gene expression signature of fibroblast serum response predicts human cancer progression: similarities between tumors and wounds. PLoS Biol. 2004 Feb;2(2):E7.
43. Erez N, Truitt M, Olson P, Arron ST, Hanahan D. Cancer-Associated Fibroblasts Are Activated in Incipient Neoplasia to Orchestrate Tumor-Promoting Inflammation in an NF-kappaB-Dependent Manner. Cancer Cell. 2010 Feb 17;17(2):135-47. doi: 10.1016/j.ccr.2009.12.041
44. Condeelis J, Pollard JW. Macrophages: obligate partners for tumor cell migration, invasion, and metastasis. Cell. 2006 Jan 27;124(2):263-6.
45. Smolarz B, Łukasiewicz H, Samulak D, Piekarska E, Kołaciński R,Romanowicz H. Lung Cancer—Epidemiology, Pathogenesis, Treatment and Molecular Aspect (Review of Literature). IJMS. 2025 Feb 26;26(5):2049.
46. Li Y, Yan B, He S. Advances and challenges in the treatment of lung cancer. Biomedicine & Pharmacotherapy. 2023 Dec;169:115891.
47. Yoon SM, Shaikh T, Hallman M. Therapeutic management options for stage III non-small cell lung cancer. WJCO. 2017;8(1):1
48. Wang M, Herbst RS, Boshoff C. Toward personalized treatment approaches for non-small-cell lung cancer. Nat Med. 2021 Aug;27(8):1345–56.
49. Boumahdi S, De Sauvage FJ. The great escape: tumour cell plasticity in resistance to targeted therapy. Nat Rev Drug Discov. 2020 Jan;19(1):39–56.
50. Gandhi L, Rodríguez-Abreu D, Gadgeel S, Esteban E, Felip E, De Angelis F, et al. Pembrolizumab plus Chemotherapy in Metastatic Non–Small-Cell Lung Cancer. N Engl J Med. 2018 May 31;378(22):2078–92.
51. Pio R, Ajona D, Ortiz-Espinosa S, Mantovani A, Lambris JD. Complementing the Cancer-Immunity Cycle. Front Immunol. 2019 Apr 12;10:774.
52. Cesano A, Augustin R, Barrea L, Bedognetti D, Bruno TC, Carturan A, et al. Advances in the understanding and therapeutic manipulation of cancer immune responsiveness: a Society for Immunotherapy of Cancer (SITC) review. J Immunother Cancer. 2025 Jan;13(1):e008876.
53. Gubin MM, Vesely MD. Cancer Immunoediting in the Era of Immunooncology. Clinical Cancer Research. 2022 Sept 15;28(18):3917–2
54. Centanni M, Moes DJAR, Trocóniz IF, Ciccolini J, Van Hasselt JGC. Clinical Pharmacokinetics and- Pharmacodynamics of Immune Checkpoint Inhibitors. Clin Pharmacokinet. 2019 July 1;58(7):835–57.
55. Alard E, Butnariu AB, Grillo M, Kirkham C, Zinovkin DA, Newnham L, et al. Advances in Anti-Cancer Immunotherapy: Car-T Cell, Checkpoint Inhibitors, Dendritic Cell Vaccines, and Oncolytic Viruses, and Emerging Cellular and Molecular Targets. Cancers. 2020 July 7;12(7):1826.
56. Wang F, Wang S, Zhou Q. The Resistance Mechanisms of Lung Cancer Immunotherapy. Front Oncol. 2020 Oct 20;10:568059
57. Chargaff, E. and R. West, The biological significance of the thromboplastic protein of blood. J Biol Chem, 1946. 166(1): p. 189-97
58. Wolf, P., The nature and significance of platelet products in human plasma. Br J Haematol, 1967. 13(3): p. 269-88.
59. De Broe, M., R. Wieme, and F. Roels, Letter: Membrane fragments with koinozymic properties released from villous adenoma of the rectum. Lancet, 1975. 2(7946): p. 1214-5
60. Benz, E.W., Jr. and H.L. Moses, Small, virus-like particles detected in bovine sera by electron microscopy. J Natl Cancer Inst, 1974. 52(6): p. 1931-4.

61. Dalton, A.J., Microvesicles and vesicles of multivesicular bodies versus "virus-like" particles. J Natl Cancer Inst, 1975. 54(5): p. 1137-48
62. Stegmayr, B. and G. Ronquist, Promotive effect on human sperm progressive motility by prostasomes. Urol Res, 1982. 10(5): p. 253-7.
63. Ronquist, G., et al., An Mg2+ and Ca2+-stimulated adenosine triphosphatase in human prostatic fluid: part I. Andrologia, 1978. 10(4): p. 261-72
64. Taylor, D.D., H.D. Homesley, and G.J. Doellgast, Binding of specific peroxidase-labeled antibody to placental-type phosphatase on tumorderived membrane fragments. Cancer Res, 1980. 40(11): p. 4064-9.
65. Dvorak, H.F., et al., Tumor shedding and coagulation. Science, 1981. 212(4497): p. 923-4Pan, B.T. and R.M. Johnstone, Fate of the transferrin receptor during maturation of sheep reticulocytes in vitro: selective externalization of the receptor. Cell, 1983. 33(3): p. 967-78
66. Pan, B.T. and R.M. Johnstone, Fate of the transferrin receptor during maturation of sheep reticulocytes in vitro: selective externalization of the receptor. Cell, 1983. 33(3): p. 967-78
67. Raposo, G., et al., B lymphocytes secrete antigen-presenting vesicles. J Exp Med, 1996. 183(3): p. 1161-72
68. Théry C, Witwer KW, Aikawa E, Alcaraz MJ, Anderson JD Andriantsitohaina R, et al. Minimal information for studies of extracellular vesicles 2018 (MISEV2018): a position statement of the International Society for Extracellular Vesicles and update of the MISEV2014 guidelines. J of Extracellular Vesicle. 2018 Dec;7(1):1535750.
69. Welsh JA, Goberdhan DCI, O'Driscoll L, Buzas EI, Blenkiron C, Bussolati B, et al. Minimal information for studies of extracellular vesicles (MISEV2023): From basic to advanced approaches. J of Extracellular Vesicle. 2024 Feb;13(2):e12404
70. Russo E., Alberti G., Corrao S., Borlongan C.V., Miceli V., Conaldi P.G., Di Gaudio F., La Rocca G. The Truth Is Out There: Biological Features and Clinical Indications of Extracellular Vesicles from Human Perinatal Stem Cells. Cells. 2023;12:2347. doi: 10.3390/cells12192347
71. Johnstone R.M., Adam M., Hammond J.R., Orr L., Turbide C. Vesicle formation during reticulocyte maturation. Association of plasma membrane activities with released vesicles (exosomes) J. Biol. Chem. 1987;262:9412–9420. doi: 10.1016/S0021-9258(18)48095-7.
72. Di Bella M.A. Overview and Update on Extracellular Vesicles: Considerations on Exosomes and Their Application in Modern Medicine. Biology. 2022;11:804. doi: 10.3390/biology11060804.
73. Sailliet N., Ullah M., Dupuy A., Silva A.K.A., Gazeau F., Le Mai H., Brouard S. Extracellular Vesicles in Transplantation. Front. Immunol. 2022;13:800018. doi: 10.3389/fimmu.2022.800018.
74. Gurung S., Perocheau D., Touramanidou L., Baruteau J. The exosome journey: From biogenesis to uptake and intracellular signalling. Cell Commun. Signal. CCS. 2021;19:47. doi: 10.1186/s12964-021-00730-1.
75. Guo H., Chitiprolu M., Roncevic L., Javalet C., Hemming F.J., Trung M.T., Meng L., Latreille E., Tanese de Souza C., McCulloch D., et al. Atg5 Disassociates the V(1)V(0)-ATPase to Promote Exosome Production and Tumor Metastasis Independent of Canonical Macroautophagy. Dev. Cell. 2017;43:716–730.e717. doi: 10.1016/j.devcel.2017.11.018
76. Zubkova E., Kalinin A., Bolotskaya A., Beloglazova I., Menshikov M. Autophagy-Dependent Secretion: Crosstalk between Autophagy and Exosome Biogenesis. Curr. Issues Mol. Biol. 2024;46:2209–2235. doi: 10.3390/cimb46030142.
77. O'Neill C.P., Gilligan K.E., Dwyer R.M. Role of Extracellular Vesicles (EVs) in Cell Stress Response and Resistance to Cancer Therapy. Cancers. 2019;11:136. doi: 10.3390/cancers11020136.
78. Peinado H., Alečković M., Lavotshkin S., Matei I., Costa-Silva B., Moreno-Bueno G., Hergueta-Redondo M., Williams C., García-Santos G., Nitadori-Hoshino A., et al. Melanoma exosomes educate bone marrow progenitor cells toward a pro-metastatic phenotype through MET. Nat. Med. 2012;18:883–891. doi: 10.1038/nm.2753.

79. Albanese M., Chen Y.A., Huls C., Gartner K., Tagawa T., Mejias-Perez E., Keppler O.T., Gobel C., Zeidler R., Shein M., et al. MicroRNAs are minor constituents of extracellular vesicles that are rarely delivered to target cells. PLoS Genet. 2021;17:e1009951. doi: 10.1371/journal.pgen.1009951.
80. Rabinowits G., Gercel-Taylor C., Day J.M., Taylor D.D., Kloecker G.H. Exosomal microRNA: A diagnostic marker for lung cancer. Clin. Lung Cancer. 2009;10:42–46. doi: 10.3816/CLC.2009.n.006.
81. Balaj L., Lessard R., Dai L., Cho Y.J., Pomeroy S.L., Breakefield X.O., Skog J. Tumour microvesicles contain retrotransposon elements and amplified oncogene sequences. Nat. Commun. 2011;2:180. doi: 10.1038/ncomms1180.
82. Sanchez C.A., Andahur E.I., Valenzuela R., Castellon E.A., Fulla J.A., Ramos C.G., Trivino J.C. Exosomes from bulk and stem cells from human prostate cancer have a differential microRNA content that contributes cooperatively over local and pre-metastatic niche. Oncotarget. 2016;7:3993–4008. doi: 10.18632/oncotarget.6540
83. Kim I.A., Hur J.Y., Kim H.J., Kim W.S., Lee K.Y. Extracellular Vesicle-Based Bronchoalveolar Lavage Fluid Liquid Biopsy for EGFR Mutation Testing in Advanced Non-Squamous NSCLC. Cancers. 2022;14:2744. doi: 10.3390/cancers14112744.
84. Paramanantham A., Asfiya R., Das S., McCully G., Srivastava A. Extracellular Vesicle (EVs) Associated Non-Coding RNAs in Lung Cancer and Therapeutics. Int. J. Mol. Sci. 2022;23:13637. doi: 10.3390/ijms232113637.
85. Ferreira, L.P.; Gaspar, V.M.; Mano, J.F. Design of Spherically Structured 3D in Vitro Tumor Models-Advances and Prospects. Acta Biomater. 2018, 75, 11–34.
86. Breslin, S.; O'Driscoll, L. Three-Dimensional Cell Culture: The Missing Link in Drug Discovery. Drug Discov. Today 2013, 18, 240–249.
87. Chiono, V. Appunti di New Advances in Alternative Preclinical Trials. (2021).
88. Habanjar O, Diab-Assaf M, Caldefie-Chezet F, Delort L. 3D Cell Culture Systems: Tumor Application, Advantages, and Disadvantages. Int J Mol Sci. 2021 Nov 11;22(22):12200. doi: 10.3390/ijms222212200. PMID: 34830082; PMCID: PMC8618305.
89. Shen, H. et al. Recent advances in three-dimensional multicellular spheroid culture and future development. Micromachines 12, 1–21 (2021).
90. Ishiguro T, Ohata H, Sato A, Yamawaki K, Enomoto T, Okamoto K. Tumor-derived spheroids: Relevance to cancer stem cells and clinical applications. Cancer Sci. 2017 Mar;108(3):283-289. doi: 10.1111/cas.13155. PMID: 28064442; PMCID: PMC5378268.
91. Bonnet, D. & Dick, J. E. Human acute myeloid leukemia is organized as a hierarchy that originates from a primitive hematopoietic cell. Nat. Med. 3, 730–737 (1997).
92. Batlle, E. & Clevers, H. Cancer stem cells revisited. Nat. Med. 23, 1124–1134 (2017).
93. Plaks, V., Kong, N. & Werb, Z. The cancer stem cell niche: how essential is the niche in regulating stemness of tumor cells? Cell Stem Cell 16, 225–238 (2015).
94. Reya T, Morrison SJ, Clarke MF, and Weissman IL. Stem Cells, Cancer, and Cancer Stem Cells. Nature 2001; 414(issue):105-11.
95. O'Brien CA, Pollett A, Gallinger S, and Dick JE. A Human Colon Cancer Cell Capable of Initiating Tumour Growth in Immunodeficient Mice. Nature 2007; 445(issue):106-10.
96. Cheng L, Ramesh AV, Flesken-Nikitin A, Choi J, and Nikitin AY. Mouse Models for Cancer Stem Cell Research. Toxicol Pathol 2010; 38(issue):62-71.
97. Michor F, and Polyak K. The Origins and Implications of Intratumor Heterogeneity. Cancer Prev Res (Phila) 2010; 3(issue):1361-4.
98. Meacham CE, and Morrison SJ. Tumour Heterogeneity and Cancer Cell Plasticity. Nature 2013; 501(issue):328-37
99. Vlashi E, and Pajonk F. Cancer Stem Cells, Cancer Cell Plasticity and Radiation Therapy. Semin Cancer Biol 2015; 31(issue):28-35.
100. Boman BM, Wicha MS, Fields JZ, and Runquist OA. Symmetric Division of Cancer Stem Cells--a Key Mechanism in Tumor Growth That Should Be Targeted in Future Therapeutic Approaches. Clin Pharmacol Ther 2007; 81(issue):893-8.

101. Morrison SJ, and Kimble J. Asymmetric and Symmetric Stem-Cell Divisions in Development and Cancer. Nature 2006; 441(issue):1068-74
102. Skvortsov S, Debbage P, Lukas P, and Skvortsova I. Crosstalk between DNA Repair and Cancer Stem Cell (Csc) Associated Intracellular Pathways. Semin Cancer Biol 2015; 31(issue):36-42.
103. Diehn M, Cho RW, Lobo NA, Kalisky T, Dorie MJ, Kulp AN, Qian D, Lam JS, Ailles LE, Wong M, Joshua B, Kaplan MJ, Wapnir I, Dirbas FM, Somlo G, Garberoglio C, Paz B, Shen J, Lau SK, Quake SR, Brown JM, Weissman IL, and Clarke MF. Association of Reactive Oxygen Species Levels and Radioresistance in Cancer Stem Cells. Nature 2009; 458(issue):780-3.
104. Yang AD, Fan F, Camp ER, van Buren G, Liu W, Somcio R, Gray MJ, Cheng H, Hoff PM, and Ellis LM. Chronic Oxaliplatin Resistance Induces Epithelial-to-Mesenchymal Transition in Colorectal Cancer Cell Lines. Clin Cancer Res 2006; 12(issue):4147-53.
105. Touil Y, Igoudjil W, Corvaisier M, Dessein AF, Vandomme J, Monte D, Stechly L, Skrypek N, Langlois C, Grard G, Millet G, Leteurtre E, Dumont P, Truant S, Pruvot FR, Hebbar M, Fan F, Ellis LM, Formstecher P, Van Seuningen I, Gespach C, Polakowska R, and Huet G. Colon Cancer Cells Escape 5fu Chemotherapy-Induced Cell Death by Entering Stemness and Quiescence Associated with the C-Yes/Yap Axis. Clin Cancer Res 2014; 20(issue):837-46.
106. Ye X, and Weinberg RA. Epithelial-Mesenchymal Plasticity: A Central Regulator of Cancer Progression. Trends Cell Biol 2015; 25(issue):675-86
107. Beerling E, Seinstra D, de Wit E, Kester L, van der Velden D, Maynard C, Schafer R, van Diest P, Voest E, van Oudenaarden A, Vrisekoop N, and van Rheenen J. Plasticity between Epithelial and Mesenchymal States Unlinks Emt from Metastasis-Enhancing Stem Cell Capacity. Cell Rep 2016; 14(issue):2281-8.
108. Mani SA, Guo W, Liao MJ, Eaton EN, Ayyanan A, Zhou AY, Brooks M, Reinhard F, Zhang CC, Shipitsin M, Campbell LL, Polyak K, Brisken C, Yang J, and Weinberg RA. The Epithelial-Mesenchymal Transition Generates Cells with Properties of Stem Cells. Cell 2008; 133(issue):704-15.
109. Hsu CL, Chung FH, Chen CH, Hsu TT, Liu SM, Chung DS, Hsu YF, Chen CL, Ma N, and Lee HC. Genotypes of Cancer Stem Cells Characterized by Epithelial-to-Mesenchymal Transition and Proliferation Related Functions. Sci Rep 2016; 6(issue):32523.
110. Ricci, C.; Moroni, L.; Danti, S. Cancer Tissue Engineering—New Perspectives in Understanding the Biology of Solid Tumours—A Critical Review. OA Tissue Eng. 2013, 1, 1–7.
111. Basu AK. DNA damage, mutagenesis and cancer. Int J Mol Sci. (2018) 19:970 10.3390/ijms19040970
112. Blackadar CB. Historical review of the causes of cancer. World J Clin Oncol. (2016) 7:54–86. 10.5306/wjco.v7.i1.54
113. Hanahan D, Weinberg RA. Hallmarks of cancer: the next generation. Cell. (2011) 144:646–74. 10.1016/j.cell.2011.02.013
114. Ricci-Vitiani L, Lombardi DG, Pilozzi E, Biffoni M, Todaro M, Peschle C, and De Maria R. Identification and Expansion of Human Colon-Cancer-Initiating Cells. Nature 2007; 445(issue):111-5.
115. O'Brien CA, Pollett A, Gallinger S, and Dick JE. A Human Colon Cancer Cell Capable of Initiating Tumour Growth in Immunodeficient Mice. Nature 2007; 445(issue):106-10
116. Basakran NS. Cd44 as a Potential Diagnostic Tumor Marker. Saudi Med J 2015; 36(issue):273-9.
117. Du L, Wang H, He L, Zhang J, Ni B, Wang X, Jin H, Cahuzac N, Mehrpour M, Lu Y, and Chen Q. Cd44 Is of Functional Importance for Colorectal Cancer Stem Cells. Clin Cancer Res 2008; 14(issue):6751-60.
118. Huh JW, Kim HR, Kim YJ, Lee JH, Park YS, Cho SH, and Joo JK. Expression of Standard Cd44 in Human Colorectal Carcinoma: Association with Prognosis. Pathol Int 2009; 59(issue):241-6.
119. David Wei-MinTan N. Chapter Three - Intestinal Stem Cells and Their Defining Niche. Current Topics in Developmental Biology 2014; 107(issue):77-107.
120. Plaks V, Kong N, and Werb Z. The Cancer Stem Cell Niche: How Essential Is the Niche in Regulating Stemness of Tumor Cells? Cell Stem Cell 2015; 16(issue):225-38.

121. Li, X. et al. Mesenchymal/stromal stem cells: necessary factors in tumour progression. Cell Death Discov. 8, 333 (2022)
122. Coughlan C, Bruce KD, Burgy O, Boyd TD, Michel CR, Garcia-Perez JE, Adame V, Anton P, Bettcher BM, Chial HJ, Königshoff M, Hsieh EWY, Graner M, Potter H. Exosome Isolation by Ultracentrifugation and Precipitation and Techniques for Downstream Analyses. Curr Protoc Cell Biol. 2020 Sep;88(1):e110. doi: 10.1002/cpcb.110. PMID: 32633898; PMCID: PMC8088761.
123. Roy, J.W., Taylor, C.A., Beauregard, A.P. et al. A multiparametric extraction method for Vn96-isolated plasma extracellular vesicles and cell-free DNA that enables multi-omic profiling. Sci Rep 11, 8085 (2021). https://doi.org/10.1038/s41598-021-87526-
124. Bachurski D, Schuldner M, Nguyen PH, Malz A, Reiners KS, Grenzi PC, … Pogge von Strandmann E (2019). Extracellular vesicle measurements with nanoparticle tracking analysis - An accuracy and repeatability comparison between NanoSight NS300 and ZetaView. J Extracell Vesicles, 8(1), 1596016. doi: 10.1080/20013078.2019.1596016
125. Nazarenko I. Extracellular Vesicles: Recent Developments in Technology and Perspectives for Cancer Liquid Biopsy. Recent Results Cancer Res. 2020;215:319–344. doi: 10.1007/978-3-030-26439-0_17.
126. Wiśniewski JR. Filter Aided Sample Preparation - A tutorial. Anal Chim Acta. 2019 Dec 20;1090:23-30. doi: 10.1016/j.aca.2019.08.032. Epub 2019 Aug 17. PMID: 31655642.
127. Rappsilber J, Ishihama Y, Mann M. Stop and go extraction tips for matrix-assisted laser desorption/ionization, nanoelectrospray, and LC/MS sample pretreatment in proteomics. Anal Chem. 2003 Feb 1;75(3):663-70. doi: 10.1021/ac026117i. PMID: 12585499.
128. Tyanova S et al. The Perseus computational platform for comprehensive analysis of (prote)omics data. Nat Methods (2016). https://doi.org/10.1038/nmeth.3901
129. Walcher L, Kistenmacher AK, Suo H, Kitte R, Dluczek S, Strauß A, Blaudszun AR, Yevsa T, Fricke S, Kossatz-Boehlert U. Cancer Stem Cells-Origins and Biomarkers: Perspectives for Targeted Personalized Therapies. Front Immunol. 2020 Aug 7;11:1280. doi: 10.3389/fimmu.2020.01280. PMID: 32849491; PMCID: PMC7426526.
130. Musielak M, Piwocka O, Kulcenty K, Ampuła K, Adamczyk B, Piotrowski I, Fundowicz M, Kruszyna-Mochalska M, Suchorska WM, Malicki J. Biological heterogeneity of primary cancer-associated fibroblasts determines the breast cancer microenvironment. Am J Cancer Res. 2022 Sep 15;12(9):4411-4427. PMID: 36225645; PMCID: PMC9548006.
131. Zhou JY, Chen M, Ma L, Wang X, Chen YG, Liu SL. Role of CD44(high)/CD133(high) HCT-116 cells in the tumorigenesis of colon cancer. Oncotarget. 2016 Feb 16;7(7):7657-66. doi: 10.18632/oncotarget.7084. PMID: 26840024; PMCID: PMC4884945.
132. Akamine T, Tagawa T, Ijichi K, Toyokawa G, Takamori S, Hirai F, Okamoto T, Oda Y, Maehara Y. The Significance of CD44 Variant 9 in Resected Lung Adenocarcinoma: Correlation with Pathological Early-Stage and EGFR Mutation. Ann Surg Oncol. 2019 May;26(5):1544-1551. doi: 10.1245/s10434-018-07137-2. Epub 2019 Feb 24. PMID: 30798450.
133. Yang, Y., Yang, Y., Yang, J., Zhao, X. & Wei, X. Tumor microenvironment in ovarian cancer: Function and therapeutic strategy. Front. cell. Dev. Biology. 8, 758 (2020).
134. Zheng Y, Wang L, Yin L, Yao Z, Tong R, Xue J, Lu Y. Lung Cancer Stem Cell Markers as Therapeutic Targets: An Update on Signaling Pathways and Therapies. Front Oncol. 2022 May 26;12:873994. doi: 10.3389/fonc.2022.873994. PMID: 35719973; PMCID: PMC9204354
135. Kodama H, Murata S, Ishida M, Yamamoto H, Yamaguchi T, Kaida S, Miyake T, Takebayashi K, Kushima R, Tani M. Prognostic impact of CD44-positive cancer stem-like cells at the invasive front of gastric cancer. Br J Cancer. 2017 Jan 17;116(2):186-194. doi: 10.1038/bjc.2016.401. Epub 2016 Dec 8. PMID: 27931044; PMCID: PMC5243989. Zheng Y, Wang L, Yin L, Yao Z, Tong R, Xue J, Lu Y. Lung Cancer Stem Cell Markers as Therapeutic Targets: An Update on Signaling Pathways and Therapies. Front Oncol. 2022 May 26;12:873994. doi: 10.3389/fonc.2022.873994. PMID: 35719973; PMCID: PMC9204354
136. Yang, Y., Yang, Y., Yang, J., Zhao, X. & Wei, X. Tumor microenvironment in ovarian cancer: Function and therapeutic strategy. Front. cell. Dev. Biology. 8, 758 (2020).

137. Horowitz, M., Esakov, E., Rose, P. & Reizes, O. Signaling within the epithelial ovarian cancer tumor microenvironment: The challenge of tumor heterogeneity. Annals Translational Med.8, 905 (2020).
138. Flörkemeier I, Antons LK, Weimer JP, Hedemann N, Rogmans C, Krüger S, Scherließ R, Dempfle A, Arnold N, Maass N, Bauerschlag DO. Multicellular ovarian cancer spheroids: novel 3D model to mimic tumour complexity. Sci Rep. 2024 Oct 9;14(1):23526. doi: 10.1038/s41598-024-73680-6. PMID: 39384844; PMCID: PMC11464915.
139. Mendoza-Martinez, A. K., Loessner, D., Mata, A. & Azevedo, H. S. Modeling the tumor microenvironment of ovarian cancer: The application of self-assembling biomaterials. Cancers13 (2021).
140. Rodrigues, J., Heinrich, M. A., Teixeira, L. M. & Prakash, J. 3D in Vitro Model (R)evolution: Unveiling tumor-stroma interactions. Trends cancer. 7, 249–264 (2021).
141. Carter, E. P., Roozitalab, R., Gibson, S. V. & Grose, R. P. Tumour microenvironment 3D-modelling: simplicity to complexity and back again. Trends cancer. 7, 1033–1046 (2021).
142. Lee, K. H. & Kim, T. H. Recent advances in multicellular tumor spheroid generation for drug screening. Biosensors11 (2021).
143. Tomas, E. & Shepherd, T. G. Insights into high-grade serous carcinoma pathobiology using three-dimensional culture model systems. J. Ovarian Res.16, 70 (2023).
144. Patrone D, Alessio N, Antonucci N, Brigida AL, Peluso G, Galderisi U, etal. Optimization of Peripheral Blood Mononuclear Cell Extraction from Small Volume of Blood Samples: Potential Implications for Children- Related Diseases. MPs. 2022 Feb 24;5(2):20.
145. Zhu, Y.; Kang, E.; Wilson, M.; Basso, T.; Chen, E.; Yu, Y.; Li, Y.-R. 3D Tumor Spheroid and Organoid to Model Tumor Microenvironment for Cancer Immunotherapy. Organoids 2022 , 1 , 149-167. https://doi.org/10.3390/organoids1020012
146. Wu Y, Yu G, Jin K, Qian J. Advancing non-small cell lung cancer treatment: the power of combination immunotherapies. Front Immunol. 2024 Jul 2;15:1349502. doi: 10.3389/fimmu.2024.1349502. PMID: 39015563; PMCID: PMC11250065.
147. Paredes R, Borea R, Drago F, Russo A, Nigita G, Rolfo C. Genetic drivers of tumor microenvironment and immunotherapy resistance in non-small cell lung cancer: the role of KEAP1, SMARCA4, and PTEN mutations. Journal for ImmunoTherapy of Cancer. 2025;13:e012288. https://doi.org/10.1136/jitc-2025-012288
148. Salas-Benito D, Pérez-Gracia JL, Ponz-Sarvisé M, Rodriguez-Ruiz ME, Martínez-Forero I, Castañón E, López-Picazo JM, Sanmamed MF, Melero I. Paradigms on Immunotherapy Combinations with Chemotherapy. Cancer Discov. 2021 Jun;11(6):1353-1367. doi: 10.1158/2159-8290.CD-20-1312. Epub 2021 Mar 12. PMID: 33712487.
149. Weiss, F., Atlasy, N., van Reijmersdal, V. et al. 3D spheroid culture to examine adaptive therapy response in invading tumor cells. In vitro models 1, 463–471 (2022). https://doi.org/10.1007/s44164-022-00040-x
150. Yu J, Kong X, Feng Y. Tumor microenvironment-driven resistance to immunotherapy in non-small cell lung cancer: strategies for Cold-to-Hot tumor transformation. Cancer Drug Resist. 2025 Apr 24;8:21. doi: 10.20517/cdr.2025.14. PMID: 40342732; PMCID: PMC12059482.
151. Cecilia Lindskog (2016) The Human Protein Atlas – an important resource for basic and clinical research, Expert Review of Proteomics, 13:7, 627-629, DOI: 10.1080/14789450.2016.1199280
152. Chen E.Y., Tan C.M., Kou Y., Duan Q., Wang Z., Meirelles G.V., et al. Enrichr: interactive and collaborative HTML5 gene list enrichment analysis tool. BMC Bioinform. 2013;14:128. doi: 10.1186/1471-2105-14-128.
153. Maxim V. Kuleshov, Matthew R. Jones, Andrew D. Rouillard, Nicolas F. Fernandez, Qiaonan Duan, Zichen Wang, Simon Koplev, Sherry L. Jenkins, Kathleen M. Jagodnik, Alexander Lachmann, Michael G. McDermott, Caroline D. Monteiro, Gregory W. Gundersen, Avi Ma'ayan, Enrichr: a comprehensive gene set enrichment analysis web server 2016 update, Nucleic Acids Research, Volume 44, Issue W1, 8 July 2016, Pages W90–W97, https://doi.org/10.1093/nar/gkw377

154. Damian Szklarczyk, Annika L Gable, Katerina C Nastou, David Lyon, Rebecca Kirsch, Sampo Pyysalo, Nadezhda T Doncheva, Marc Legeay, Tao Fang, Peer Bork, Lars J Jensen, Christian von Mering, The STRING database in 2021: customizable protein–protein networks, and functional characterization of user-uploaded gene/measurement sets, Nucleic Acids Research, Volume 49, Issue D1, 8 January 2021, Pages D605–D612, https://doi.org/10.1093/nar/gkaa1074
155. Bafiti V, Thanou E, Ouzounis S, Kotsakis A, Georgoulias V, Lianidou E, Katsila T, Markou A. Profiling Plasma Extracellular Vesicle Metabotypes and miRNAs: An Unobserved Clue for Predicting Relapse in Patients with Early-Stage NSCLC. Cancers. 2024; 16(22):3729. https://doi.org/10.3390/cancers16223729
156. Schousboe I. beta 2-Glycoprotein I: a plasma inhibitor of the contact activation of the intrinsic blood coagulation pathway. Blood. 1985 Nov;66(5):1086-91. PMID: 4052628.
157. Barbié, V. and Lefranc, M.-P., Exp. Clin. Immunogenet., 15, 171-183 (1998) PMID: 9813414
158. Anjana Soman, S. Asha Nair - Unfolding the cascade of SERPINA3: Inflammation to cancer-Biochimica et Biophysica Acta (BBA) - Reviews on Cancer, Volume 1877, Issue 5, 2022,188760,ISSN 0304-419X,https://doi.org/10.1016/j.bbcan.2022.188760.
159. Andrea Sánchez-Navarro, Isaac González-Soria, Rebecca Caldiño-Bohn, and Norma A. Bobadilla An integrative view of serpins in health and disease: the contribution of SerpinA3American Journal of Physiology-Cell Physiology 2021 320:1, C106-C118
160. Jin, Y., Zhang, Y., Huang, A., Chen, Y., Wang, J., Liu, N. ... Pan, J. (2023). Overexpression of SERPINA3 suppresses tumor progression by modulating SPOP/NF-κB in lung cancer. International Journal of Oncology, 63, 96. https://doi.org/10.3892/ijo.2023.5544
161. Zhao J, Liu Y, Zhou L, Liu Y. Retinol-Binding Protein 4 as a Biomarker in Cancer: Insights from a Pan-Cancer Analysis of Expression, Immune Infiltration, and Methylation. Genes (Basel). 2025 Jan 25;16(2):150. doi: 10.3390/genes16020150. PMID: 40004479; PMCID: PMC11855459.
162. Wajda A, Sowińska A, Haładyj E, Stypińska B, Nałęcz-Janik J, Jagodziński PP, Majewski D, Olesińska M, Paradowska-Gorycka A. Tissue factor and human apolipoprotein H genetic variants and pro-inflammatory cytokines in systemic lupus erythematosus patients. Clin Exp Rheumatol. 2021 May-Jun;39(3):587-600. doi: 10.55563/clinexprheumatol/5lkj3f. Epub 2020 Sep 3. PMID: 32896248.
163. Ge Y, Ye T, Fu S, Jiang X, Song H, Liu B, Wang G and Wang J (2023) Research progress of extracellular vesicles as biomarkers in immunotherapy for non-small cell lung cancer. Front.Immunol. 14:1114041. doi: 10.3389/fimmu.2023.1114041 40366616; PMCID: PMC12077270. Analysis and Machine Learning. J Extracell Vesicles. 2025 May;14(5):e70078. doi: 10.1002/jev2.70078. PMID: 40366616; PMCID: PMC12077270.
164. Hajjar, K. A., and Krishnan, S. (1999). Annexin II: A mediator of the plasmin/plasminogen activator system. Trends Cardiovasc Med. 9 (5), 128–138. doi:10.1016/s1050-1738(99)00020-1
165. Wang, C. Y., and Lin, C. F. (2014). Annexin A2: Its molecular regulation and cellular expression in cancer development. Dis. Markers 2014, 308976. doi:10.1155/2014/308976
166. Wang, T., Wang, Z., Niu, R., and Wang, L. (2019). Crucial role of Anxa2 in cancer progression: Highlights on its novel regulatory mechanism. Cancer Biol. Med. 16 (4), 671–687. doi:10.20892/j.issn.2095-3941.2019.0228
167. Huang, Y., Jia, M., Yang, X., Han, H., Hou, G., Bi, L., et al. (2022). Annexin A2: The diversity of pathological effects in tumorigenesis and immune response. Int. J. Cancer 151 (4), 497–509. doi:10.1002/ijc.34048
168. Tan, H.T., Low, J., Lim, S.G. and Chung, M.C.M. (2009), Serum autoantibodies as biomarkers for early cancer detection. The FEBS Journal, 276: 6880-6904. https://doi.org/10.1111/j.1742-4658.2009.07396.x
169. Huang, Chen Kai et al. ENO1 and Cancer Molecular Therapy - Oncolytics, Volume 24, 288 - 298
170. Tian T., Li X., Hua Z., Ma J., Wu X., Liu Z., Chen H., Cui Z. S100A7 promotes the migration, invasion and metastasis of human cervical cancer cells through epithelial–mesenchymal

transition. Oncotarget. 2017; 8: 24964-24977. Retrieved from https://www.oncotarget.com/article/15329/text/

171. Rotondo R, Barisione G, Mastracci L, Grossi F, Orengo AM, Costa R, Truini M, Fabbi M, Ferrini S, Barbieri O. IL-8 induces exocytosis of arginase 1 by neutrophil polymorphonuclears in nonsmall cell lung cancer. Int J Cancer. 2009 Aug 15;125(4):887-93. doi: 10.1002/ijc.24448. PMID: 19431148.
172. Aaboe Jørgensen M, Ugel S, Linder Hübbe M, Carretta M, Perez-Penco M, Weis-Banke SE, Martinenaite E, Kopp K, Chapellier M, Adamo A, De Sanctis F, Frusteri C, Iezzi M, Zocca MB, Hargbøll Madsen D, Wakatsuki Pedersen A, Bronte V, Andersen MH. Arginase 1-Based Immune Modulatory Vaccines Induce Anticancer Immunity and Synergize with Anti-PD-1 Checkpoint Blockade. Cancer Immunol Res. 2021 Nov;9(11):1316-1326. doi: 10.1158/2326-6066.CIR-21-0280. Epub 2021 Sep 13. PMID: 34518197.
173. Georgila, K.; Vyrla, D.; Drakos, E. Apolipoproteina AI (ApoA-I), Immunità, infiammazione e cancro. Cancers 2019, 11 , 1097. https://doi.org/10.3390/cancers11081097
174. Qiu, K., Ding, D., Zhang, F. et al. LTF as a Potential Prognostic and Immunological Biomarker in Glioblastoma. Biochem Genet 63, 2347–2362 (2025). https://doi.org/10.1007/s10528-024-10716-6
175. Goel S, Wozniak C, Sabri A, Haddad B, Lopo B, Cobos A, Sarofim S, Guthrie J, Heyl D, Evans HG. Lactoferrin treatment activates acetylcholinesterase, decreasing acetylcholine levels in non-small cell lung cancer (NSCLC) cell culture supernatants, inhibiting cell survival. FEBS Open Bio. 2025 Sep 23. doi: 10.1002/2211-5463.70125. Epub ahead of print. PMID: 40985115.
176. Cao L, Li B, Zheng S, Zhang Q, Qian Y, Ren Y, Wang H, Wang M, Wu X, Zhang J, Xu K. Reprogramming of fibroblasts into cancer-associated fibroblasts via IGF2-mediated autophagy promotes metastasis of lung cancer cells. iScience. 2024 Oct 28;27(12):111269. doi: 10.1016/j.isci.2024.111269. PMID: 39759028; PMCID: PMC11700637.
177. Ting Wang, Ge Du, Dong Wang. The S100 protein family in lung cancer,Clinica Chimica Acta, Volume 520, 2021,Pages 67-70,ISSN 0009-8981,https://doi.org/10.1016/j.cca.2021.05.028.
178. Heizmann CW. S100 proteins: Diagnostic and prognostic biomarkers in laboratory medicine. Biochim Biophys Acta Mol Cell Res. 2019 Jul;1866(7):1197-1206. doi: 10.1016/j.bbamcr.2018.10.015. Epub 2018 Oct 28. PMID: 30392897.
179. Brodin, O.; Hackler, J.; Misra, S.; Wendt, S.; Sun, Q.; Laaf, E.; Stoppe, C.; Björnstedt, M.; Schomburg, L. Selenoprotein P as Biomarker of Selenium Status in Clinical Trials with Therapeutic Dosages of Selenite. Nutrients 2020, 12, 1067. https://doi.org/10.3390/nu12041067
180. Razaghi, A.; Björnstedt, M. Exploring Selenoprotein P in Liver Cancer: Advanced Statistical Analysis and Machine Learning Approaches. Cancers 2024, 16, 2382. https://doi.org/10.3390/cancers16132382
181. Tianjie Tian, Chuang Qi, Xianqing Luo et al. Molecular mechanisms and prognostic value of the selenoprotein gene family in lung adenocarcinoma and lung squamous cell carcinoma, 11 May 2023, PREPRINT (Version 1) available at Research Square [https://doi.org/10.21203/rs.3.rs-2901655/v1]
182. Pilat JM, Brown RE, Chen Z, Berle NJ, Othon AP, Washington MK, Anant SA, Kurokawa S, Ng VH, Thompson JJ, Jacobse J, Goettel JA, Lee E, Choksi YA, Lau KS, Short SP, Williams CS. SELENOP modifies sporadic colorectal carcinogenesis and WNT signaling activity through LRP5/6 interactions. J Clin Invest. 2023 Jul 3;133(13):e165988. doi: 10.1172/JCI165988. PMID: 37166989; PMCID: PMC10313376.
183. De Lucia A, Mazzotti L, Gaimari A, Zurlo M, Maltoni R, Cerchione C, Bravaccini S, Delmonte A, Crinò L, Borges de Souza P, Pasini L, Nicolini F, Bianchi F, Juan M, Calderon H, Magnoni C, Gazzola L, Ulivi P, Mazza M. Non-small cell lung cancer and the tumor microenvironment: making headway from targeted therapies to advanced immunotherapy. Front Immunol. 2025 Feb 10;16:1515748. doi: 10.3389/fimmu.2025.1515748. PMID: 39995659; PMCID: PMC11847692.

184. Li H, Zhang D, Li B, Zhen H, Chen W, Men Q. PRDX6 Overexpression Promotes Proliferation, Invasion, and Migration of A549 Cells in vitro and in vivo. Cancer Manag Res. 2021 Feb 10;13:1245-1255. doi: 10.2147/CMAR.S284195. PMID: 33603470; PMCID: PMC7883393.
185. Lee SH, Suh IB, Lee EJ, Hur GY, Lee SY, Lee SY, Shin C, Shim JJ, In KH, Kang KH, Yoo SH, Kim JH. Relationships of coagulation factor XIII activity with cell-type and stage of non-small cell lung cancer. Yonsei Med J. 2013 Nov;54(6):1394-9. doi: 10.3349/ymj.2013.54.6.1394. PMID: 24142643; PMCID: PMC3809885.
186. l FVII espresso dal tumore ha indotto l'espressione genica prometastatica
187. Luo JH, Zhang XX, Sun WH. F12 as a reliable diagnostic and prognostic biomarker associated with immune infiltration in papillary thyroid cancer. Aging (Albany NY). 2022 Apr 28;14(8):3687-3704. doi: 10.18632/aging.204037. Epub 2022 Apr 28. PMID: 35483340; PMCID: PMC9085229.
188. Valiente M, Obenauf AC, Jin X, Chen Q, Zhang XH, Lee DJ, Chaft JE, Kris MG, Huse JT, Brogi E, Massagué J. Serpins promote cancer cell survival and vascular co-option in brain metastasis. Cell. 2014 Feb 27;156(5):1002-16. doi: 10.1016/j.cell.2014.01.040. PMID: 24581498; PMCID: PMC3988473.
189. Mirandola, L., Chiriva-Internati, M., Bresalier, R. et al. A novel method for efficient generation of antigen-specific effector T-cells using dendritic cells transduced with recombinant adeno-associated virus and p38 kinase blockade. J Transl Med 17, 424 (2019). https://doi.org/10.1186/s12967-019-02163-4
190. Ge Y, Ye T, Fu S, Jiang X, Song H, Liu B, Wang G, Wang J. Research progress of extracellular vesicles as biomarkers in immunotherapy for non-small cell lung cancer. Front Immunol. 2023 Apr 21;14:1114041. doi: 10.3389/fimmu.2023.1114041. PMID: 37153619; PMCID: PMC10162406.
191. Whiteside TL. Biology of extracellular vesicles and the potential of tumor-derived vesicles for subverting immunotherapy of cancer. Journal for ImmunoTherapy of Cancer 2025;13:e010376. doi:10.1136/jitc-2024-010376
192. Yehonatan E. et al. Meeting Abstract: 2025 ASCO Annual Meeting J Clin Oncol 43, 8579(2025)-Volume 43, Number 16_suppl - DOI: 10.1200/JCO.2025.43.16_suppl.8579
193. Bar J, Leibowitz R, Reinmuth N, Ammendola A, Jacob E, Moskovitz M, Levy-Barda A, Lotem M, Katsenelson R, Agbarya A, Abu-Amna M, Gottfried M, Harkovsky T, Wolf I, Tepper E, Loewenthal G, Yellin B, Brody Y, Dahan N, Yanko M, Lahav C, Harel M, Raveh Shoval S, Elon Y, Sela I, Dicker AP, Shaked Y. Biological insights from plasma proteomics of non-small cell lung cancer patients treated with immunotherapy. Front Immunol. 2024 Feb 29;15:1364473. doi: 10.3389/fimmu.2024.1364473. PMID: 38487531; PMCID: PMC10937428.
194. Sun, J., Xie, T., Jamal, M. et al. CLEC3B as a potential diagnostic and prognostic biomarker in lung cancer and association with the immune microenvironment. Cancer Cell Int 20, 106 (2020). https://doi.org/10.1186/s12935-020-01183-1
195. Sun, J., Xie, T., Jamal, M. et al. CLEC3B as a potential diagnostic and prognostic biomarker in lung cancer and association with the immune microenvironment. Cancer Cell Int 20, 106 (2020). https://doi.org/10.1186/s12935-020-01183-1
196. Qian, S., He, Y., Li, R. et al. Polymeric immunoglobulin receptor (pIgR) in cancer progression: a critical role and potential therapeutic target. Apoptosis 30, 1751–1775 (2025). https://doi.org/10.1007/s10495-025-02116-x
197. Luo B, Sen S, Dasari S, et al. Longitudinal plasma proteomics for NSCLC ICI response monitoring. J Clin Oncol. 2025;43(16_suppl):8579. DOI: 10.1200/JCO.2025.43.16_suppl.8579
198. Vandooren J, Itoh Y. Alpha-2-Macroglobulin in Inflammation, Immunity and Infections. Front Immunol. 2021 Dec 14;12:803244. doi: 10.3389/fimmu.2021.803244. PMID: 34970276; PMCID: PMC8712716.
199. Olbromski M, Mrozowska M, Piotrowska A, Kmiecik A, Smolarz B, Romanowicz H, Blasiak P, Maciejczyk A, Wojnar A, Dziegiel P. Prognostic significance of alpha-2-macrglobulin and low-density lipoprotein receptor-related protein-1 in various cancers. Am J Cancer Res. 2024 Jun 15;14(6):3036-3058. doi: 10.62347/VUJV9180. PMID: 39005669; PMCID: PMC11236788.

200. Lu J., Wang Y., Yan M., Feng P., Yuan L., Cai Y., Xia X., Liu M., Luo J., Li L. High serum haptoglobin level is associated with tumor progression and predicts poor prognosis in non-small cell lung cancer. Oncotarget. 2016; 7: 41758-41766.
201. Semeradtova, A., Liegertova, M., Herma, R. et al. Extracellular vesicles in cancer´s communication: messages we can read and how to answer. Mol Cancer 24, 86 (2025). https://doi.org/10.1186/s12943-025-02282-1
202. Ye Z, Zhang X, Luo Y, Li S, Huang L, Li Z, Li P, Chen G. Prognostic Values of Vimentin Expression and Its Clinicopathological Significance in Non-Small Cell Lung Cancer: A Meta-Analysis of Observational Studies with 4118 Cases. PLoS One. 2016 Sep 22;11(9):e0163162. doi: 10.1371/journal.pone.0163162. PMID: 27657690; PMCID: PMC5033348.
203. Zu R, Ren H, Yin X, Zhang X, Rao L, Xu P, Wang D, Li Y, Luo H. The FLNA Gene in Tumour-Educated Platelets Can Be Utilised to Identify High-Risk Populations for NSCLCs. J Cell Mol Med. 2025 Apr;29(7):e70544. doi: 10.1111/jcmm.70544. PMID: 40208200; PMCID: PMC11984322.
204. Chen Y, Zhao H, Feng Y, Ye Q, Hu J, Guo Y, Feng Y. Pan-Cancer Analysis of the Associations of TGFBI Expression With Prognosis and Immune Characteristics. Front Mol Biosci. 2021 Oct 4;8:745649. doi: 10.3389/fmolb.2021.745649. PMID: 34671645; PMCID: PMC8521171.
205. Kunapuli SP, Singh H, Singh P, Kumar A. Ceruloplasmin gene expression in human cancer cells. Life Sci. 1987 Jun 8;40(23):2225-8. doi: 10.1016/0024-3205(87)90057-9. PMID: 3586857.
206. Balmaña M, Sarrats A, Llop E, Barrabés S, Saldova R, Ferri MJ, Figueras J, Fort E, de Llorens R, Rudd PM and Peracaula R: Identification of potential pancreatic cancer serum markers: Increased sialyl-Lewis X on ceruloplasmin. Clin Chim Acta 442: 56-62, 2015. PMID: 25595436. DOI: 10.1016/j.cca.2015.01.007
207. Schneider MA, Rozy A, Wrenger S, Christopoulos P, Muley T, Thomas M, Meister M, Welte T, Chorostowska-Wynimko J, Janciauskiene S. Acute Phase Proteins as Early Predictors for Immunotherapy Response in Advanced NSCLC: An Explorative Study. Front Oncol. 2022 Jan 31;12:772076. doi: 10.3389/fonc.2022.772076. PMID: 35174082; PMCID: PMC8841510.
208. Repetto O, Mussolin L, Elia C, Martina L, Bianchi M, Buffardi S, Sala A, Burnelli R, Mascarin M and De Re V: Proteomic identification of plasma biomarkers in children and adolescents with recurrent hodgkin lymphoma. J Cancer 9(24): 4650-4658, 2018. PMID: 30588249. DOI: 10.7150/jca.27560
209. Li N, Hu H, Wu G and Sun B: Value of immune factors for monitoring risk of lung cancer in patients with interstitial lung disease. Journal of International Medical Research 47(7): 3344-3353, 2020. DOI: 10.1177/0300060519847403
210. Zhevak T, Shelekhova T, Chesnokova N, Tsareva O, Chanturidze A, Litvitsky P, Andriutsa N, Samburova N and Budnik I: The relationship between oxidative stress and cytogenetic abnormalities in B-cell chronic lymphocytic leukemia. Exp Mol Pathol 116: 104524, 2020. PMID: 32882207. DOI: 10.1016/j.yexmp.2020.104524
211. Mukae Y, Ito H, Miyata Y, Araki K, Matsuda T, Aibara N, Nakamura Y, Matsuo T, Sakai H, Ohyama K.- Ceruloplasmin Levels in Cancer Tissues and Urine Are Significant Biomarkers of Pathological Features and Outcome in Bladder Cancer. Anticancer Res. 2021 Aug;41(8):3815-3823. doi: 10.21873/anticanres.15174. PMID: 34281841.
212. Shimazaki R, Takano S, Satoh M, Takada M, Miyahara Y, Sasaki K, Yoshitomi H, Kagawa S, Furukawa K, Takayashiki T, Kuboki S, Sogawa K, Motohashi S, Nomura F, Miyazaki M, Ohtsuka M. Complement factor B regulates cellular senescence and is associated with poor prognosis in pancreatic cancer. Cell Oncol (Dordr). 2021 Aug;44(4):937-950. doi: 10.1007/s13402-021-00614-z. Epub 2021 Jun 1. PMID: 34075561; PMCID: PMC8338870.
213. He C., Y. Li, R. Zhang, J. Chen, X. Feng, Y. Duan Low CFB expression is independently associated with poor overall and disease-free survival in patients with lung adenocarcinoma Oncol. Lett., 21 (6) (2021), p. 478
214. He C, Wang X, Jiang B, Zhu M, Zhang H, Duan Y, Li Y. Complement Factor B (CFB) inhibits the malignant progression of lung adenocarcinoma by downregulating the Ras/MAPK signaling

pathway. Arch Biochem Biophys. 2024 Oct;760:110130. doi: 10.1016/j.abb.2024.110130. Epub 2024 Aug 20. PMID: 39173700.
215. Tinari N.; Lattanzio R.; Querzoli P.; Natoli C.; Grassadonia A.; Alberti S.; Hubalek M.; Reimer D.; Nenci I.; Bruzzi P.; Piantelli M.; Iacobelli S. High expression of 90K (Mac-2 BP) is associated with poor survival in node-negative breast cancer patients not receiving adjuvant systemic therapies. Int. J. Cancer 2009, 124 (2), 333–8. 10.1002/ijc.23970.
216. Marchetti A.; Tinari N.; Buttitta F.; Chella A.; Angeletti C. A.; Sacco R.; Mucilli F.; Ullrich A.; Iacobelli S. Expression of 90K (Mac-2 BP) correlates with distant metastasis and predicts survival in stage I non-small cell lung cancer patients. Cancer Res. 2002, 62 (9), 2535–9.
217. Zhang X.; Ding H.; Lu Z.; Ding L.; Song Y.; Jing Y.; Hu Q.; Dong Y.; Ni Y. Increased LGALS3BP promotes proliferation and migration of oral squamous cell carcinoma via PI3K/AKT pathway. Cell Signal 2019, 63, 109359. 10.1016/j.cellsig.2019.109359.
218. Inohara H.; Raz A. Identification of human melanoma cellular and secreted ligands for galectin-3. Biochem. Biophys. Res. Commun. 1994, 201 (3), 1366–75. 10.1006/bbrc.1994.1854.
219. Lobb, R.J., Visan, K.S., Wu, LY. et al. An epithelial-to-mesenchymal transition induced extracellular vesicle prognostic signature in non-small cell lung cancer. Commun Biol 6, 68 (2023). https://doi.org/10.1038/s42003-022-04350-4
220. Mirzapoiazova T, Mambetsariev N, Lennon FE, Mambetsariev B, Berlind JE, Salgia R, Singleton PA. HABP2 is a Novel Regulator of Hyaluronan-Mediated Human Lung Cancer Progression. Front Oncol. 2015 Jul 21;5:164. doi: 10.3389/fonc.2015.00164. PMID: 26258071; PMCID: PMC4508840.
221. Feng, S., Zhang, L., Sun, T., Xu, L., Quan, X., Zhao, G. and Zhang, H. (2025), OVOL1 Promotes Proliferation and Metastasis of Non-Small Cell Lung Cancer by Regulating APOE-Mediated Cholesterol Metabolism. J Cell Mol Med, 29: e70634. https://doi.org/10.1111/jcmm.70634
222. Montenegro, R.C., de Souza, P.F.N., Mesquita, F.P. (2025). APOE and Cancer Immunology. In: Oria, R., Ashford, J.W., Smith, C.J. (eds) Apolipoprotein E. Springer, Cham. https://doi.org/10.1007/978-3-031-52641-1_34-1
223. Darwish, N.M.; Al-Hail, M.K.; Mohamed, Y.; Al Saady, R.; Mohsen, S.; Zar, A.; Al-Mansoori, L.; Pedersen, S. The Role of Apolipoproteins in the Commonest Cancers: A Review. Cancers 2023, 15, 5565. https://doi.org/10.3390/cancers15235565
224. Gu, Y., Tang, S., Wang, Z., Cai, L., Lian, H., Shen, Y., & Zhou, Y. (2021). A pan-cancer analysis of the prognostic and immunological role of β-actin (ACTB) in human cancers. Bioengineered, 12(1), 6166–6185. https://doi.org/10.1080/21655979.2021.1973220
225. Huang ZC, Li H, Sun ZQ, Zheng J, Zhao RK, Chen J, Sun SG, Wu CJ. Distinct prognostic roles of HSPB1 expression in non-small cell lung cancer. Neoplasma. 2018;65(1):161-166. doi: 10.4149/neo_2018_102. PMID: 29017331.
226. National Comprehensive Cancer Network. Non-small cell lung cancer (Version3.2020) (2020). Available from: https://www.nccn.org/professionals/physician_gls/pdf/nscl.pdf
227. Batra U, Nathany S. Biomarker testing in lung cancer: from bench to bedside. Oncol Rev. 2025 Jan 6;18:1445826. doi: 10.3389/or.2024.1445826. PMID: 39834530; PMCID: PMC11743711.
228. Naryzhny S, Ronzhina N, Zorina E, Kabachenko F, Klopov N, Zgoda V. Construction of 2DE Patterns of Plasma Proteins: Aspect of Potential Tumor Markers. Int J Mol Sci. 2022 Sep 21;23(19):11113. doi: 10.3390/ijms231911113. PMID: 36232415; PMCID: PMC9 Geyer P.E., Kulak N.A., Pichler G., Holdt L.M., Teupser D., Mann M. Plasma Proteome Profiling to Assess Human Health and Disease. Cell Syst. 2016;2:185–195. doi: 10.1016/j.cels.2016.02.015. 569744.
229. Irmer B, Chandrabalan S, Maas L, Bleckmann A, Menck K. Extracellular Vesicles in Liquid Biopsies as Biomarkers for Solid Tumors. Cancers (Basel). 2023 Feb 18;15(4):1307. doi: 10.3390/cancers15041307. PMID: 36831648; PMCID: PMC9953862.
230. Kratka K, Sistik P, Olivkova I, Kusnierova P, Svagera Z, Stejskal D. Mass Spectrometry-Based Proteomics in Clinical Diagnosis of Amyloidosis and Multiple Myeloma: A Review (2012-2024).

J Mass Spectrom. 2025 Mar;60(3):e5116. doi: 10.1002/jms.5116. PMID: 39967472; PMCID: PMC11836596.
231. Thiele JA, Bethel K, Kralickova M, Kuhn P (2017) Circulating tumor cells: fluid surrogates of solid tumors. Annu Rev Pathol 12:419–447
232. Perakis S, Speicher MR (2017) Emerging concepts in liquid biopsies. BMC Med 15(1):017–0840
233. Yeung TM, Gandhi SC, Bodmer WF. Hypoxia and lineage specification of cell line-derived colorectal cancer stem cells. Proc Natl Acad Sci U S A 2011;108:4382-4387.
234. Eramo, A., Haas, T. & De Maria, R. Lung cancer stem cells: tools and targets to fight lung cancer. Oncogene 29, 4625–4635 (2010). https://doi.org/10.1038/onc.2010.207
235. Hirschhaeuser F, Menne H, Dittfeld C, West J, Mueller-Klieser W, Kunz-Schughart LA. Multicellular tumor spheroids: an underestimated tool is catching up again. J Biotechnol 2010;148:3-15.
236. Dalal, V., Dhankhar, P., Biswas, S. (2022). Proteomics as a Potential Tool for Biomarker Discovery. In: Sharma, N.K., Arya, A. (eds) High Altitude Sickness – Solutions from Genomics, Proteomics and Antioxidant Interventions. Springer, Singapore. https://doi.org/10.1007/978-981-19-1008-1_8
237. Mann M, Kulak NA, Nagaraj N, Cox J (2013) The coming age of complete, accurate, and ubiquitous proteomes. Mol Cell 49(4):583–590. https://doi.org/10.1016/j.molcel.2013.01.029
238. Chen F., Chandrashekar D.S., Varambally S., Creighton C.J. Pan-cancer molecular subtypes revealed by mass-spectrometry-based proteomic characterization of more than 500 human cancers. Nat. Commun. 2019;10:5679. doi: 10.1038/s41467-019-13528-0.
239. Hanash S., Taguchi A. Application of proteomics to cancer early detection. Cancer J. 2011;17:423–428. doi: 10.1097/PPO.0b013e3182383cab
184ii. Sun J, Xie T, Jamal M, Tu Z, Li X, Wu Y, Li J, Zhang Q, Huang X. CLEC3B as a potential diagnostic and prognostic biomarker in lung cancer and association with the immune microenvironment. Cancer Cell Int. 2020 Apr 1;20:106. doi: 10.1186/s12935-020-01183-1. PMID: 32265595; PMCID: PMC7110733.

7.0 Scientific Products

Papers:

2025

• Gristina V, Bazan V, Barraco N, Taverna S, Manno M, Raccosta S, Carreca AP, Bono M, Bazan Russo TD, Pepe F, Pisapia P, Incorvaia L, Badalamenti G, Troncone G, Malapelle U, Santini D, Russo A, Galvano A. On-treatment dynamics of circulating extracellular vesicles in the first-line setting of patients with advanced non-small cell lung cancer: the LEXOVE prospective study. Mol Oncol. 2025 Jan 9. doi: 10.1002/1878-0261.13737. Epub ahead of print. PMID: 39780749.

2024

• Palumbo FS, Calligaris M, Calzà L, Fiorica C, Baldassarro VA, Carreca AP, Lorenzini L, Giuliani A, Carcione C, Cuscino N, Pitarresi G, Scilabra SD, Conaldi PG, Chinnici CM. Topical application of a hyaluronic acid-based hydrogel integrated with secretome of human mesenchymal stromal cells for diabetic ulcer repair. Regen Ther. 2024 Jul 27;26:520-532. doi: 10.1016/j.reth.2024.07.008. PMID: 39156755; PMCID: PMC11327949.

• Carreca AP, Tinnirello R, Miceli V, Galvano A, Gristina V, Incorvaia L, Pampalone M, Taverna S, Iannolo G. Extracellular Vesicles in Lung Cancer: Implementation in Diagnosis and Therapeutic Perspectives. Cancers (Basel). 2024 May 22;16(11):1967. doi: 10.3390/cancers16111967. PMID: 38893088; PMCID: PMC11171234.

• Calligaris M, Zito G, Busà R, Bulati M, Iannolo G, Gallo A, Carreca AP, Cuscino N, Castelbuono S, Carcione C, Centi C, Amico G, Bertani A, Chinnici CM, Conaldi PG, Scilabra SD, Miceli V. Proteomic analysis and functional validation reveal distinct therapeutic capabilities related to priming of mesenchymal stromal/stem cells with IFN-γ and hypoxia: potential implications for their clinical use. Front Cell Dev Biol. 2024 May 31;12:1385712. doi: 10.3389/fcell.2024.1385712. PMID: 38882056; PMCID: PMC11179434.

• Candore G, Accardi G, Aiello A, Baggio G, Bellini T, Calabrese V, Carreca AP, Carreca I, Masucci A, Cattaneo M, Dato S, Di Bona D, Fabris L, Gambino C, Di Lorenzo G, Franceschi C, Ligotti ME, Manfrinato MC, Puca AA, Tamburello M, Vassallo R, Caruso C. Sex and Gender in Ageing and Longevity: Highlights From an International Course. Transl Med UniSa. 2024 Feb 27;26(1):15-29. doi: 10.37825/2239-9747.1049. PMID: 38560614; PMCID: PMC10980291.

• Bonsignore R, Trippodo E, Di Gesù R, Carreca AP, Rubino S, Spinello A, Terenzi A, Barone G. Novel half Salphen cobalt(III) complexes: synthesis, DNA binding and anticancer studies. Dalton Trans. 2024 Apr 2;53(14):6311-6322. doi:

10.1039/d4dt00092g. PMID: 38487871.

• Palumbo FS, Fiorica C, Carreca AP, Iannolo G, Pitarresi G, Amico G, Giammona G, Conaldi PG, Chinnici CM. Modulating the release of bioactive molecules of human mesenchymal stromal cell secretome: Heparinization of hyaluronic acid-based hydrogels. Int J Pharm. 2024 Mar 25;653:123904. doi: 10.1016/j.ijpharm.2024.123904. Epub 2024 Feb 12. PMID: 38355074.

2023

• Schiera G, Cancemi P, Di Liegro CM, Naselli F, Volpes S, Cruciata I, Cardinale PS, Vaglica F, Calligaris M, Carreca AP, Chiarelli R, Scilabra SD, Leone O, Caradonna F, Di Liegro I. An In Vitro Model of Glioma Development. Genes (Basel). 2023 Apr 27;14(5):990. doi: 10.3390/genes14050990. PMID: 37239349; PMCID: PMC10217752.

2022

• Alfayez E, Veschini L, Dettin M, Zamuner A, Gaetani M, Carreca AP, Najman S, Ghanaati S, Coward T, Di Silvio L. DAR 16-II Primes Endothelial Cells for Angiogenesis Improving Bone Ingrowth in 3D-Printed BCP Scaffolds and Regeneration of Critically Sized Bone Defects. Biomolecules. 2022 Nov 2;12(11):1619. doi: 10.3390/biom12111619. PMID: 36358970; PMCID: PMC9687468.

• Spanò DP, Bonelli S, Calligaris M, Carreca AP, Carcione C, Zito G, Nicosia A, Rizzo S, Scilabra SD. High-Resolution Secretome Analysis of Chemical Hypoxia Treated Cells Identifies Putative Biomarkers of Chondrosarcoma. Proteomes. 2022 Jul 20;10(3):25. doi: 10.3390/proteomes10030025. PMID: 35893766; PMCID: PMC9326515.

• Carreca, A.P.; et al. Galectin-9 and Interferon-Gamma Are Released by Natural Killer Cells upon Activation with Interferon-Alpha and Orchestrate the Suppression of Hepatitis C Virus Infection. Viruses 2022, 14, 1538. https:// doi.org/10.3390/v14071538 IF:5.818

• Yang CY, Bonelli S, Calligaris M, Carreca AP, Müller SA, Lichtenthaler SF, Troeberg L, Scilabra SD. Quantitative Proteomics Reveals That ADAM15 Can Have Proteolytic-Independent Functions in the Steady State. Membranes (Basel). 2022 May 31;12(6):578. doi: 10.3390/membranes12060578. PMID: 35736286; PMCID: PMC9227920.

• G. Di Mento,et al. “A retrospective molecular epidemiological scenario of carbapenemaseproducing Klebsiella pneumoniae clinical isolates in a Sicilian transplantation hospital shows a swift polyclonal divergence among sequence types, resistome and virulome”. Microbiological Research, Volume

256,2022,126959,ISSN 0944-5013, https://doi.org/10.1016/j.micres.2021.126959 IF: 5.415

Posters:

- Carreca Anna Paola, Bongiorno Angela, Amico Giandomenico , Labbozzetta Manuela, Pampalone Mariangela; - Extracellular Vesicles from Placental MSCs Modulate Anti-Tumor Immunity interacting with Immune Checkpoints in Lung Cancer- Abstract num P2.49- 4TH Evita Symposium- Favignana (TP) 24-26 September 2025
- Cammarata G , di Fazio G , Poppa G , Carreca AP , D'Ascenzo S , Megiorni F , Ceccarelli S., Dolo V. , Giusti I., Taverna S. - Selective Enrichment of Circular RNAs in Extracellular Vesicles released by Ovarian Cancer Cells: A New Frontier in Liquid Biopsy- Abstract num. P1.46 - 4TH Evita Symposium- Favignana (TP) 24-26 September 2025

Oral presentation:

- "Consideration of sex and gender aspects in oncology" at I course on sex and gender in ageing and longevity- International School of Medical Sciences c/o Ettore Majorana Foundation- Erica (Trapani) 7-8 November 2023.

Other publications – outreach and educational texts

- Trattato Italiano di Medicina d'Ambiente HECO 2023 Consensus on Health, Environment, Economy:Tomo II Chapter 62; Tomo III Chapters 38- 39 - Editor Aldo Ferrara
- Role of Sex and Gender in Aging and Longevity- Chapter 11- Editor Caruso Calogero
- Vademecum della Salute, distributed during the Freccia Rosa initiative by the IncontraDonna Foundation, both in 2024 and 2025.

Reviewer for journals:

- Cancers;
- International Journal of Molecular Sciences;
- Journal of Tissue Engineering and Regenerative Medicine
- Translational Lung Cancer Research